Architecture, tectonic control and instability of the submarine continental margin offshore Mount Etna, Italy

DISSERTATION

zur Erlangung des Doktorgrades

an der Mathematisch-Naturwissenschaftlichen Fakultät

der Christian-Albrechts-Universität zu Kiel

vorgelegt von

Felix Michael Gross

Kiel, 2015

Referent:	Prof. Dr. Sebastian Krastel-Gudegast
Koreferent:	Prof. Dr. Jan Behrmann
Tag der mündlichen Prüfung:	03. Juni 2015
Zum Druck genehmigt:	

……

Der Dekan

Hiermit erkläre ich eidesstattlich, dass ich die vorliegende Dissertation selbständig und ohne zuhilfenahme unerlaubter Hilfsmittel angefertigt habe. Bisher ist die Arbeit noch nicht an anderer Stelle im Rahmen eines Prüfungsverfahrens vorgelegt worden. Die Arbeit ist unter Einhaltung der Regeln guter wissenschaftlicher Praxis der Deutschen Forschungsgemeinschaft entstanden.

Kiel, den

Felix Gross

Abstract

The Island of Sicily (southern Italy) is located at the collision zone of the Eurasian Plate and the subducting African Plate. It is one of the most active areas in terms of seismicity in Europe; the trend of the subduction zone and its subducting mechanism, however, are still debated. The structural unrest of the area is documented by large plate ruptures in historical times like the prominent 1693, 1783 and 1908 earthquakes. Especially the 1908 Messina earthquake (~ 80,000 casualties) is of major interest as it was associated with the worst tsunami Italy experienced in the historical time (~2000 casualties). It is still debated whether a plate rupture at the seafloor or a massive submarine landslide triggered the tsunami, which hits the coast of East Sicily and Calabria.

Related to this geodynamic setting, the area is also famous for its active volcanism. The Aeolian Island in the Tyrrhenian Sea form the highly active backarc-volcanism of the Calabrian subduction regime. Another type of volcano is observed directly at the shore of East Sicily – Mt Etna. Mt Etna is not only Europe's largest volcano edifice with a recent height of 3323 m a.s.l, furthermore it is well known for its frequent eruptions. Compared to Earth's history, Mt Etna is a relatively young volcano with an active volcanic history of ~500 ka. The origin of Mt Etna is still debated in several theories have been proposed (e.g., asymmetrical rifting processes, intersection of structural elements, hot spot, extensional tectonics). Mt Etna's edifice can be traced mostly onshore and is directly adjacent to the continental margin of the Ionian Sea east of Sicily.

Mt Etna is well known for its onshore edifice flank instability, as its eastern and southern flanks are gliding towards the continental margin in the east. The part of the flank gliding to the east is bound by prominent volcano-tectonic fault systems. The continental margin offshore of the gliding flank is characterized by a prominent bulge, which is not found further to the north or south. The onshore flank movement is well documented and monitored, but the potential continuation of this process towards the continental margin is not well investigated due to a lack of offshore data.

In order to investigate and evaluate the phenomenon of volcano flank instability and its link to continental margin instability, a new high resolution new 2D/3D hydro/seismo-acoustic and geological dataset was acquired during RV METEOR research cruise M86/2 in December 2011/January 2012.

The new dataset shows that not only the volcano edifice reveals an instability; furthermore, the entire continental margin east of the gliding sector of Mt Etna shows indications for recent extensional tectonics related to gravitational spreading. Whereas the northern boundary of the moving volcano flank is well defined by the sharp Pernicana-Provenzana Fault onshore, the offshore continuation reveals a diffuse grade of deformation and cannot be traced as a distinct sharp boundary. In contrast, the offshore southern boundary of the moving flank is clearly imaged by the new data set. It is identified as a right

lateral oblique fault north of Catania Canyon. Two anticlines are present directly in front of the continental margin bulge. These anticlines are bound to half-graben basins towards the east and mark the eastern limits of the volcano flank and continental margin instability. As volcano-tectonic structures like the southern boundary fault can be traced from the volcano edifice across the continental margin towards the continental toe, the whole system is considered as a coupled volcano flank / continental margin gravitational instability and collapse.

During M86/2 a new high-resolution 3D seismic cube at the center of the continental margin between the funnel shaped depositional system of Valle di Archirafi and a prominent amphitheater-like headwall, was collected. By assessing this 3D seismic data, a secondary spreading center was mapped at the center of the continental margin affected by the continental margin gravitational instability. It is located at a structural high, directly adjacent to the massive amphitheater headwall. The structural high hosts a set of normal faults, dipping towards steep amphitheater's headwall. These faults show indications for recent and ongoing activity, as most of the fault planes are striking out at the seafloor. This fault activity makes to structural high to one of the most striking areas in terms of possible future hazards, related to submarine landslides, in the entire survey area. Next to mass transport deposits, traced in the funnel shaped Valle di Archirafi, the entire continental margin and the continental toe is strongly overprinted by a variety of mass transport deposits in the upper 750 m of the sedimentary record. A typical succession of mass transport deposits directly overlain by tephra layers indicate that volcano induced seismicity and flank deformation prior to an eruption act as important trigger mechanisms for catastrophic slope failures on the continental margin east of Mt Etna. The near-surface mass transport deposits are relatively small but seismic data illustrate significantly larger buried mass transport deposits, which were most likely triggered by similar volcanic processes in the past. The new dataset does not support the theory that the 1908 tsunami was triggered by a massive submarine landslide north of Mt Etna's continental margin. The proposed slide deposit is overlain by a ~150 m thick succession of in-situ strata. The mass transport deposits seems to be the product of an ancient landslide event and has not occurred just ~100 years ago.

All these findings imply a recently active coupled volcano edifice / continental margin system, which results in instable slopes and submarine mass movements. These findings even increase the geo-hazard potential of the area, which is already very high due to the ongoing seismic activity.

Zusammenfassung

Die Insel Sizilien (Süditalien) ist an der Kollisionszone zwischen der eurasischen- und der sich subduzierenden afrikanischen Platte gelegen. Die Gegend ist bekannt als eine der seismisch aktivsten Zonen in Europa, wobei der genaue Verlauf und die Mechanismen der Subduktionszone immer noch unklar sind. Diese strukturelle Unruhe geht mit großen Plattenverschiebungen einher, die schwerwiegende Erdbeben wie das 1693, 1783 und das 1908 Erdbeben in historischen Zeiten auslösten. Hierbei ist das 1908 Messina Erdbeben (~ 80,000 Opfer) von großem Interesse, da es von dem fatalsten Tsunami (~2000 Opfer), den die Küsten von Italien seit der Zeitaufzeichnung erfahren haben, begleitet wurde. Es ist nach wie vor nicht geklärt, ob dieser Tsunami, der an den Küsten von Sizilien und Kalabrien anbrandete, von einem Meeresbodenversatz oder einer großen submarinen Hangrutschung ausgelöst wurde.

Einhergehend mit seiner geodynamischen Besonderheit ist die Gegend zudem für den auftretenden aktiven Vulkanismus bekannt. Die Äolischen Inseln in der tyrrhenischen See bilden hierbei den hoch-aktiven Backarc-Vulkanismus der kalabrischen Subduktionszone. Ein anderer Typ von Vulkanismus kann direkt an der Küste von Ost-Sizilien beobachtet werden – der Vulkan Ätna. Mit seiner aktuellen Erhebung von 3323 m über dem Meeresspiegel, ist Ätna nicht nur als das höchste Vulkangebäude Europas, sondern auch für seine oft auftretenden Eruptionen, bekannt. Im Vergleich zur Erdgeschichte handelt es sich bei Ätna um einen relativ jungen Vulkan, dessen erste Aktivität ca. 500 ka zurückliegt. Der Ursprung von Ätna ist noch nicht endgültig geklärt und es gibt verschiede Ansätze seine Entstehung zu erklären (z.B. asymmetrische Kluft Bildung, Überschneiden von strukturellen Elementen, Hot Spot Vulkanismus, extensionelle Tektonik). Das Vulkangebäude von Ätna kann hauptsächlich am Festland von Ost-Sizilien kartiert werden. Zudem erhebt sich das Vulkangebäude direkt westlich des submarinen Kontinentalhanges der ionischen See.

Das terrestrische Vulkangebäude von Ätna ist für seine Flankeninstabilität bekannt, da sich seine östliche- und südliche Flanke langsam in Richtung des im Osten gelegenen Kontinentalhangs gleiten. Dieses Gleiten wird von ausgeprägten Störungssystemen am Vulkangebäude geleitet. Der Kontinentalhang vor dem Vulkangebäude ist durch eine Aufwölbung geprägt, die nicht Nördlich oder Südlich von Ätna zu beobachten ist. Die Bewegungen der Flanke des Vulkangebäudes sind sehr gut dokumentiert und werden ständig beobachtet. Auf Grund eines Mangels an Daten im marinen Bereich, ist die Fortsetzung dieses Prozesses in Richtung des submarinen Kontinentalhangs allerdings nicht gut erforscht.

Um den Zusammenhang zwischen Vulkangebäude-Instabilität und die Auswirkungen und Verbindungen auf den Kontinentalhang zu untersuchen, wurde ein neuer hochauflösender mariner Datensatz während der Forschungsreise M86/2 mit dem deutschen Forschungsschiff METEOR im

Dezember 2011 und Januar 2012 aufgenommen. Der neue Datensatz enthält sowohl 2D/3D seismische, Hydro-akustische sowie geologische Daten.

Der neue Datensatz zeigt, dass nicht nur das Vulkangebäude Hinweise auf Flankeninstabilität liefert. Vielmehr zeigt der Kontinentalhang östlich der gleitenden Vulkanflanke Indikationen für aktive, ausdehnende Tektonik, welche auf das schwerkraftbedingte Ausbreiten des Meeresbodens hinweisen.

Wobei die nördliche Grenze der sich bewegenden Vulkanflanke an Land gut durch die Pernicna-Provenzana Störung dargestellt ist, zeigt die submarine Verlängerung dieses Störungssystems einen diffusen Grad an Deformation und kann daher nicht als scharfe Grenze im marinen Bereich verfolgt werden. Im Gegensatz zur nördlichen Grenze, ist es mit dem neuen Datensatz möglich die südliche Grenze der sich bewegenden Vulkanflanke auf dem Kontinentalhang zu verfolgen. Die Störung wird als eine dextrale Diagonalverwerfung nördlich des Catania Canyon charakterisiert. Dem aufgewölbten Kontinentalhang sind zwei Antiklinen vorgelagert. Diese Antiklinen grenzen östlich an Halbgraben-Becken und stellen die östliche Grenze der Instabilität des Vulkangebäudes und des Kontinentalhanges dar. Da sich Strukturen wie die südliche Grenze der Flankeninstabilität vom Vulkangebäude über den Kontinentalhang in Richtung des Kontinentalfußes verfolgen lassen, wird das gesamte System als eine gekoppelte, schwerkraftbedingte Instabilität und Kollaps des Vulkangebäudes und des Kontentalhanges angesehen.

Während der Forschungsfahrt M86/2 wurde zudem ein hochauflösender 3D seismischer Würfel im zentralen Bereich des Kontinentalhangs, zwischen dem trichterförmigen Ablagerungssystem des Valle di Archirafi und einer markanten Abrisskante einer Amphitheater-Struktur, aufgezeichnet. Mit Hilfe des 3D seismischen Würfels wurde ein sekundäres Spreizungszentrum am Meeresboden in diesem Bereich kartiert. Dieses Spreizungszentrum ist an einer strukturellen Erhebung direkt westlich der Amphitheater-Struktur gelegen. Diese strukturelle Erhebung ist durch Abschiebungen, die in Richtung der steilen Abrisskante der Amphitheater-Struktur einfallen, geprägt. Die Abschiebungen weisen auf eine rezente Aktivität des Systems hin, da die meisten Störungsflächen am Meeresboden ausstreichen. Dieses aktive Störungssystem macht die strukturelle Erhebung am Rande der Amphitheater-Struktur zu einer der wichtigsten Gegenden für zukünftig auftretende Gefahren, die mit Hangrutschungen assoziiert werden.

Neben Ablagerungen von Hangrutschungen, die im trichterförmigen Valle di Archirafi beobachtet werden können, weist der gesamte Kontinentalhang und der Kontinentalfuß auf eine Überprägung durch Hangrutschungen hin, da eine Vielzahl von Ablagerungen von Hangrutschungen in den oberen 750 m der Sedimentmächtigkeit gefunden wurden.

Eine typische Sedimentabfolge von Hangrutschungs-Ablagerungen, die direkt von Tephren überlagert sind, wurde in Sedimentkernen festgestellt. Dies impliziert, dass vom Vulkan ausgehende Seismizität und einhergehende Flankendeformation vor einer Eruption als ein wichtiger Auslösemechanismus für katastrophale Hangrutschungen am Kontinentalhang östlich des Ätna in Betracht gezogen werden müssen. Die oberflächennahen Ablagerungen von Hangrutschungen weisen relativ geringe Mächtigkeiten auf, jedoch können mit Hilfe der Reflektions-Seismik signifikant mächtigere Ablagerungen von Hangrutschungen kartiert werden, die sehr wahrscheinlich von ähnlichen vulkanischen Prozessen in der Vergangenheit generiert wurden. Der neue Datensatz zeigt keine Indikationen dafür, dass der 1908 Tsunami von einer submarinen Hangrutschung, die nördlich des Kontinentalhangs von Ätna gefunden wurde, ausgelöst wurde. Die vermutete Ablagerung einer Hangrutschung ist von einer ca. 150 m mächtigen, gut stratifizierten in-situ Sedimentfazies überlagert, die wenig bis gar keine Deformation aufweist. Dies impliziert, dass die Ablagerung ein Resultat einer wesentlich älteren Hangrutschung sind, die vor westlich mehr als ~100 Jahren stattfand.

Die neuen Forschungsergebnisse implizieren die Aktivität der Instabilität von einem gekoppelten Vulkangebäude und Kontinentalhang, die zu der Instabilität des Hanges und resultierenden submarinen Hangrutschungen führt. Die neuen Ergebnisse deuten auf eine Erhöhung des Gefahrenpotentials in der Gegend hin, die sowieso schon auf Grund von hoher Seismizität als gefährlich eingestuft wird.

Content

Outline of the Thesis

Chapter 1 introduces the survey area at Mt Etna. General information on volcano flank- and continental margin instability are presented. In addition, the tectonic setting, the geology and the flank instability at Mt Etna are described.

Chapter 2 presents the objectives of this thesis, which include descriptive and process oriented questions.

Chapter 3 gives an insight to the used methods for this thesis. General information on 2D/3D seismics, multi-beam bathymetry and PARASOUND sediment echo-sounder, as well as the acquisition parameters used during RV Meteor Cruise M/86/2 are presented. A short introduction into the processing of the data is given as well.

Chapter 4: Manuscript I - The limits of seaward spreading and slope instability at the continental margin offshore Mt Etna, imaged by high-resolution 2D seismic data (In review at 'Tectonophysics')

This chapter includes the analysis of the architecture of the continental margin and the continental toe offshore Mt Etna by means of 2D high-resolution reflection seismic data. The chapter focuses on the different surface and sub-surface structures observed at the continental margin and continental toe offshore Mt Etna. By compiling all data, a new model for the continental margin and volcano flank architecture will be introduced in this chapter.

Chapter 5: Manuscript II - High-Resolution 3D seismic imaging of spreading and gravitational instability next to a giant amphitheater headwall at the continental margin offshore Mt Etna, Italy (in preparation for submission to 'Geochemistry; Geophysics, Geosystems')

This chapter focusses on the 3D P-Cable cube acquired at the central continental margin offshore Mt Etna. It includes the analysis of seafloor morphology, as well as the subsurface sedimentary and tectonic processes. The chapter will give insights into the tectonic control of the Valle di Archirafi and the structural high at the prominent amphitheater-like structure off Mt Etna. In addition, the dataset is evaluated in its regional context.

Chapter 6: Manuscript III - Evidence for landslides offshore Mt. Etna, Italy (Published as Gross, F., Krastel, S., Chiocci, F.L., Ridente, D., Schwab, J., Beier, J., Cukur, D., Winkelmann, D. (2014) New implications on submarine landslides offshore Mt. Etna, Italy. In: Submarine mass movements and their consequences (eds: Krastel et al). Advances in Natural and Technological Hazards Research, 37, 307-316.)

This chapter focusses on mass transport deposits on the continental margin east off Mt Etna. A new distribution map of submarine mass transport deposits is presented. Another topic of this chapter is the

falsification of the theory by *Billi et al. [2008]* that the 1908 tsunami was caused by a landslide. Furthermore, the theory of volcanic tremor and coherent seismicity as a possible trigger mechanism for submarine landslides offshore Mt Etna will be introduced based on the analysis of sediment cores,.

Chapter 7 summarizes the outcome of this thesis and gives an outlook for potential future work at the continental margin offshore Mt Etna.

1 Introduction

1.1 Motivation

Southern Italy is one of most active seismic regions in Europe *[e.g. Orecchio et al. 2014]*. This seismic activity is expressed by numerous deep to shallow earthquakes, occurring in the Calabrain Arc at the transition of the Tyrrhenian- and the Ionian Sea *[Monaco and Tortorici, 2000]* (Fig. 1). Especially the occurrence of large magnitude earthquakes like the 1693 *[e.g. Tinti et al. 2001]*, 1783 *[e.g. Jacques et al. 2001]* and 1908 earthquake with high numbers of causalities underline the hazardous potential of these ruptures. The 1908 Messina Earthquake (Ms=7.3; 80,000 casualties) and its ensuing tsunami (~2000 causalities) *[Baratta, 1910]*, is known as the most devastating tsunami in historical times striking the Italian coastline *[Tinti et al. 1999; Billi et al. 2008]*. This event is of major interest, as it is still uncertain, whether a plate boundary rupture at the seafloor or a submarine landslide triggered the tsunami *[e.g. Billi et al. 2008; Argnani et al. 2009; Favalli et al. 2009]*. In addition to a high seismicity, the area is strongly affected by volcanism in the Tyrrhenian Sea (Aeolian Islands) and the volcanism of Mount Etna on the Sicilian mainland (Fig. 1).

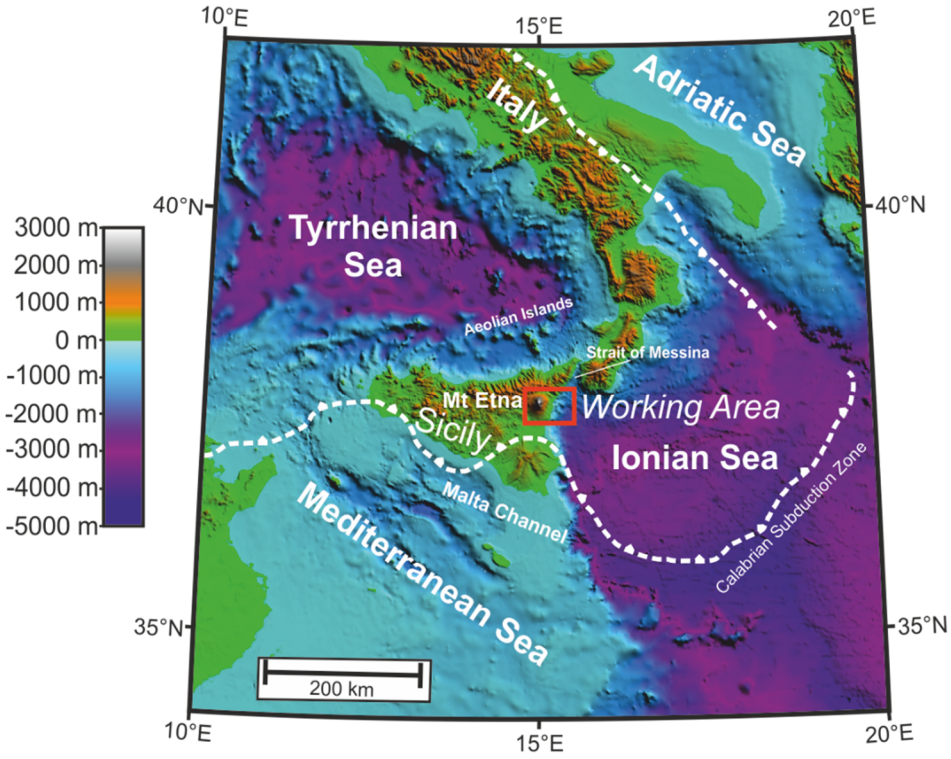

Figure 1: Sicily is located between the Tyrrhenian- and the Ionian Sea. It is separated from the Italian mainland by the Strait of Messina. The working area of this thesis is located offshore Mt Etna, which is Europe's largest active volcano and piles up to a height of 3323 m a.s.l. The red box marks the working area (Fig. 2). (Projection: Universal Transverse Mercator (UTM))

Mt Etna is known as Europe's largest and one of the most active volcanoes, worldwide. It piles up to a recent height of 3323 m a.s.l. and established its edifice ~500 kyr ago *[Branca et al. 2004]* on continental crust directly on the coastline of eastern Sicily *[e.g. Gvirtzman and Nur 1999; Doglioni et al. 2001]*. First settlements in direct vicinity to Mt. Etna were established in pre-roman times, as the fertile volcano flank offered outstanding quality for farmland and agriculture. Over the past 3000 years the region around Mt Etna developed to a densely populated area. The largest city of the region is Catania, home to ~315.000 inhabitants, directly at the southern slope of Mt Etna. Mt Etna is also known to be the cradle of volcanology as the Greek historian Diodorus Siculus first mentioned and described the active volcano in East Sicily ~ 60 BC *[Diodorus Siculus in Vogel and Fisher 1888-1906]*. A description and summary of historical eruptions of Mt Etna was presented by *Branca [2004]*. Due to its impressive volcano edifice forming a unique landscape and its cultural significance, the area of Mt Etna was added by the UNESCO to the World Heritage Sites in 2013 *[http://whc.unesco.org/en/news/1042 , 25.02.2015]*.

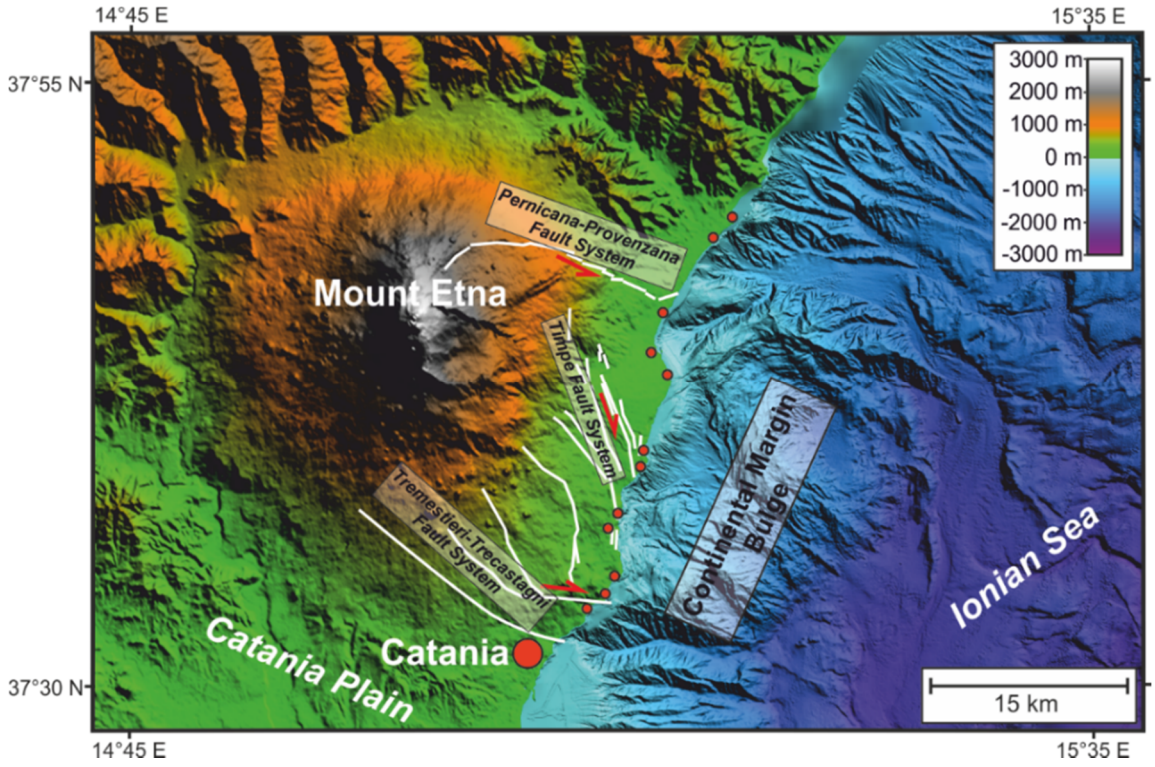

Figure 2: Mt Etna and its adjacent continental margin (see Fig. 1 for location). Mt Etna's volcano edifice can mostly be traced onshore. The continental margin is described as a prominent bulge, which cannot be observed north and south of the volcano edifice in the Ionian Sea. (Projection: Universal Transverse Mercator (UTM))

In addition to several eruptions per year *[Branca 2004]*, Mt Etna is known for its edifice instability, as its eastern and southern flanks are slowly gliding towards the Ionian Sea in the east and the Catania Plain in the south *[e.g. Borgia et al. 1992]* (Fig. 2). In comparison to the well-studied and monitored onshore realm, only little is known about the adjacent continental margin, which is expressed as a morphological bulge in front of Mt. Etna (Fig. 2). Surveying of the continental margin has only started ~10 years ago *[Marani et al. 2004; Argnani and Bonazzi 2005; Pareschi et al. 2006; Chiocci et al.*

2011; Argnani et al. 2013]. It is still unclear, if the continental margin is affected by the slope instability, observed at Mt Etna, or the continental margin is an important precursor for this movement. This lack of information is the motivation of this thesis. Providing a description and explaining the situation of the continental margin and its bulging by means of high-resolution hydro/seismo-acoustic and geological data is the main objective of this dissertation.

1.2 Volcanic Flank and Continental Margin instability

In order to understand the complex geologic, tectonic and geodynamic setting at Mt Etna, general volcano flank instability and continental margin instability have to be considered. Mt Etna is a unique type of volcano, as it sits on top of continental curst; volcanic activity is characterized by plinian eruptions at its strato volcano edifice and fissure type eruptions at the volcano flanks for the past ~40 kyr *[Branca 2004]*. No comparable setting is known worldwide. However, the general effects and precursors for volcano instability *[e.g. McGuire 1996 and references therein]* and continental margin *[e.g. Winker and Edwards 1983; Morley et al. 2011; Peel 2014]* instability were studied during the last decades and some of them can be applied to the setting at Mount Etna.

1.2.1 Volcanic Flank instability

After the 1980 Mt St. Helens eruption *[Christiansen and Peterson 1981]*, which might have been triggered by a massive landslide *[Lipman and Mullineaux, 1981]*, volcano instability of large scale volcano edifices and associated geo-hazards are well known. Many studies at different volcanoes like the Hawaiian Island *[e.g. Moore et al. 1989]*, the Canary Island *[e.g. Krastel et al. 2001; Mason et al. 2002]*, the Aeolian Islands *[e.g. Kokelaar et al. 1995]* and Casita Volcano Nicaragua *[e.g. van Wyk de Vries et al. 2000]* show the importance of volcano flank instability, as most of the active volcanos reveal sector collapses and instable flanks, worldwide.

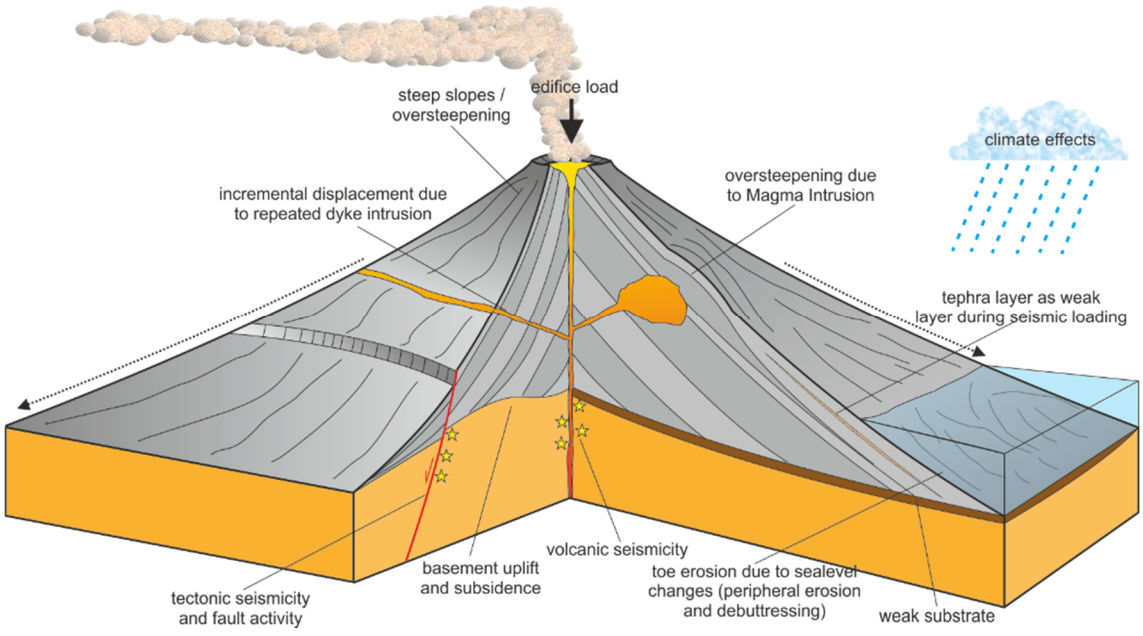

Figure 3: Schematic drawing of possible contributors to volcano edifice structural instability at active volcanos including precursors for flank instability and possible trigger mechanisms for flank failures. Precursors and trigger mechanisms for volcano flank instability can be divided into endogenic and exogenic factors (Table 1).

Precursors and triggers (Fig. 3) for volcano edifice instability can be classified into internal forcing (endogenic) and external forcing (exogenic) (Table 1) and can generate a volcano edifice instability in periods of weeks to months or thousand to tens of thousands of years *[McGuire 1996]*. Some of the most prominent endogenic precursors for volcano flank instability at active volcano edifices are slope over-steepening due to magma intrusion *[e.g. Begét and Kienle 1992]* and incremented displacement due to repeated dyke intrusions *[Swanson et al. 1976; McGuire et al. 1990; 1991]*. Especially dike intrusions can lead to a lateral flank displacement during fissure type eruptions, affecting volcano flanks like at Mt Etna *[Acocella et al. 2003]*. Furthermore, exogenic influences on volcano edifice like climate effects *[Cervelli et al. 2002]* and also toe erosion during sea-level changes can lead to peripheral weakening and debuttressing *[e.g. Tibaldi 2001]*. Another important mechanism for volcano edifice instability is the weight of the volcano edifice, which is mostly observed at large scale volcanos *[e.g. Münn et al. 2006]*. This can lead, like at Mt. Etna, to a gravitational collapse of the entire edifice and result in large-scale spreading and deformation of the volcano edifice *[Borgia et al. 1992]*.

Table 1: Internal and external forcing for volcano flank instability, worldwide (Fig. 2):

Trigger / Precursor	Internal Forcing	Example	Reference
Precursor	Over-steepening due to magma intrusion	Augustine, Alaska	*[Begét and Kienle, 1992]*
Precursor / Trigger	Incremental displacement due to repeated dyke intrusion	Kilauea, Hawaii Mt Etna, Italy	*[Swanson et al. 1976]* *[McGuire et al. 1990, 1991; Acocella et al. 2003]*
Precursor	Basement uplift or subsidence	Mt Etna, Italy	*[Stewart et al. 1993; Firth et al. 1996]*
Trigger	Volcanic seismicity	Stromboli, Italy Casita, Nicaragua	*[Telesca et al. 2010]* *[Van Wyk de Vries et al. 2000]*
Precursor	Weak substrate	Mt Etna, Italy	*[Rust et al. 2005]*
Trigger / Precursor	**External Forcing**	**Example**	**Reference**
Precursor	Steep slope / over steepening due accumulation of eruptive products on the volcano edifice	Mt Etna, Italy	*[Murray and Voight 1996]*
Trigger	Climate effects	Kilauea ,Hawaii	*[Cervelli et al. 2002]*
Precursor	Toe erosion due to sea level changes (peripheral erosion and debuttressing)	Stromboli, Italy	*[Tibaldi 2001]*
Precursor	Edifice load and gravitational spreading	El Hierro, Canary Islands Mt Etna, Italy	*[Münn et al. 2006]* *[Borgia et al. 1992]*
Trigger	Tephra layer as weak layer during seismic loading*	Offshore central America	*[Harders et al. 2010]*
Precursor	Pre-Existing volcano rift- and fault zones	Cumbre Vieja, Canary Islands	*[Day et al. 1999]*

* Only observed at the continental margin and not at volcano edifice

1.2.2 Continental Margin Instability due to gravity driven processes

The occurrence of large-scale lateral movements at mountain belts lead to the development of the concept of gravity-driven tectonics and deformation *[e.g. Bucher 1956; van Bemmelen 1960; Kehle, 1970; Elliott 1976]*. It was used to explain the coherence of extensional faults in the up-dip portion and contraction in the down-dip region of sloping landscapes *[Peel 2014]*. This phenomenon is not only observed in active orogenic complexes. Furthermore, the presence of gravity-driven deformation of sedimentary sequences can be observed at most passive continental margins worldwide *[Rowan et al. 2004; Morley et al. 2011; Peel 2014]*. Gravity-driven processes can be observed in the range from the meter scale *[e.g. Alsop and Marco, 2013]* to giant system, which are many kilometers thick and hundreds of kilometers long *[Peel et al. 1995]*.

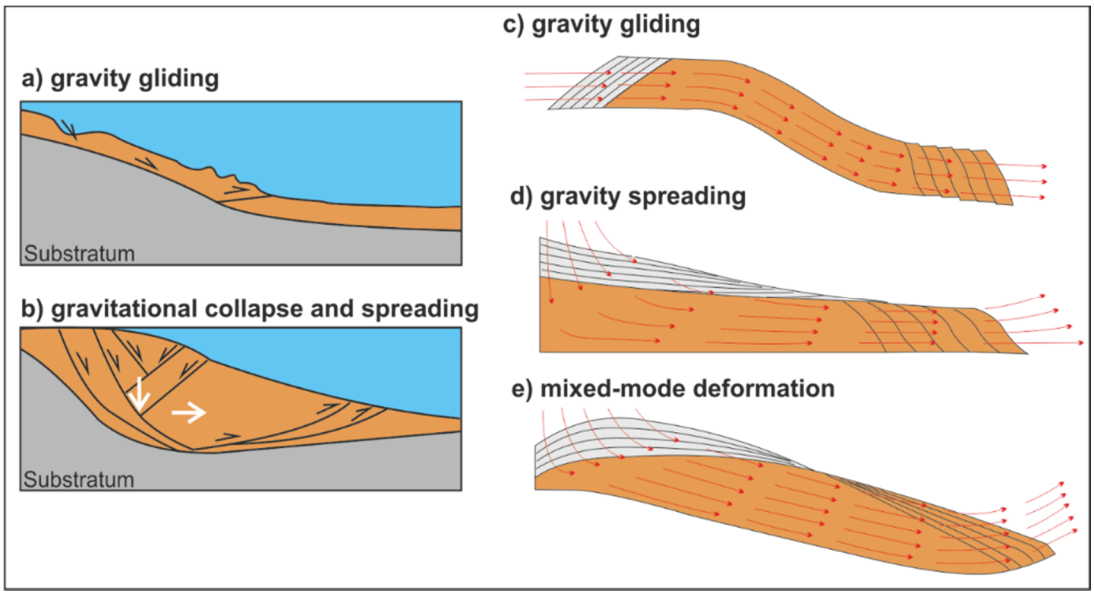

Figure 4: Types of passive continental margin Instability – spreading vs. gliding *[modified after Peel et al. 2014]* a) gravity gliding is defined as a process, where the system releases its energy parallel to its base by lowering the center of gravity due to a movement along an inclined surface b) gravitational collapse and spreading describes a system in which the system releases its energy due to vertical and lateral thinning of material. In this type, intense internal deformation and related faulting can be observed c) vector displacements during gravity gliding d) vector displacements during gravity spreading e) vector displacements in a mixed-mode deformation, in which spreading and gliding occur in a coherent system.

Two basic modes of gravity driven deformation were described by *de Jong and Scholten [1973]* and *Ramberg [1967; 1977; 1981]*, as they distinguish between gravity gliding and gravity spreading. Gravity gliding is classified by a system that releases its energy by lowering the center of gravity due to movement along an inclined surface *[Peel 2014]*; the internal structure of the sediments stays relatively intact. In this case, the system's energy is released parallel to the base (Fig. 4). Compressional features can be observed at the distal extends of such systems *[Peel 2014]* (Fig. 4). Gravity spreading is described by a system that releases its gravitational energy due to thinning of the material *[Peel 2014]*. The energy released by this process is mostly transferred to faulting and deformation. This phenomenon leads to the

strong overprint of extensional faults at continental margins, as the energy releases its energy perpendicular to the base (Fig. 4). In addition a mixed-mode deformation may be observed, where the continental margin is affected as well by gliding due to an inclined surface as spreading due its internal gravitational deformation *[Peel 2014]* (Fig. 4). In this case, the energy is released parallel and perpendicular to the base (Fig. 4). The definition by *Peel [2014]* does not distinguish between the lithology and rheology, as it can be applied to brittle, ductile, viscous or plastic material behavior. Whereas brittle deformation will lead to faulting, ductile deformation will be expressed by folding.

The processes of gravity gliding and spreading are relatively slow processes *[Peel 2014]* affecting the continental margin. Hence, they differ from massive mass transport events, which are faster events and do have a higher hazardous potential. However, gravity gliding and spreading on continental margins can lead to over-steepening and sediment weakening, which in turn can be a preconditioning factor for sudden failures and mass wasting on continental margins.

1.3 Tectonic setting and Geologic Evolution of Mount Etna

1.3.1 The Tectonic Setting at Mount Etna

Mt Etna, Europe's largest volcano, rises to a height of 3323 m (Fig. 2). The composite volcanic edifice sitting on top of continental crust *[Gvirtzman and Nur 1999]* is highly active with an eruption history of ~500 kyr *[Branca and Del Carlo 2004; Branca et al. 2004]*. Its recent volcanic unrest is documented by several eruptions per year during the past decades *[Branca and Del Carlo 2004]*.

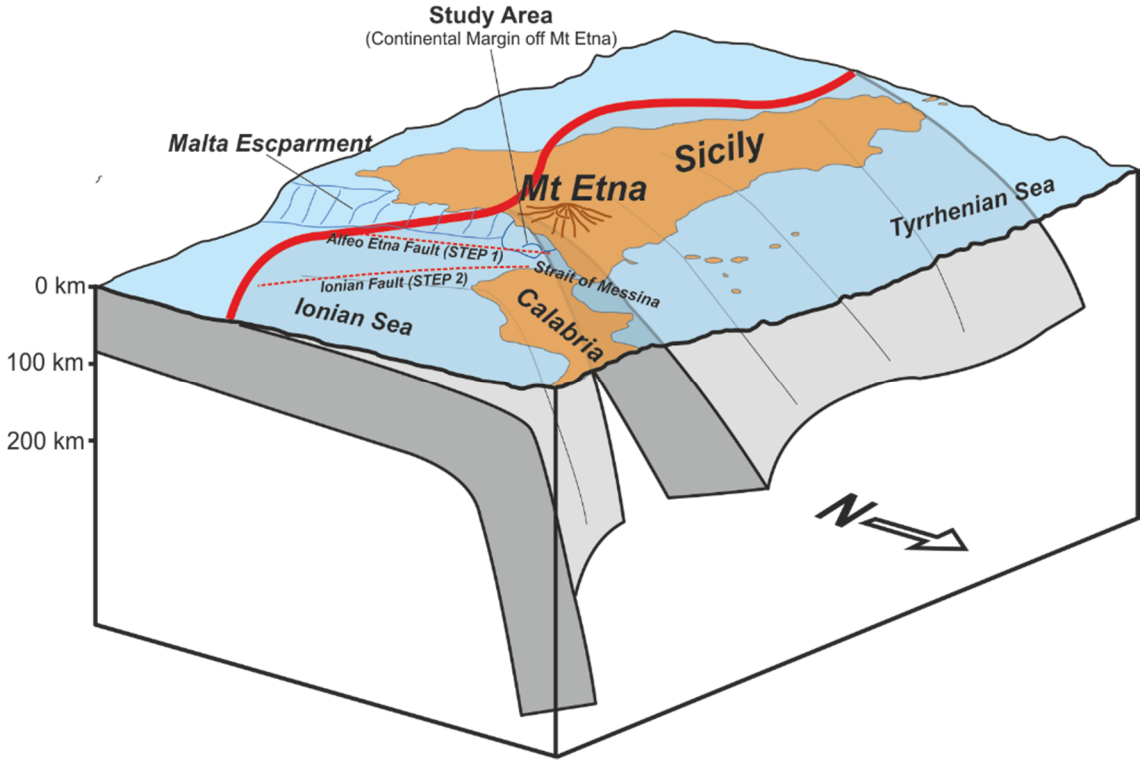

Figure 5: The geodynamic setting of Sicily and Calabria. The Calabrian subduction zone is characterized by a complex subduction. Between the two slabs of the Calabrian Subduction zone, a window opens due to oblique subduction. At this window, Mt Etna established on top of continental crust in East Sicily *[modified after Doglioni et al. 2012]*.

Mt Etna's geological setting is characterized by the complex compressional tectonics of the Appenine-Maghrebian Fold and Thrust Belt to the south (Fig. 6), and the northwest dipping Calabrian subduction zone to the southeast *[e.g. Doglioni et al. 2001; Doglioni et al. 2012]* (Figs. 1, 5, 6). The Malta Escarpment (Figs. 5, 6), a large northward trending crustal discontinuity between eastern Sicily's continental crust and the oceanic crust making up the Ionian Sea, is a prominent morphological feature at the seafloor. It can be traced southward and passes east of the Maltese Islands *[Lentini et al. 2006; Argnani and Bonazzi, 2005]*, thereby affecting the subduction regime underneath Calabria (Figs. 5, 6) *[e.g. Gvirtzman and Nur 1999; Argnani and Bonazzi 2005]*. Because of its regional importance as a deep-seated fault, a link between the Malta Escarpment and Mt Etna's edifice has been proposed *[Rust*

and Kershaw, 2000]. However, the complex structure and morphology of the continental margin (Fig. 6) makes it difficult to trace the Malta Escarpment as far north as Mt Etna's coastal offshore extension, and into the onshore volcanic edifice *[Argnani and Bonazzi 2005; Nicolich et al. 2000]*.

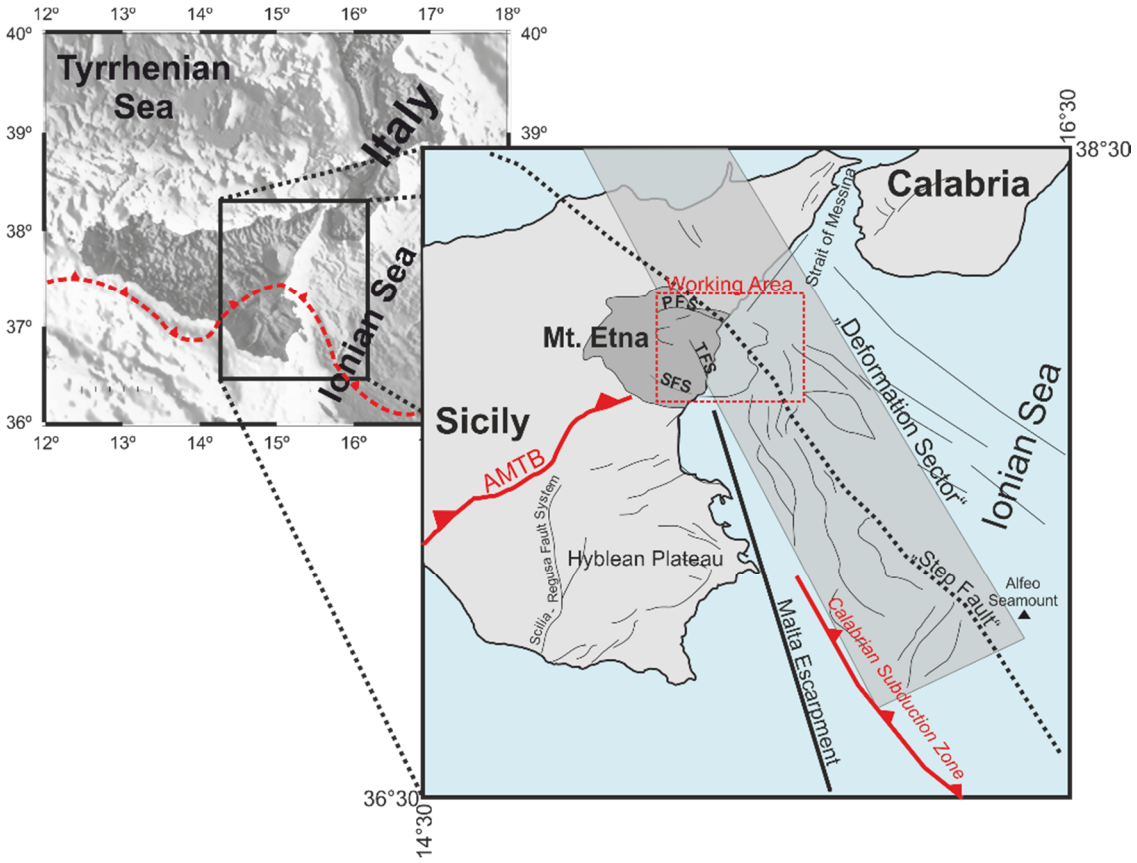

Figure 6: Overview map of the geographical setting of Sicily and Tectonic map of East Sicily modified after *Argnani [2014]*. Sicily is separated from the Italian mainland by the Strait of Messina, which opens towards the Ionian Sea east of Sicily. PFS=Pernicana-Provenzana-Fault-System, TFS=Timpe-Fault-System, SFS=Southern-Fault-System, AMTB=Appenine-Maghrebian Fold and Thrust Belt. The working area of this thesis is marked by a red box.

The NNE trending right-lateral Scilia-Regusa fault system, heading towards Mt Etna at the western boundary of the Hyblean Plateau (Fig. 6), was also invoked to explain the location of Mt Etna *[e.g. Lo Guidice and Rasà 1992]*. Furthermore, recent interpretations based on refraction and reflection seismic data favor the existence of a distinct southeast trending Subduction Transform Edge Propagator Fault (STEP-Fault), passing by Mt Etna's northern flank (Figs. 5, 6) *[Polonia et al. 2012; Gallais et al. 2013; Gallais et al. 2014]*. Such a fault is required to delimit the retreating Calabrian subduction front towards the southwest, and opening an asthenospheric window at sub-lithospheric depths. The proposed STEP-fault is somewhat oblique to the Malta Escarpment (Figs. 5, 6) *[Gallais et al. 2013]*. However, *Argnani [2014]* does not find indications for a distinct near-surface STEP-fault in a dense grid of seismic lines from offshore eastern Sicily. Instead, he suggests a 20-30 km wide corridor of SSE trending faults (Fig. 6) affecting the entire area from Alfeo Seamount to Sicily (Fig. 6) to be the surface expression of a deep crustal-scale structure, controlling the regional tectonics in this area *[Argnani 2014]*. *Argnani [2014]* bases his interpretation on a series of asymmetric half-grabens, bound to eastward dipping normal faults

[Hirn et al. 1997; Nicolich et al. 2000; Bianca et al. 1999, Argnani and Bonazzi, 2005]. These normal faults are proposed to have generated paleo-earthquakes like the 1693 Catania event *[Bianca et al. 1999; Argnani et al. 2012]*.

The entire region around Mt Etna is seismically highly active *[Orecchio et al. 2014]* (Fig. 7). Large earthquakes like the disastrous Messina 1908 event *[e.g. Pino et al. 2009]* occurred in the Strait of Messina north of Mt Etna. Furthermore, deep (20-30 km) compressive earthquakes, probably related to thrusting in the Appennine-Maghrebian Thrust Belt, have been recorded close to the volcano *[Lavecchia et al. 2007]*. Another set of seismic events (hypocenter depths <10km) were observed underneath the eastern flank of Mt Etna. This small scale variation in location and kinematics of seismic events leads to the interpretation that the stress field underneath Mt Etna is highly heterogeneous *[Cocina et al. 1997]*.

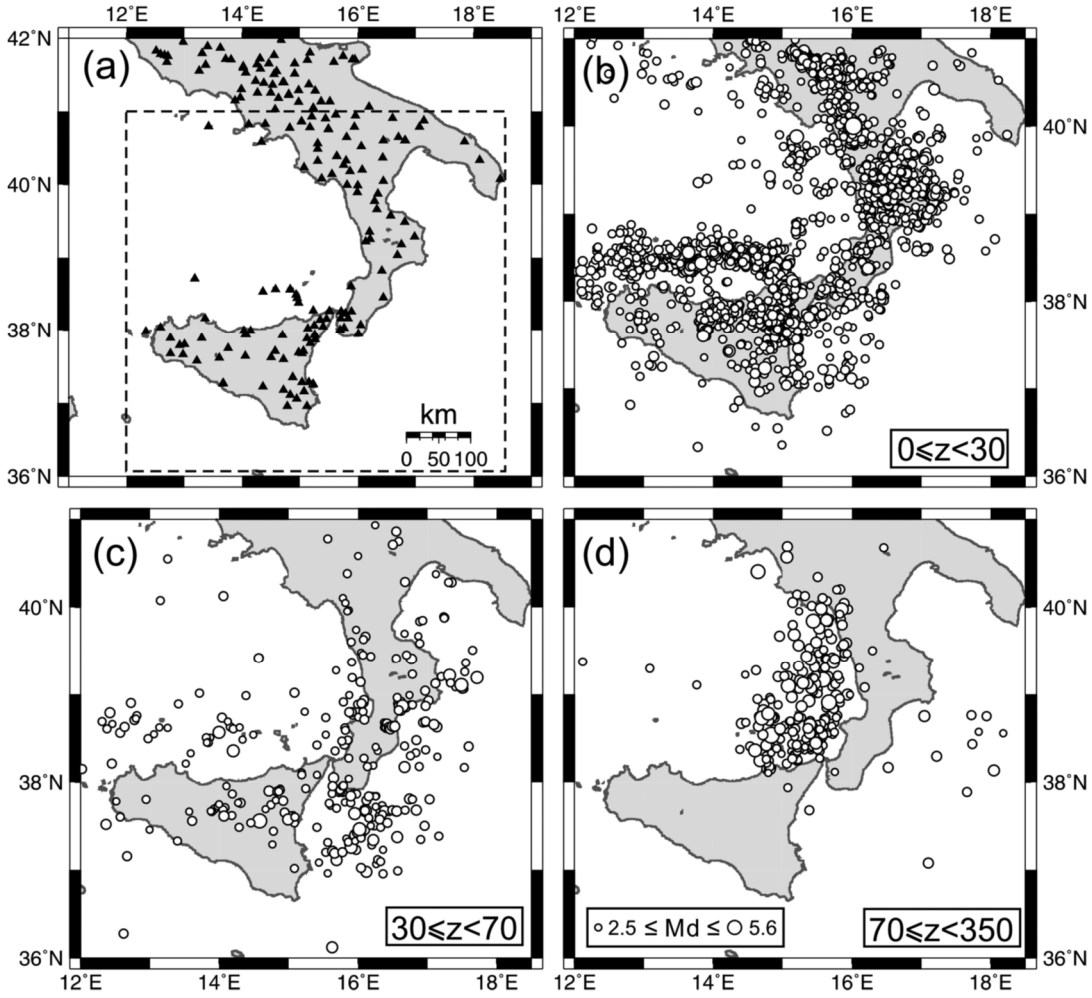

Figure 7: Epicenter locations of earthquakes duration magnitude $M_d \geq 2.5$ in Sicily and Calabria between January 1997 and May 2011 *[Orecchio et al. 2014]* a) Seismic stations in Southern Italy b) Seismicity from 0 to 30 km depth. c) Seismicity from 30 to 70 km depth. d) Seismicity from 70 to 350 km depth. Especially shallow seismic activity can be observed in the area at M Etna and its offshore continental margin.

1.3.2 The Geologic Evolution of Mount Etna

Compared with Earth's History, the ~500 kyr ongoing eruptive history, Mt. Etna can be characterized as a relatively young volcano *[Branca et al. 2004]*. It reveals different types of volcanism and coherent changes in its mineralogical expression over time; the volcano is still active.

The first period of Mt. Etna's eruptive history (~500-200 kyr BP) is characterized as a dispersed fissure-type volcanism with a tholeiitic affinity *[Branca et al. 2004]*. The areal extent of this proto-volcano is described as the northward extension of the Plio-Pleistocene Hyblean volcanism, which extended northwards to the Etnean region (Fig. 8a).

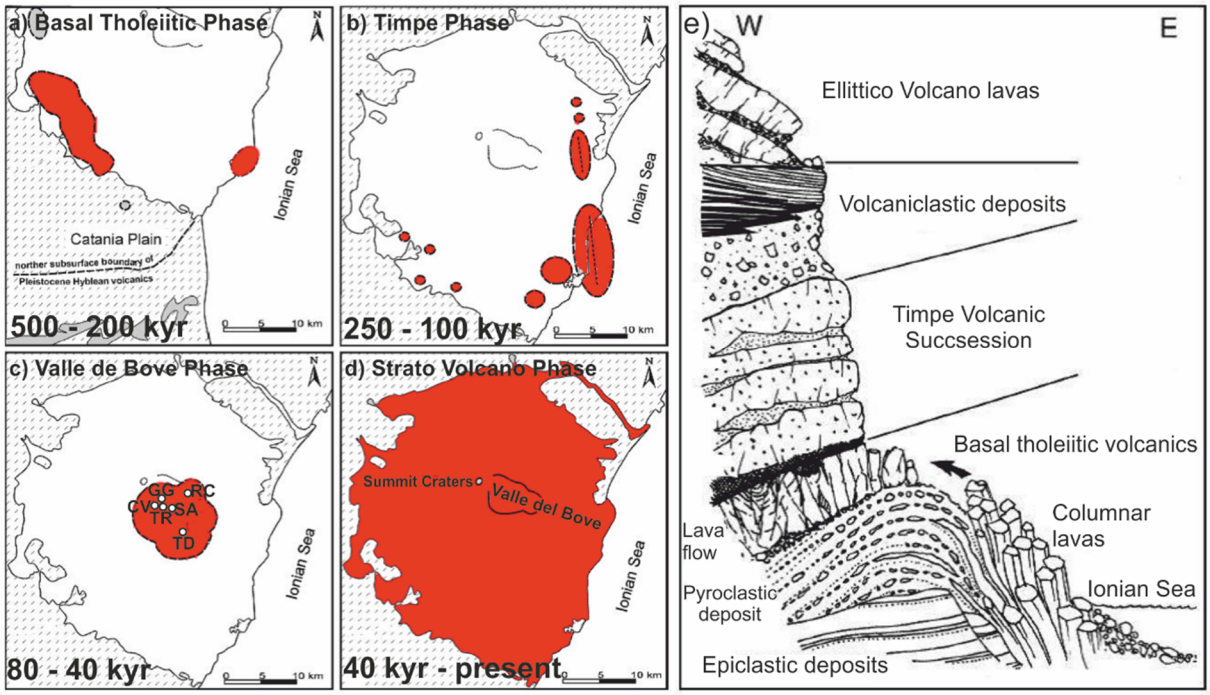

Figure 8: Evolutionary stages of Mt Etna during the last ~500 kyrs *[modified after Branca et al. 2004]* a) Basal Tholeiitic phase ~500-200 kyr b) Timpe phase ~250-100 kyr c) Valle del Bove volcanos phase ~80-40 kyr TR = Trifoglietto, GG = Giannicola Grande, SA = Salifizio, CV = Cuvigghiuni , RC = Rocche, TD = Tardeira d) Strato volcano phase <40 kyr. e) Schematic drawing of the volcanic succession outcropping at the Acireale Timpa fault *[Branca et al. 2004]*

The second phase of volcanism (~250-100 kyr BP) is defined by the onset of the Timpe eruptive activity, which concentrates along the Ionian coast at the NNW-SSE oriented Timpe Fault System; this period of activity did not build up major edifices (Fig. 8b). The first volcanic edifices, expressed as the nested volcano centers Tardeira and Rocche, were established during the Valle del Bove Crater Phase (80-40 kyr BP) by an eastward shift of the volcanism (Fig. 8c). A strong variation of the plumbing system created the southern Trifoglietto as well as the Giannicola Grande, Salifizio and Cuvigghiuni craters (Figs. 8, 9). The largest, and recently observable strato-volcano edifice is the Ellittico, which was created

during the stabilization of the plumbing system at Mt Etna and makes up the bulk of the present edifice. This phase was terminated with four major caldera forming plinian eruptions at ~15 kyr BP *[all after Branca et al. 2004]*.

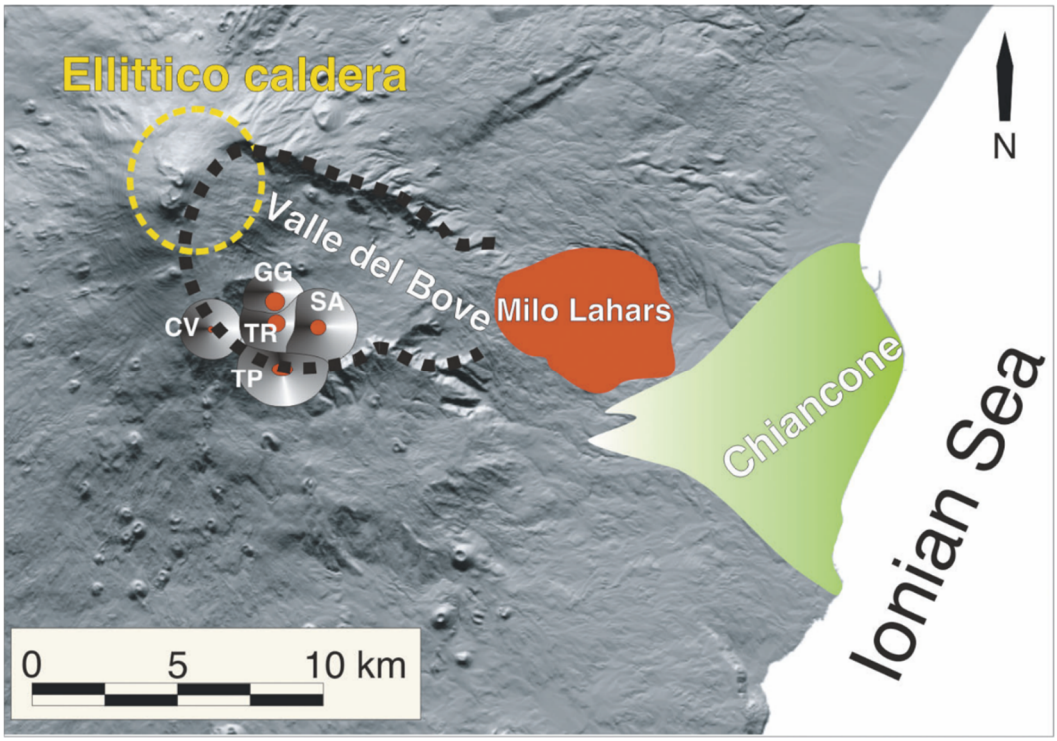

Figure 9: Valle de Bove scar and the Chiancone Fanglomerate, which was so far only mapped onshore. TR = Trifoglietto, GG = Giannicola Grande, SA= Salifizio, CV = Cuvigghiuni , TP = Tripodo *[Calvari et al. 2004]*

During the Holocene, the Mongibello volcano established on top of the ancient volcanic edifices. Its eruptive material covers an area of at least 85% of the recent volcano edifice and generated the recent appearance of Mount Etna. A major sector collapse, which created the Valle Del Bove scar, occurred ~8000 yr ago *[Calvari et al. 2004]*. The debris created by this collapse is known as the Chiancone fanglomerate, which can mostly be traced onshore directly adjacent to the Ionian coastline *[Calvari et al. 2004]*.

1.3.3 Volcano Edifice Instability at Mt Etna's eastern flank

Mt Etna's flank instability, first described in the early 1990's as gravitational instability by *Borgia et al. [1992]*, is one of the best-monitored and studied examples for volcano flank instability around the world. In the following years, evidence for both, episodic and continuous flank movement was reported *[e.g. Froger et al. 2001, Acocella et al. 2003, Bonforte and Puglisi 2003]*. With the help of a dense network of GPS and geodetic stations *[Lundgren et al. 2003; Puglisi et al. 2008; Bonforte et al. 2009; Neri et al. 2009]*, gas monitoring *[Neri et al. 2007; Bonforte et al. 2013]*, and geologic fieldwork *[Groppelli and Tibaldi 1999; Neri et al. 2004]*, it was possible to locate and characterize the instability of Mt Etna's eastern flank. The anatomy of the flank and related fault systems were assessed by means of Permanent Scatters analysis, which were used to characterize the main kinematic domains of the flank *[Bonforte et al. 2011]*.

The northern boundary of the moving flank is described as the left lateral Pernicana-Provenzana Fault (Figs. 10, 11, 12) with a continuous horizontal displacement of ~2.,8 cm/a *[Bonforte and Puglisi 2003]* that may accelerate during volcanic activity *[Bonforte et al. 2007]*. The Pernicana-Provenzana Fault system represents the fault system with the highest set of displacements at the edifice of Mt Etna (Fig. 10).

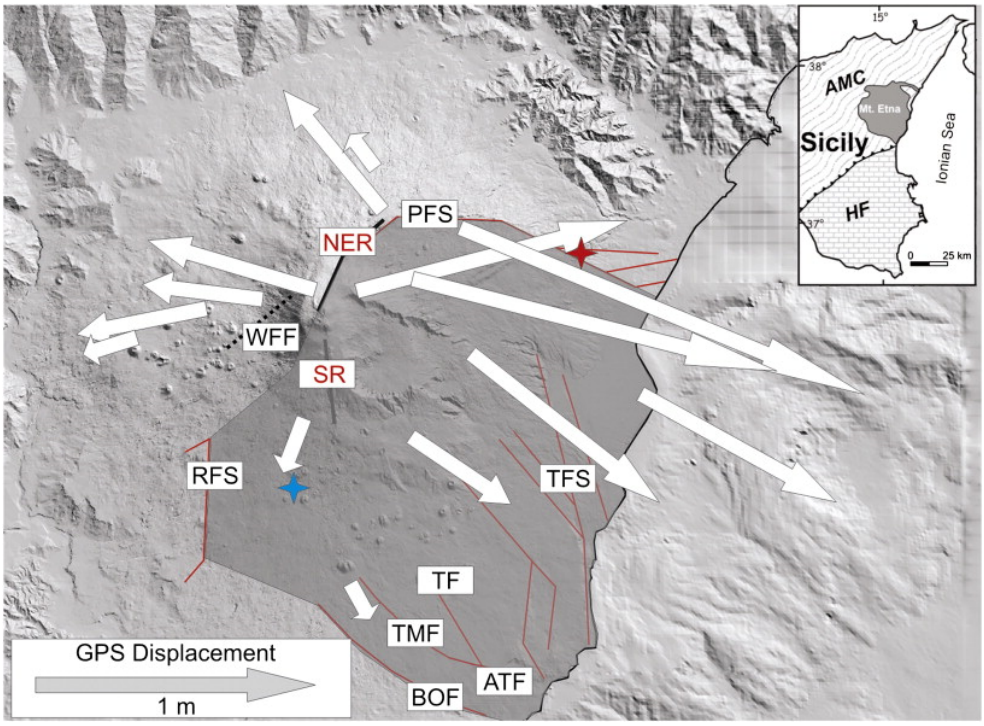

Figure 10: GPS Displacement of selected stations at the eastern and southern flank of Mt. Etna. The vectors represent the total displacements between 1993 and 2006 recorded at selected benchmarks (located at the beginning of each vector arrow) of the GPS network. Highest displacements can be observed at the northern region at the Pernicana-Provenzana Fault system at Mt Etna's eastern flank. PFS = Pernicana-Provenzana Fault System, TFS = Timpe Fault System, TMF= Tremestieri Fault, TF=Trecastagni Fault *[Acocella and Puglisi 2013]*.

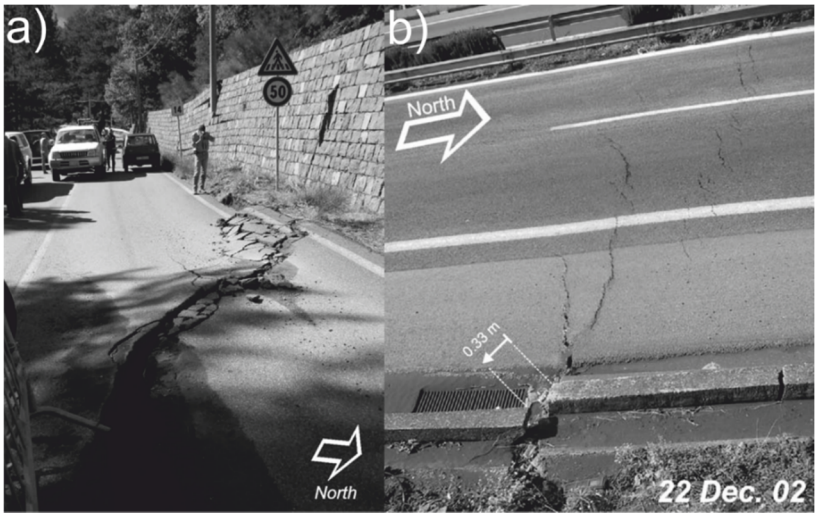

Figure 11: a) Road at the westernmost portion of the Pernicana-Provenzana Fault at Mt Etna's northern flank on November 12th, 2002. Total horizontal displacement of the fractures is >1.25 m, with a vertical component of ~0.5 m *[Neri et al. 2004]*. b) The eastern extends of the Pernicana-Provenzana Fault at the A18 Catania Messina Highway. Total vertical displacement at the border of the highway, 0.33 m (of which 0.05 m is related to movement through December 22nd 2002 and 0.28 m is due to previous episodes since 1971, when the highway was constructed) *[Neri et al. 2004]*

The Timpe Fault System (Figs. 10, 12) separates the NE-Block to the Medium East Block and is well documented by geodetic and InSAR measurements onshore (Fig. 12) *[Bonforte et al. 2011]*. The southern boundary (Fig. 10) of the moving flank is only constrained by InSAR measurements and Soil Gas emissions and is described by the faults of the Tremestieri-Trecastagni Fault System (Fig. 10) *[Froger et al. 2001; Bonforte et al. 2013]*.

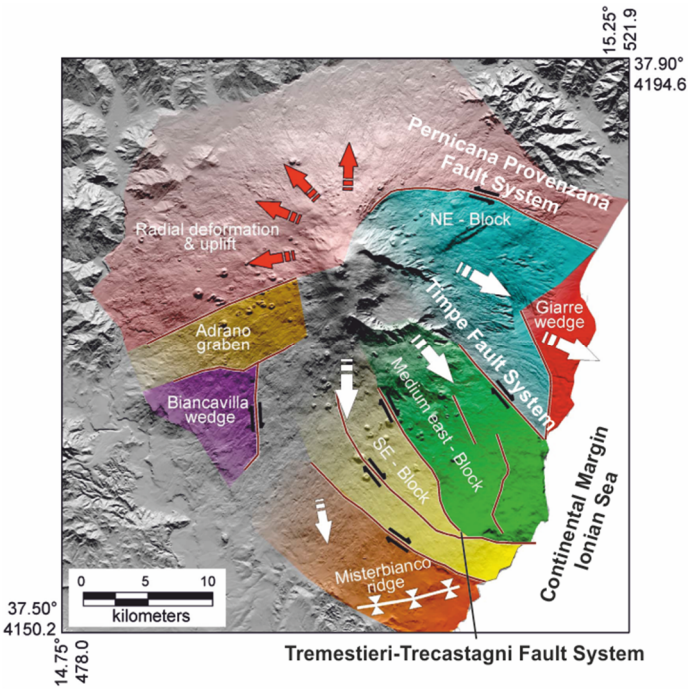

Figure 12: Main Kinematic domains at the edifice of Mt Etna *[modified after Bonforte et al. 2011]*. Northern boundary of the moving flank: Pernicana-Provenzana Fault System. Southern boundary of the moving flank: Tremestieri-Trecastagni Fault System. The Timpe Fault System can be observed at the central part of Mt Etna's eastern flank.

1.3.4 Continental Margin Instability offshore Mt Etna

Mt Etna established its edifice directly at the Ionian coastline of eastern Sicily. In comparison to the Ionian continental margin north and south of the volcano edifice, a clear bulging and extension can be observed at the continental margin directly in front of Mt Etna by its morphological expression (Fig. 13) *[Chiocci et al. 2011]*. In contrast to the well-studied onshore volcano edifice of Mt Etna *[e.g. Bonforte et al. 2011]*, only few information is available concerning the continental margin offshore east of Mt Etna. A first multi-beam bathymetric map of the Ionian Sea illustrated the major morphologic features in the area off Mt Etna *[Marani et al. 2004]*. The first detailed interpretation of the continental margin's seafloor morphology was carried out by *Chiocci et al. [2011]*. Next to deeply incised valleys and gullies, a prominent bulge, between Fiumefreddo Valley and Catania Canyon (Fig. 13), was recognized. This bulging of the continental margin can only be observed directly in front of Mt Etna and cannot be traced further north or south *[Chiocci et al. 2011; Argnani et al. 2013]*.

Argnani et al. [2013] interpret the bulge at the continental margin as the northernmost extent of the Hyblean Foreland, which is the onshore region south of Catania (Fig. 1). However, *Chiocci et al. [2011]* interpret the bulge to be a response to intrusive inflation of a pre-Etnean continental margin. By using high-resolution multi-beam bathymetry, *Chiocci et al. [2011]* proposed the idea of an upslope propagating instability, caused by a large scale mass wasting event offshore Mt. Etna, creating a prominent amphitheater (Fig. 13) offshore the village of Riposto (Fig. 13). Reflection seismic data indicate that the offshore area around the volcano is dominated by extensional faulting with thrust faults close to the coast and towards the distal extends of the continental margin *[Argnani et al. 2013]*. However, *Argnani et al. [2013]* interpret the bulge to be generated rather by thrusting than to a simple inflation due to magmatic intrusion related to Mt Etna. So far it was not possible to determine the limits of instability, affecting the continental margin *[Argnani et al. 2013]*.

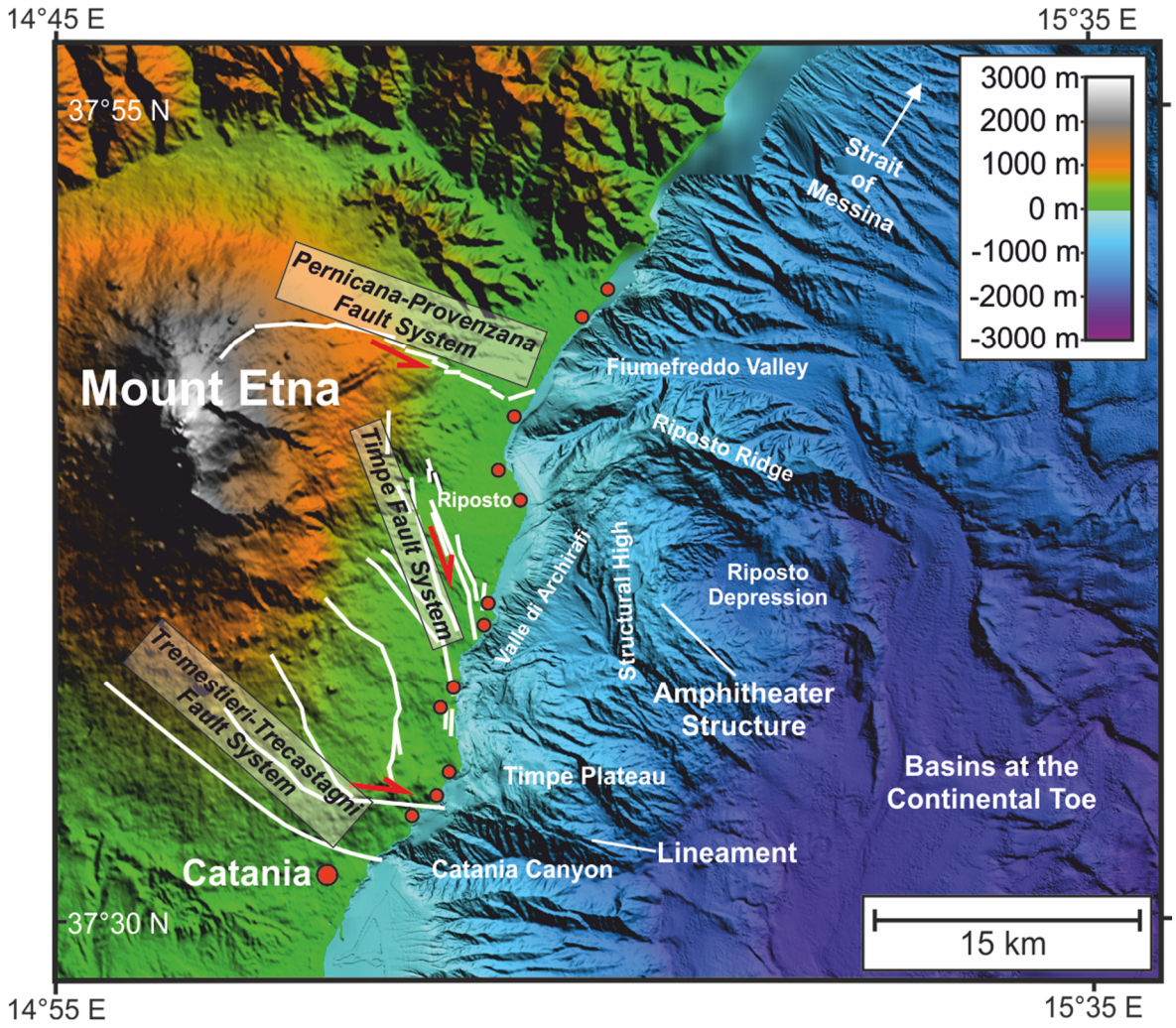

Figure 13: Mt Etna and its adjacent continental margin. The continental margin is characterized by bulging, what cannot be observed at the continental margins north and south of Mt Etna's edifice. The continental margin is strongly overprinted by channels and gullies. The continental margin can be subdivided into three major regions. The southern region is characterized by the Timpe Plateau, which is strongly overprinted by gullies and channels. It is terminated towards the south by Catania Canyon. The central region shows the morphological expressions of the funnel shaped Valle di Archirafi, a structural high with prominent ridges and a massive amphitheater structure with its enclosed Riposto Depression. The northern region is marked by the E-W trending anticline of Riposto Ridge. In front of the continental margin, the seafloor morphology flattens abruptly. In this region, large sedimentary basins can be observed. The entire continental margin and its structures will be described and examined in detail in chapters 5, 6 and 7. The digital elevation model was created by using the SRTM dataset *[Farr et al. 2007]*, the MaGIC dataset *[Chiocci and Ridente 2011]* and the bathymetry, acquired during RV Meteor Cruise M86/2 – Map shown with UTM Projection.

1.3.5 Recent studies on the origin of volcano edifice and continental margin instability on- and offshore Mt Etna

Instability can be driven by magma pressure, lack of buttressing support, loading of the edifice on a weak basement, increasing pore pressure associated with volcanism, dike emplacement, and/or tectonic stress *[e.g. Voight and Elsworth 1997; McGuire 1996]*. Explaining flank instability of Mt Etna is particularly challenging as deformation due to magma overpressure reaches its maximum at the summit, whereas the larger subsidence and seaward movements are recorded along the coast *[Acocella and Puglisi 2013]*. Moreover, displacement measurements are yet limited to the onshore part of the volcano, while the continental margin, affected by the volcano buildup, lies offshore in the Ionian Sea. Recent hypotheses that have been brought forward to explain instability of Mt Etna's eastern flank include:

i) Magmatically induced: Flank dynamics have been interpreted as a passive effect of gravity instability and magma intrusion *[e.g. Bonforte and Puglisi 2003]*. More recently, *Le Corvec et al. [2014]* used analogue modelling to shed light on the complex interplay interaction of magmatism, flank instability, and tectonic activity. Their model not only explains the different spatial displacement rates, but also temporally variable activity of the Timpe Fault System before, during and after eruptions.

ii) Missing mass: *Chiocci et al. [2011]* analyze bathymetric data offshore Mt Etna. The authors find that the entire continental margin is affected by large deformations that develop from the base of the slope up to the shoreline. Moreover, both submarine instability and subaerial flank sliding are bounded by two regional tectonic lineaments. Hence, they propose that continental margin instability drives the eastern flank's seaward movement.

iii) Basement landslide: *Nicolosi et al. [2014]* use magnetic data to model the non-volcanic strata that is underlying Mt Etna. Their results indicate that Mt Etna is growing on a pre-existing basement landslide and the authors show that its eastern flank moves coherently with the underlying landslide.

References

Acocella, V., Behncke, B., Neri, M., D'Amico, S., 2003. Link between major flank slip and 2002–2003 eruption at Mt. Etna (Italy). Geophysical Research Letters 30. 2286. DOI:10.1029/2003GL018642

Acocella, V., Puglisi, G., 2013. How to cope with volcano flank dynamics? A conceptual model behind possible scenarios for Mt. Etna. Journal of Volcanology and Geothermal Research 251. 137–148. DOI:10.1016/j.jvolgeores.2012.06.016

Alsop, G.I., Marco, S., 2013. Seismogenic slump folds formed by gravity-driven tectonics down a negligible subaqueous slope. Tectonophysics 605. 48–69.

Argnani, A., Bonazzi, C., 2005. Malta Escarpment fault zone offshore eastern Sicily: Pliocene-Quaternary tectonic evolution based on new multichannel seismic data. Tectonics 24. DOI:10.1029/2004TC001656

Argnani A., Chiocci F.L., Tinti S., Bosman A., Lodi M.V., Pagnoni G., Zaniboni F., 2009. Comment on "On the cause of the 1908 Messina tsunami, southern Italy" by Andrea Billi et al. Geophysical Research Letters 36. L13307.

Argnani, A., Armigliato, A., Pagnoni, G., Zaniboni, F., Tinti, S., Bonazzi, C., 2012. Active tectonics along the submarine slope of south-eastern Sicily and the source of the 11 January 1693 earthquake and tsunami. Natural Hazards Earth System Sciences. 12. 1311–1319. DOI:10.5194/nhess-12-1311-2012

Argnani, A., Mazzarini, F., Bonazzi, C., Bisson, M., Isola, I., 2013. The deformation offshore of Mount Etna as imaged by multichannel seismic reflection profiles. Journal of Volcanology and Geothermal Research 251. 50–64. DOI:10.1016/j.jvolgeores.2012.04.016

Argnani, A., 2014. Comment on the article "Propagation of a lithospheric tear fault (STEP) through the western boundary of the Calabrian accretionary wedge offshore eastern Sicily (Southern Italy)" by Gallais et al., 2013 Tectonophysics. Tectonophysics 610. 195–199. DOI:10.1016/j.tecto.2013.06.035

Baratta, M., 1910. La Catastrofe Sismica Calabro-Messinese (28 Dicembre 1908). Soc. Geogr. Ital., Rome. 496.

Begét, J. E., Kienle, J., 1992. Cyclic formation of debris avalanches at Mount St Augustine volcano. Nature 356. 701–704. DOI: 10.1038/356701a0

Bianca, M., Monaco, C., Tortorici, L., Cernobori, L., 1999. Quaternary normal faulting in southeastern Sicily (Italy): a seismic source for the 1693 large earthquake. Geophysical Journal International 139. 370–394. DOI:10.1046/j.1365-246x.1999.00942.x

Billi A., Funiciello R., Minelli L., Faccenna C., Neri G., Orecchio B., Presti D., 2008. On the cause of the 1908 Messina tsunami, Southern Italy. Geophysical Research Letters 35; L06301 DOI:10.1029/2008GL033251

Bonforte, A., Puglisi, G., 2003. Magma uprising and flank dynamics on Mount Etna volcano, studied using GPS data (1994–
1995). Journal of Geophysical Research 108. 2153. DOI:10.1029/2002JB001845.

Bonforte, A., Branca, S., Palano, M., 2007. Geometric and kinematic variations along the active Pernicana fault: Implication for the dynamics of Mount Etna NE flank (Italy). Journal of Volcanology and Geothermal Research 160. 210–222. DOI:10.1016/j.jvolgeores.2006.08.009

Bonforte, A., Gambino, S., Neri, M., 2009. Intrusion of eccentric dikes: The case of the 2001 eruption and its role in the dynamics of Mt. Etna volcano. Tectonophysics 471. 78–86. DOI:10.1016/j.tecto.2008.09.028

Bonforte, A., Guglielmino, F., Coltelli, M., Ferretti, A., Puglisi, G., 2011. Structural assessment of Mount Etna volcano from Permanent Scatterers analysis. Geochemistry Geophysics Geosystems 12. DOI:10.1029/2010GC003213

Bonforte, A., Federico, C., Giammanco, S., Guglielmino, F., Liuzzo, M., Neri, M., 2013. Soil gases and SAR measurements reveal hidden faults on the sliding flank of Mt. Etna (Italy). Journal of Volcanology and Geothermal Research 251. 27–40. DOI:10.1016/j.jvolgeores.2012.08.010

Borgia, A., Ferrari, L., Pasquarè, G., 1992. Importance of gravitational spreading in the tectonic and volcanic evolution of Mount Etna. Nature 357. 231–235. DOI:10.1038/357231a0

Branca, S., Del Carlo, P., 2004. Eruptions of Mt Etna during the past 3,200 years: a revised compilation integrating the historical and stratigraphic records. Bonaccorso, A., Calvari, S., Coltelli, M., Del Negro, C., Falsaperla, S. (Eds.). Mt. Etna: Volcano Laboratory. Geophysical Monograph Series 143. American Geophysical Union, Washington, D.C.. 1–27.

Branca, S., Coltelli, M., Groppelli, G., 2004. Geological evolution of Etna volcano. Bonaccorso, A., Calvari, S., Coltelli, M., Del Negro, C., Falsaperla, S. (Eds.), Mt. Etna: Volcano Laboratory. Geophysical Monograph Series, 143. American Geophysical Union, Washington, D.C.. 49–63.

Bucher, W.H., 1956. Role of gravity in orogenesis. Geological Society of America Bulletin. 67, 1295–1318.

Calvari, S., Tanner, L. H., Groppelli, G., Norini, G., 2004. Valle del Bove, eastern flank of Etna Volcano: A comprehensive model for the opening of the depression and implications for future hazards. Alessandro Bonaccorso, Sonia Calvari, Mauro Coltelli, Ciro Del Negro und Susanna Falsaperla (Eds.): Mt. Etna: Volcano Laboratory, Bd. 143. Washington, D. C: American Geophysical Union (Geophysical monograph series). 65–75.

Cervelli, P., Segall, P., Johnson, K., Lisowski, M., Miklius, A., 2002. Sudden aseismic fault slip on the south flank of Kilauea volcano. Nature 415. 1014–1018. DOI: 10.1038/4151014a

Chiocci, F.L., Coltelli, M., Bosman, A., Cavallaro, D., 2011. Continental margin large-scale instability controlling the flank sliding of Etna volcano. Earth and Planetary Science Letters 305. 57–64. DOI:10.1016/j.epsl.2011.02.040

Chiocci, F.L., Ridente, D., 2011. Regional-scale seafloor mapping and geohazard assessment. The experience from the Italian project MaGIC (Marine Geohazards along the Italian Coasts). Marine Geophysical Research 32. 13–23. DOI: 10.1007/s11001-011-9120-6

Christiansen, R.I., Peterson, D.W., 1981. Chronology of the 1980 eruptive activity. In: Lipman, P. W. & Mullineaux, D. R. (Eds) The 1980 eruptions of Mount St Helens. US Geological Survey Professional Paper 1250. 17-30.

Cocina, O., Neri, G., Privitera, E., Spampinato, S., 1997. Stress tensor computations in theMount Etna area (Southern Italy) and tectonic implications. Journal of Geodynamics 23. 109–127. DOI:10.1016/S0264-3707(96)00027-0

Day, S.J., Carracedo, J.C, Guillou, H., Gravestock, P., 1999. Recent structural evolution of the Cumbre Vieja volcano, La Palma, Canary Islands: volcanic rift zone reconfiguration as a precursor to volcano flank instability? Journal of Volcanology and Geothermal Research 94. 135–167. DOI: 10.1016/S0377-0273(99)00101-8

De Jong, K.A., Scholten, R., 1973. Preface. In: De Jong, K.A., Scholten, R. (Eds.), Gravity and Tectonics. John Wiley and Sons, New York. ix–xviii.

Doglioni, C., Innocenti, F., Mariotti, G., 2001. Why Mt Etna?. Terra Nova 13. 25–31. DOI:10.1046/j.1365-3121.2001.00301.x

Doglioni, C., Ligi, M., Scrocca, D., Bigi, S., Bortoluzzi, G., Carminati, E., et al., 2012. The tectonic puzzle of the Messina area (Southern Italy): Insights from new seismic reflection data. Scientific Reports 2. DOI: 10.1038/srep00970

Elliott, D., 1976. The energybalance and deformation mechanisms of thrust sheets. Philosophical Transactions of the Royal Society A 283. 289–312.

Farr, T. G., Rosen, A., Caro, E., Crippen, R., Duren, R., Hensley, S., Kobrick, S., Rodriguez, E., Roth, L., Seal, D., Shaffer, S., Shimada, J., Umland, J., Werner, M., Oskin, M., Burbank, D., Alsdorf, D., 2007. The Shuttle Radar Topography Mission. Reviews of Geophysics 45. DOI:10.1029/2005RG000183

Favalli, M., Boschi, E., Mazzarini, F., Pareschi, M.T., 2009. Seismic and landslide source of the 1908 Straits of Messina tsunami (Sicily, Italy). Geophysical Research Letters 36. DOI: 10.1029/2009GL039135.

Firth, C., Stewart, I., McGuire, W.J., Kershaw, S., Vita-Finzi, C., 1996, Coastal elevation changes in eastern Sicily: implications for volcano instability at Mount Etna. Geological Society, London, Special Publications 110. 153–167. DOI:10.1144/GSL.SP.1996.110.01.12

Froger, J.L., Merle, O., Briole, P., 2001. Active spreading and regional extension at Mount Etna imaged by SAR interferometry. Earth and Planetary Science Letters 187. 245–258. DOI:10.1016/S0012-821X(01)00290-4

Gallais, F., Graindorge, D., Gutscher, M.A., Klaeschen, D., 2013. Propagation of a lithospheric tear fault (STEP) through the western boundary of the Calabrian accretionary wedge offshore eastern Sicily (Southern Italy). Tectonophysics 602. 141–152. DOI:10.1016/j.tecto.2012.12.026

Gallais, F., Graindorge, D., Gutscher, M.A., 2014. Reply to comment on the article "Propagation of a lithospheric tear fault (STEP) through the western boundary of the Calabrian accretionary wedge offshore eastern Sicily (Southern Italy)" by Gallais et al., 2013 Tectonophysics. Tectonophysics 610. 200–203. DOI:10.1016/j.tecto.2013.10.012.

Groppelli, G., Tibaldi, A., 1999. Control of rock rheology of deformation style and sliprate along the active Pernicana fault, Mt. Etna, Italy. Tectonophysics 305. 521–537. DOI:10.1016/S0040-1951(99)00035-9

Gvirtzman, Z., Nur, A., 1999. The formation of Mount Etna as the consequence of slab rollback. Nature 401. 782–785. DOI:10.1038/44555

Jacques, E., Monaco, C., Tapponnier, P., Tortorici, L., Winter, T., 2001. Faulting and earthquake triggering during the 1783 Calabria seismic sequence. Geophysical Journal International 147. 499–516. DOI:10.1046/j.0956-540x.2001.01518.x

Harders R., Kutterolf S., Hensen C., Moerz T., Brückmann W., 2010. Tephra layers: A controlling factor on submarine translational sliding?. Geochemistry Geophysics Geosystems 11 5. 1-18. DOI:10.1029/2009GC002844

Hirn, A., Nicolich, R., Gallart, J., Laigle, M., Cernobori, L., ETNASEIS Scientific Group, 1997. Roots of Etna volcano in faults of great earthquakes. Earth and Planetary Science Letters 148. 171–191. DOI:10.1016/S0012-821X(97)00023-X

Kehle, K.O., 1970. Analysis of gravity sliding and orogenic translation. Geological Society of America Bulletin 81. 1641–1664.

Kokelaar, P., Romagnoli, C., 1995. Sector collapse, sedimentation and clast population evolution at an active island-arc volcano: Stromboli, Italy. Bulletin of Volcanology 57. 240–262. DOI:10.1007/BF00265424

Krastel, S., Schmincke, H., Jacobs, C.L., Rihm, R., Le Bas, T.P., Alibés, B., 2001. Submarine landslides around the Canary Islands. Journal Geophysical Research. 106. DOI:10.1029/2000JB900413

Lavecchia, G., Ferrarini, F., De Nardis, R., Visini, F., Barbano, M.S., 2007. Active thrusting as a possible seismogenic source in Sicily (sourthern Italy). Some insights from integrated structural-kinematic and seismological data. Tectonophysics 445. 145–167. DOI:10.1016/j.tecto.2007.07.007

Le Corvec, N., Walter, T.R., Ruch, J., Bonforte, A., Puglisi, G., 2014. Experimental study of the interplay between magmatic rift intrusion and flank instability with application to the 2001 Mount Etna eruption. Journal of Geophysical Research Solid Earth. DOI: 10.1002/2014JB011224.

Lentini, F., Carbone, S., Guarnieri, P., 2006. Collisional and postcollisional tectonics of the Apenninic-Maghrebian orogen (southern Italy). Dilek, Y., Pavlides, S. (Eds.), Postcollisional Tectonics and Magmatism in the Mediterranean Region and Asia. Special Paper - Geological Society of America 409. 57–81. DOI:10.1130/2006.2409(04)

Lipman, P.W., Mullineaux, D. (Eds.). 1981. The 1980 eruptions of Mount St Helens. US Geological Survey Professional Paper. 1250.

Lo Giudice, E., Rasà, R., 1992. Very shallow earthquakes and brittle deformation in active volcanic areas: the Etnean region as an example. Tectonophysics 202. 257–268.

Lundgren, P., Berardino, P., Coltelli, M., Fornaro, G., Lanari, R., Puglisi, G., Sansosti, E., Tesauro, M., 2003. Coupled magma chamber inflation and sector collapse slip observed with synthetic aperture radar interferometry on Mt. Etna volcano. Journal of Geophysical Research 108. 2247, DOI:10.1029/2001JB000657.

Marani, M.P., Gamberi, F., Bortoluzzi, G., Carrara, G., Ligi, M., Penitenti, D., 2004. Seafloor bathymetry of the Ionian Sea. In: Marani, M.P., Gamberi, F., Bonatti, E. (Eds.), From Seafloor to Deep Mantle: Architecture of the Tyrrhenian Backarc Basin: Memorie Descrittive della Carta Geologica d'Italia 44. Plate 3. Roma, System Cart.

Masson, D. G., Watts, A.B., Gee, M.J.R., Urgeles, R., Mitchell, N.C., Le-Bas, T.P., Canals, M., 2002. Slope failures on the flanks of the western Canary Islands. Earth-Science Review 57. 1-35. DOIi:10.1016/S0012-8252(01)00069-1

McGuire, W.J., Pullen, A.D., Saunders, S.J., 1990. Recent dyke-induced large-scale block movement at Mount Etna and potential slope failure. Nature 343. 357-359.

McGuire, W.J., Murray, J.B., Pullen, A.D., Saunders, S.J., 1991. Ground deformation monitoring at Mount Etna; evidence for dyke emplacement and slope instability. Journal of the Geological Society, London 148. 577-583.

McGuire, W.J., 1996. Volcano instability: a review of contemporary themes. Geological Society, London, Special Publications 110. 1–23. DOI: 10.1144/GSL.SP.1996.110.01.01

Monaco, C., Tortorici, L., 2000. Active faulting in the Calabrian arc and eastern Sicily. Journal of Geodynamics 29. 407–424. DOI: 10.1016/S0264-3707(99)00052-6

Moore, J.G., Clague, D.A., Holcomb, R.T., Lipman, P.W., Normark, W.R., Torresan, M.E., 1989. Prodigious submarine landslides on the Hawaiian Ridge, Journal of Geophysical Research 94. 17. 465-484.

Morley, C.K., King, R., Hillis, R., Tingay, M., Backe, G., 2011. Deepwater fold and thrust belt classification, tectonics, structure and hydrocarbon prospectivity: A review. Earth-Science Reviews 104. 41–91. DOI:10.1016/j.earscirev.2010.09.010

Münn, S., Walter, T.R., Klügel, A., 2006. Gravitational spreading controls rift zones and flank instability on El Hierro, Canary Islands. Geological Magazine 143. 257. DOI: 10.1017/S0016756806002019

Murray, J.B., Voight, B., 1996. Slope stability and eruption prediction on the eastern flank of Mount Etna. Geological Society, London, Special Publications 110.

Neri, M., Acocella, V., Behncke, B., 2004. The role of the Pernicana Fault System in the spreading of Mt. Etna (Italy) during the 2002–2003 eruption. Bulletin of Volcanology 66, 417–430. DOI:10.1007/s00445-003-0322-x

Neri, M., Guglielmino, F., Rust, D., 2007. Flank instability on Mount Etna: radon, radar interferometry and geodetic data from the southern boundary of the unstable sector. Journal of Geophysical Research 112. DOI:10.1029/2006JB004756

Neri, M., Casu, F., Acocella, V., Solaro, G., Pepe, S., Berardino, P., Sansosti, E., Caltabiano,T., Lundgren, P., Lanari, E., 2009. Deformation and eruptions at Mt. Etna (Italy): alesson from 15 years of observations. Geophysical Research Letters 36. L02309. DOI:10.1029/2008GL036151

Nicolich, R., Laigle, M., Hirn, A., Cernobori, L., Gallart, J., 2000. Crustal structure of the Ionian margin of Sicily: Etna volcano in the frame of regional evolution. Tectonophysics 329. 121–139. DOI:10.1016/S0040-1951(00)00192-X

Nicolosi, I., D'Ajello Caracciolo, F., Branca, S., Ventura, G., Chiappini, M., 2014. Volcanic conduit migration over a basement landslide at Mount Etna (Italy). Scientific Reports 4. DOI:10.1038/srep05293

Orecchio, B., Presti, D., Totaro, C., Neri, G., 2014. What earthquakes say concerning residual subduction and STEP dynamics in the Calabrian Arc region, south Italy. Geophysical Journal International 199. 1929–1942. DOI: 10.1093/gji/ggu373

Pareschi, M.T., Boschi, E., Mazzarini, F., Favalli, M., 2006. Large submarine landslides offshore Mt. Etna. Geophysical Research Letters 33. DOI:10.1029/2006GL026064

Peel, F.J., Travis, C.J., Hossack, J.R., 1995. Genetic structural provinces and salt tectonics of the Cenozoic offshore US Gulf of Mexico: a preliminary analysis, M.P.A. Martin, D.G. Roberts, S. Snelson (Eds.), Salt Tectonics: A Global Perspective. AAPG Memoir 65. 153–175.

Peel, F.J., 2014. The engines of gravity-driven movement on passive margins: Quantifying the relative contribution of spreading vs. gravity sliding mechanisms. Tectonophysics 633. 126–142. DOI:10.1016/j.tecto.2014.06.023

Pino, N.A., Piatanesi, A., Valensise, G., Boschi, E., 2009. The 28 December 1908 Messina Straits earthquake (Mw 7.1): a great earthquake throughout a century of seismology. Seismological Research Letters 80. 243–259. DOI:10.1785/gssrl.80.2.243

Polonia, A., Torelli, L., Gasperini, L., Mussoni, P., 2012. Active faults and historical earthquakes in the Messina Straits area (Ionian Sea), Natural Hazards and Earth System Sciences 12. 2311-2328. doi:10.5194/nhess-12-2311-2012

Puglisi, G., Bonforte, A., Ferretti, A., Guglielmino, F., Palano, M., Prati, C., 2008. Dynamicsof Mount Etna before, during, and after the July–August 2001 eruption inferred from GPS and differential synthetic aperture radar interferometry data. Journal of Geophysical Research 113. B06405. DOI: 10.1029/2006JB004811

Ramberg, H., 1967. Gravity, Deformation and the Earth's Crust. Academic Press, London. 217.

Ramberg, H., 1977. Some Remarks on the Mechanism of Nappe Movement. Geol. Foremingen. Stockholm Forhandlingar. 110– 117.

Ramberg, H., 1981. The role of gravity in orogenic belts. McClay, K.R., Price, N.J. (Eds.), Thrust and Nappe Tectonics. Special Publications of the Geological Society of London 9. 125–140.

Rasa, R., Azzaro, R., Leonardi, O., 1996. Aseismic creep on faults and flank instability at Mount Etna volcano, Sicily. Geological Society, London, Special Publications 110. 179–192. DOI: 10.1144/GSL.SP.1996.110.01.14

Rowan, M.G., Peel,F.J., Vendeville, B.C., 2004. Gravity-driven fold belts on passive margins. McClay, K.R. (Ed.), Thrust Tectonics and Hydrocarbon Systems AAPG Mem. 82. 157–182

Rust, D., Kershaw, S., 2000. Holocene tectonic uplift patterns in northeastern Sicily: evidence from marine notches in coastal outcrops. Marine Geology 167. 105–126. DOI:10.1016/S0025-3227(00)00019-0

Rust, D., Behncke, B., Neri, M., Ciocanel, A., 2005. Nested zones of instability in the Mount Etna volcanic edifice, Italy. Journal of Volcanology and Geothermal Research 144. 137–153. DOI: 10.1016/j.jvolgeores.2004.11.021

Stewart, L., McGuire, W.J., Vita-Finzi, C., Firth, C., Holmes, R., Saunders, S., 1993. Active faulting and neotectonic deformation on the eastern flank of Mount Etna, Sicily. Geomorphology 94. 73-94.

Swanson, D.M., Duffield, W.A., Fiske, R.S., 1976. Displacement of the south flank of Kilauea volcano: the result of forceful intrusion of magma into the rift zones. US Geological Survey Professional Paper 963.

Telesca, L., Lovallo, M., Carniel, R., 2010. Time-dependent Fisher Information Measure of volcanic tremor before the 5 April 2003 paroxysm at Stromboli volcano, Italy. Journal of Volcanology and Geothermal Research 195. 78–82. DOI: 10.1016/j.jvolgeores.2010.06.010

Tibaldi, A., 2001. Multiple sector collapses at stromboli volcano, Italy: how they work. Bulletin of Volcanology 63. 112–125. DOI: 10.1007/s004450100129

Tinti, S., Armigliato, A., Bortolucci, E., Piatanesi, A., 1999. Identification of the source fault of the 1908 Messina earthquake through tsunami modelling. Is it a possible task? Physics and Chemistry of the Earth, Part B: Hydrology, Oceans and Atmosphere 24. 417–421. DOI: 10.1016/S1464-1909(99)00022-2

Tinti, S., Armigliato, A., Bortolucci, E., 2001. Contribution of tsunami data analysis to constrain the seismic source: the case of the 1693 eastern Sicily earthquake. Journal of Seismology 5. 41–61. DOI: 10.1023/A:1009817601760

van Bemmelen, R.W., 1960. New views on East-Alpine orogenesis. Rep. 21st International Geological Congress Copenhagen 18. 99- 116.

van Wyk de Vries, B.W., Kerle. N., Petley, D., 2000. Sector collapse forming at Casita volcano, Nicaragua. Geology 28. 167–170.

Vogel, F., Fisher, C.T., eds, Diodorus Siculus, 1888-1906. Bibliotheca Historica. Leibzig

Voight, B., Elsworth, D., 1992. Resolution of mechanics problems for prodigious Hawaiian landslides: magmatic intrusions simultaneously increase driving force and reduce driving resistance by fluid pressure enhancement. Eos, Transactions of the American Geophysical Union 73. 506.

Winker, C. D., Edwards, M. B., 1983. Unstable progradational clastic shelf margins. Daniel Jean Stanley und George T. Moore (Eds.): The Shelfbreak: SEPM Society for Sedimentary Geology. 139–157.

2 Objectives

In order to investigate the architecture and the behavior of the submarine continental margin, adjacent to Mount Etna, a new hydro/seismo-acoustic and geological dataset was acquired during RV METEOR research cruise M86/2 in December 2011/January 2012. The dataset includes high-resolution marine 2D/3D reflection seismic-, multi-beam bathymetry- and PARASOUND Echo-Sounder data, as well as gravity cores. This dataset was processed and interpreted in order to answer or contribute to the following objectives:

- **Architecture of the continental margin in front of Mt Etna's edifice:**
  The continental margin east off Mt Etna's edifice shows a prominent bulge in bathymetrical datasets. By analyzing multi-beam-bathymetry data, *Chiocci et al. [2011]* interpret this morphological bulge as the result of magmatic inflation of the pre-Etnean continental margin, as the bulge of the continental margin can only be observed adjacent to Mt. Etna and cannot be traced towards the Strait of Messina in the north and the Malta Escarpment towards the south. On the contrary, *Argnani et al. [2013]* sees indications for thrusting, affecting the continental margin, resulting in the formation of this prominent bulge offshore the volcano edifice. The new M86/2 dataset is used to evaluate near-surface structures in order to produce a new structural model of the continental margin east of Mt Etna. The combination of bathymetric and high-resolution 2D/3D reflection seismic dataset allows considering the high grade of heterogeneity in terms of its morphology and internal structure, which previously was not possible based on the sparse marine surveys done in the working area before. An important task is to evaluate the possible limits of the continental margin instability, as the onshore volcano flank instability is limited by prominent strike-slip faults *[e.g. Bonforte et al. 2011]*.

- **Characterization of continental margin instability:**
  The deformation and instability of the continental margin is suggested and based on bathymetric *[Chiocci et al. 2011*] and seismic data *[Argnani et al. 2013]*. The new high-resolution 2D and 3D seismic dataset will be used to evaluate, if the continental margin is affected by gravity gliding over a décollement (e.g. a pre-Etnean clay rich layer *[Rasà et al. 1996]* or a pre-Etnan landlslide deposit *[Nicolosi et al. 2014]* or gravitational instability and collapse, leading to intense extension and continental margin spreading.

- **Link between volcano flank instability and continental margin instability:**

  As observed onshore, Mt Etna's volcano edifice flank instability is restricted to strike-slip faults in the north (Pernicana-Provenzana Fault System (Fig. 2)) and in the south (Tremestieri-Trecastagni Fault System / Southern Fault System (Fig. 2)) *[e.g. Bonforte et al. 2011]*. As the faults are mapped towards the coastline of East Sicily, the evaluation of possible fault propagation towards the offshore realm, and therefore the continental margin, is necessary. A continuation of the prominent onshore faults towards the offshore realm would imply a strong connection of volcano edifice- and continental margin instability, as the entire system would then be restricted to the same boundaries. Furthermore, *Le Corvec et al. [2014]* proposed the idea of a strong connection between the onshore Timpe Fault System and the offshore Mt Etna, which will also be evaluated in this study. Such information is essential for future evaluation of flank instability at Mt Etna, as a definition of the region affected by slope instability is still lacking.

- **Continental margin instability in context of submarine mass movements:**

  Pareschi et al. [2006] presented indications for a strong overprint of mass transport deposits at the toe of Mt Etna and pointed to its hazardous potential. *Billi et al. [2008]* favored the mass transport deposit at the northern boundary of the continental margin to be related to the 1908 tsunami, which is highly doubted by *Argnani et al. [2009]*. Lack of high-resolution seismic data in this area made a reliable verification / falsification of this hypothesis impossible. The new dataset presented in this thesis will significantly contribute to this discussion.

  A precise evaluation and mapping of near-surface mass transport deposits in the area of the continental margin and the continental toe is done in this thesis, which is necessary for evaluation of geo-hazard potential in the working area. In addition, plausible sources, precursors and trigger mechanisms in the area will be discussed.

References

Argnani A., Chiocci F.L., Tinti S., Bosman A., Lodi M.V., Pagnoni G., Zaniboni F., 2009. Comment on "On the cause of the 1908 Messina tsunami, southern Italy" by Andrea Billi et al. Geophysical Research Letters 36. L13307.

Argnani, A., Mazzarini, F., Bonazzi, C., Bisson, M., Isola, I., 2013. The deformation offshore of Mount Etna as imaged by multichannel seismic reflection profiles. Journal of Volcanology and Geothermal Research 251. 50–64. DOI:10.1016/j.jvolgeores.2012.04.016

Billi A., Funiciello R., Minelli L., Faccenna C., Neri G., Orecchio B., Presti D., 2008. On the cause of the 1908 Messina tsunami, Southern Italy. Geophysical Research Letters 35. L06301. DOI:10.1029/2008GL033251

Bonforte, A., Guglielmino, F., Coltelli, M., Ferretti, A., Puglisi, G., 2011. Structural assessment of Mount Etna volcano from Permanent Scatterers analysis. Geochemistry Geophysics Geosystems 12. DOI:10.1029/2010GC003213

Chiocci, F. L., Coltelli, M., Bosman, A., Cavallaro, D., 2011. Continental margin large-scale instability controlling the flank sliding of Etna volcano. Earth and Planetary Science Letters 305. 57–64. DOI:10.1016/j.epsl.2011.02.040

Le Corvec, N., Walter, T. R., Ruch, J., Bonforte, A., Puglisi, G., 2014. Experimental study of the interplay between magmatic rift intrusion and flank instability with application to the 2001 Mount Etna eruption. Journal Geophysical Research Solid Earth. DOI: 10.1002/2014JB011224

Nicolosi, I., D'Ajello Caracciolo, F., Branca, S., Ventura, G., Chiappini, M., 2014. Volcanic conduit migration over a basement landslide at Mount Etna (Italy). Scientific Reports 4. DOI:10.1038/srep05293

Pareschi, M.T., Boschi, E., Mazzarini, F., Favalli, M., 2006. Large submarine landslides offshore Mt. Etna. Geophysical Research Letters 33. DOI:10.1029/2006GL026064

Rasa, R., Azzaro, R., Leonardi, O., 1996. Aseismic creep on faults and flank instability at Mount Etna volcano, Sicily. Geological Society, London, Special Publications 110. 179–192. DOI: 10.1144/GSL.SP.1996.110.01.14

3 Methods

During RV Meteor cruise M86/2 in December 2011/January 2012, a large hydro/seismo-acoustic and geological dataset was acquired in the Gioia Basin (Tyrrhenian Sea), the Strait of Messina and offshore Mt Etna (Ionian Sea) (Fig. 14) *[Krastel et al. 2014]*. The dataset includes 2D reflection seismic profiles, a 3D reflection seismic P-Cable cube of 26.6 km^2, a full coverage bathymetry, PARASOUND echo-sounder profiles, sediment gravity cores and box cores. As the acquisition and processing of this data is fundamental for this work, this chapter will give short insight to data acquisition and processing during and after Cruise M86/2. Although all acquisition and processing techniques were applied to the entire dataset acquired during M86/2, this thesis will concentrate on the region offshore Mt Etna (Fig. 14).

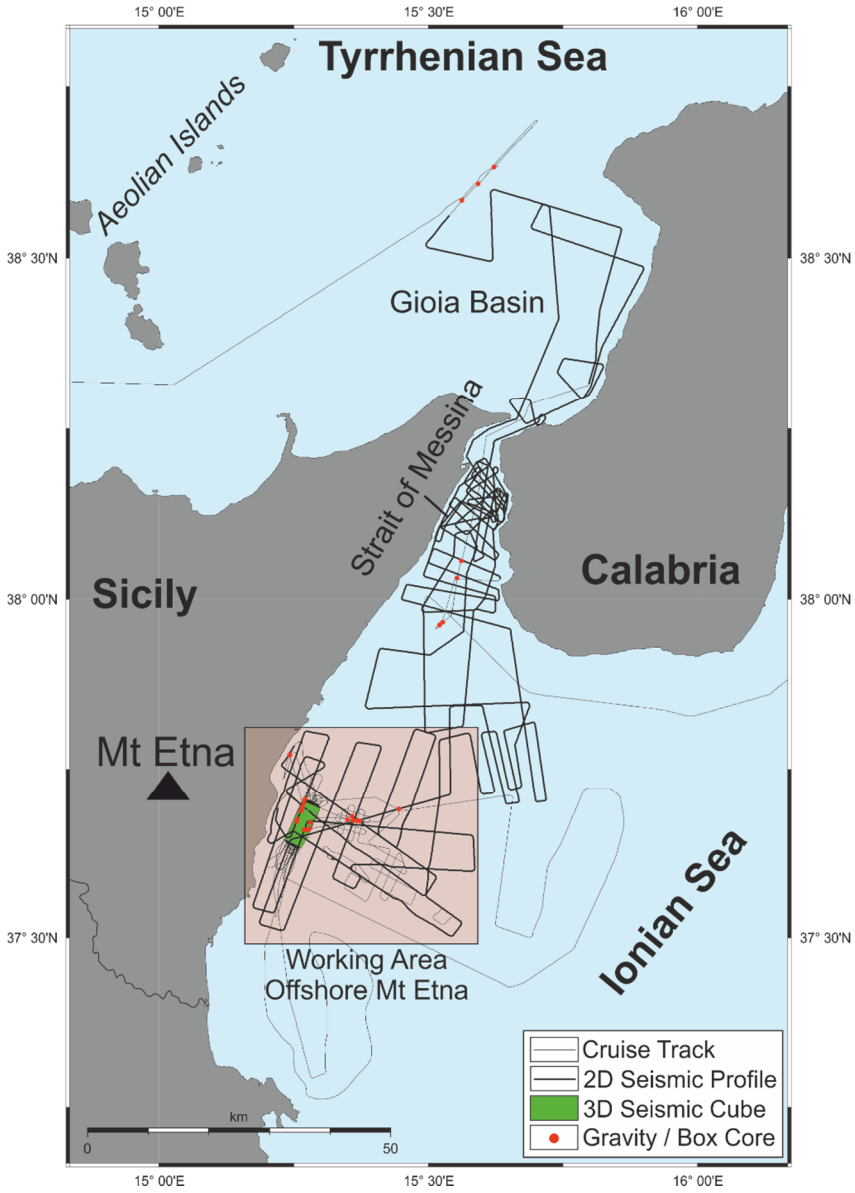

Figure 14: Cruise track of M86/2. The working area offshore Mt Etna (this thesis) is marked by the red box. Modified after *[Krastel et al. 2014]*.

3.1 2D reflection seismic Acquisition

During RV Meteor M86/2 cruise, a 104 channel digital Geometrics GeoEel Streamer system was used to gather high-resolution 2D multichannel reflection seismic profiles. The streamer system is modular set up by 12.5 m long sections, each equipped with 16 hydrophones, paired to 8 groups with a group distance of 1.5625 m. This setup allows the collection of very high-resolution seismic data, which cannot be achieved with industry-type streamers (Typical group distances of 6.25 or 12.5 m).The short hydrophone spacing enables a bin sizes down to 0.78125 m during seismic processing, as the lateral bin size has to be at least half the channel spacing of the seismic system. During M86/2, the hydrophone streamer was configured with 13 x 12.5 m long active sections, resulting in a total active length of 162.5 m and 104 channels. This short streamer length and high water depth of up to 2000 m in the working area made a dedicated velocity analysis impossible. Hence a continuous sound velocity of 1500 m/s was applied to the dataset. The seismic signal was produced by a 1.7 l Sercel GI Gun, which was operated at ~200 bar in harmonic mode. For a short streamer like the used GeoEel System, the shot interval, cruise speed and recording length are important parameters for obtaining a high coverage; these parameters were adjusted during the cruise depending on current velocities, and water depths. Offshore Mt Etna, a cruise speed of ~4 knots, a shot interval of 4 s and a recording length of 3-4 s were chosen to obtain an average CMP (Common-Mid-Point) fold of ~15 by applying a bin size of 2 m.

3.2 2D reflection seismic Processing

For 2D seismic data processing, the commercial software Gedco Vista Seismic Processing was used. In order to setup a standardized processing flow, which is applicable to other datasets, a new flow was designed for the M86/2 dataset. The flow enables even less experienced seismic processers to obtain first presentable seismic profiles with a low investment of time. The developed flow is now used for several datasets, acquired over the past years *[e.g. Elger et al. 2014]*. The processing manual and flows are available from Sebastian Krastel-Gudegast and his working group “Marine Geophysik und Hydroakustik” at the Christian-Albrechts Universität zu Kiel.

The most important steps of this processing flow are:

- Data import and header edit: Import of each shot gather file (*.sgd), which was acquired during acquisition. The shot-files are merged to a single *.sgy file, which is a standardized file type for multichannel seismic data.
- Geometry Setup, CMP (Common-Mid-Point) calculations and binning: During Geometry setup, each shot point and each channel of the streamer is merged with its exact position during

acquisition. Exact shot point and receiver locations are then written into the header of the *.sgy file. This file can then be used to calculate the mid points for each shot-receiver pair. Binning (assignment of shot-receiver pairs to bins) is then done along a crooked-line along the ship track; the bin-distance for the M86/2 dataset was set to 2 m or 3.125 m.

- Bulk-Shift and Normal-Move-Out Corrections: In order to create zero-offset sections, a bulk shift and Normal-Move-Out correction are applied to the dataset. This method guarantees that the lateral offsets of the hydrophone spacing are eliminated and a correct signal onset is given for each shot and channel. The Normal-Move-Out Corrections were carried out by applying a constant velocity of 1500 m/s.
- Filtering: The developed processing flow contains standard filters like a Band Pass Filter and a FK (Frequency / Wavenumber) filter. Filters are an important mechanism to eliminate noise during seismic processing and need to be adjusted for each profile.
- CMP Stack and Migration: The CMP-Stack is carried out in order to stack the calculated CMPs, which were addressed to specific bins during Geometry Setup. This method leads to a constructive interference of coherent reflectors and the elimination of random noise. This step is therefore one of the most important processing step for multichannel seismic processing. The seismic migration of data is realized by using the software's finite difference migration (FD Migration) algorithm and was carried out with a constant velocity of 1500 m/s.

3.3 3D reflection seismic Acquisition

Marine 3D reflection seismic acquisition is a standard industry approach for hydrocarbon exploration and is carried out worldwide by several acquisition companies *[Biondi 2006]*. As the petroleum industry is aiming for deep targets and large areas, the systems are designed to meet these requirements. Instruments for industry-standard 3D seismic acquisition require large resources in terms of acquisition platform size, staff and investments into seismic systems *[Vermeer and Beasley 2012]*. The advantages of 3D seismics in comparison to 2D seismics is the areal coverage of a survey site, making a dedicated analysis of volumes and fault strike / dips possible *[e.g. Biondi 2006]*.

In order to build a 3D seismic system, which is capable for high-resolution 3D reflection seismics, the so called P-Cable was developed *[Planke et al. 2009]*. The modular system uses 12-24 parallel towed short streamers, which are attached to a so-called cross-cable (Fig. 15) *[Planke et al. 2009]*. This enables the system to be used on relatively small platforms like medium-size research vessels *[Planke et al. 2009]*.

The GEOMAR P-cable system was used during Cruise M86/2 and the used GEOMETRICS GeoEel digital streamer segments are the same as used for 2D reflection seismic acquisition, which enables the user to use the same equipment for either 2D or 3D surveys. This synergy effect minimizes the costs of the seismic system and enables even the scientific community to use 3D seismic systems.

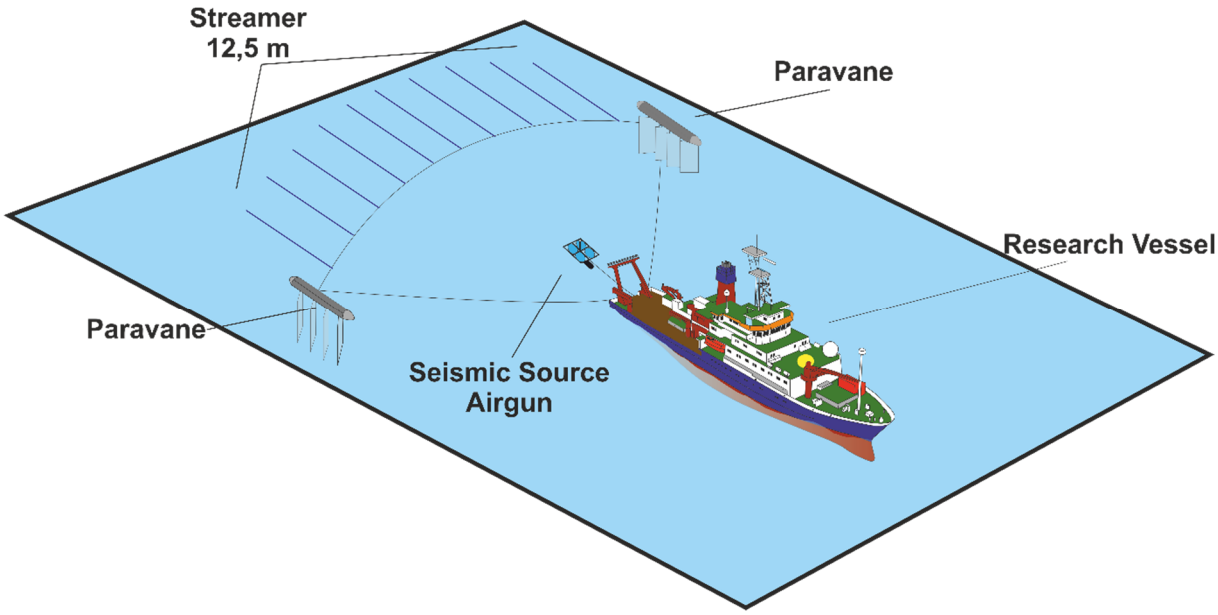

Figure 15: Schematic drawing of P-Cable 3D reflection seismic acquisition and its components. The P-Cable system consists of two paravanes, which are fanning up numerous streamers, which are attached parallel to each other at the cross-cable.

The P-Cable System is operated between two paravanes, which are trawled behind the acquisition vessel, fanning out numerous streamer segments, which are attached to the cross-cable (Figs. 15, 16). The streamer segments can either be single sections of 12.5 m or 25 m length or longer segments like the "Stingray Configuration", which hosts a longer central streamer between the two paravanes. The seismic source, typically a GI Airgun, is trawled directly behind the vessel and operates in front of the fan of streamers (Figs. 15, 16).

The paravanes are equipped with a GPS antennae, which are wirelessly connected to the acquisition laboratory on the vessel (Fig. 16). This enables geometry calculations of all system components, as all lengths like the cross-cable distances and the length of the trawl wires are known. This data is processed in real time and the positions of the paravanes can be monitored from the acquisition laboratory, which is important during track changes, bad weather conditions and strong currents like offshore Mt Etna. During seismic acquisition, real time quality control can be carried out and information about each streamer, channel and system coverage can be displayed by Seismic Unix / GMT (Generic Mapping Tool) scripts written by Dirk Klaeschen and Cord Papenberg (GEOMAR Helmholtz Centre for Ocean Research, Kiel). As the system consists of numerous short streamer segments, the system is not built for a dedicated velocity analysis. It is possible to obtain subsurface sound velocity information with OBS / OBH (Ocean Bottom Seismometer / Ocean Bottom Hydrophone) instruments, which is then implemented during seismic processing.

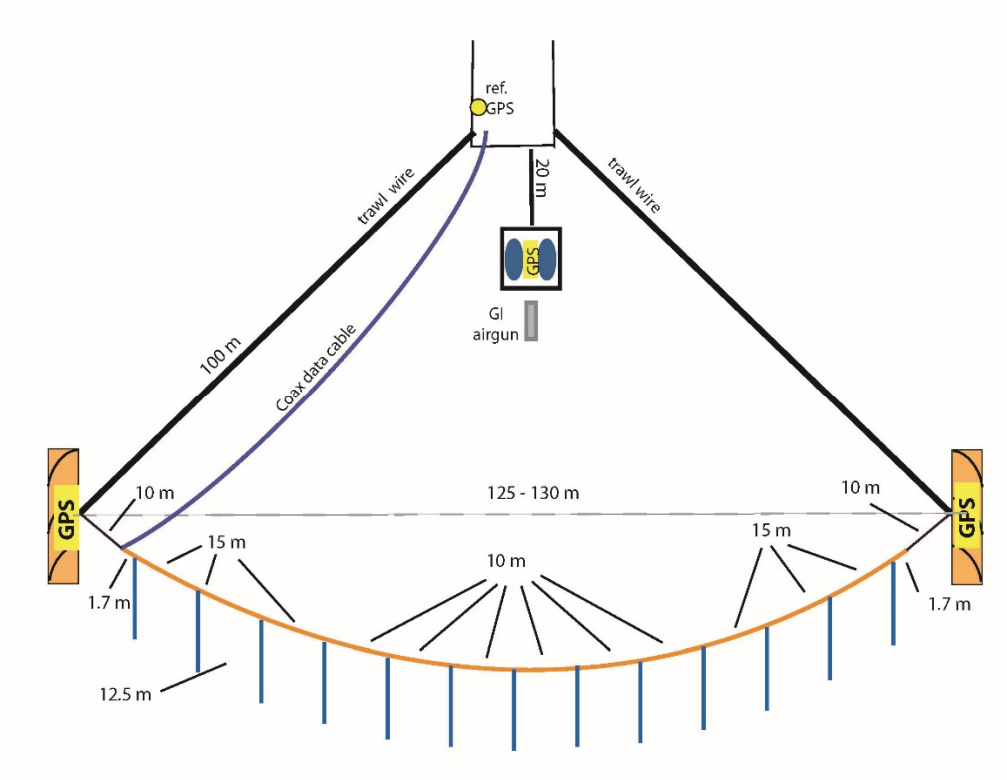

Figure 16: Sketch of the P-Cable design and setup during the M86-2 cruise. In total 13 streamers were fanned up by the paravanes and trawled behind the vessel. For navigation processing, each paravane, the GI airgun and vessel iss equipped with GPS antennae *[Krastel et al. 2014]*.

During M86/2 in total 13 Streamers, each 12.5 m long, were trawled behind RV Meteor (Fig. 17). The distance between the paravanes was constantly between 125 – 130 m and the system worked relatively smooth. The implementation of a dedicated sound velocity analysis for the working area was resigned, as only three of the four deployed OBS / OBH instruments were operating accurately during the cruise and the heterogeneous sub-seafloor structures made a representative interpolation of these three stations impossible. Therefore, like for 2D reflection seismic profiles, a constant sound velocity of 1500 m/s was applied to the dataset.

3.4 3D reflection seismic Processing

Exact navigation processing is one of the most critical steps for high-resolution 3D seismic acquisition. The navigation is recorded by using remote GPS receivers mounted to the paravanes, the seismic source and the vessel (Fig. 16). The GPS navigation information are readout in real-time and saved to navigation files. With these information, the location of the P-Cable and each streamer segment can be calculated. The exact channel positions of the streamers are defined and evaluated between first arrivals at the hydrophones and calculated streamer positions. During navigation processing, the entire survey area is defined as raster, in which each shot and channel position is assigned to a specific position. In accordance to a specific bin size (for this seismic cube bin size = 5x5 m; Table 2), the CDP-grid is calculated. This procedure will lead to the coverage map, from which the system's coverage can be obtained (Figs. 17, 18). As lack of data points in the grid can lead to inaccuracy of the entire dataset, a dense coverage of CDPs has to be ensured during acquisition.

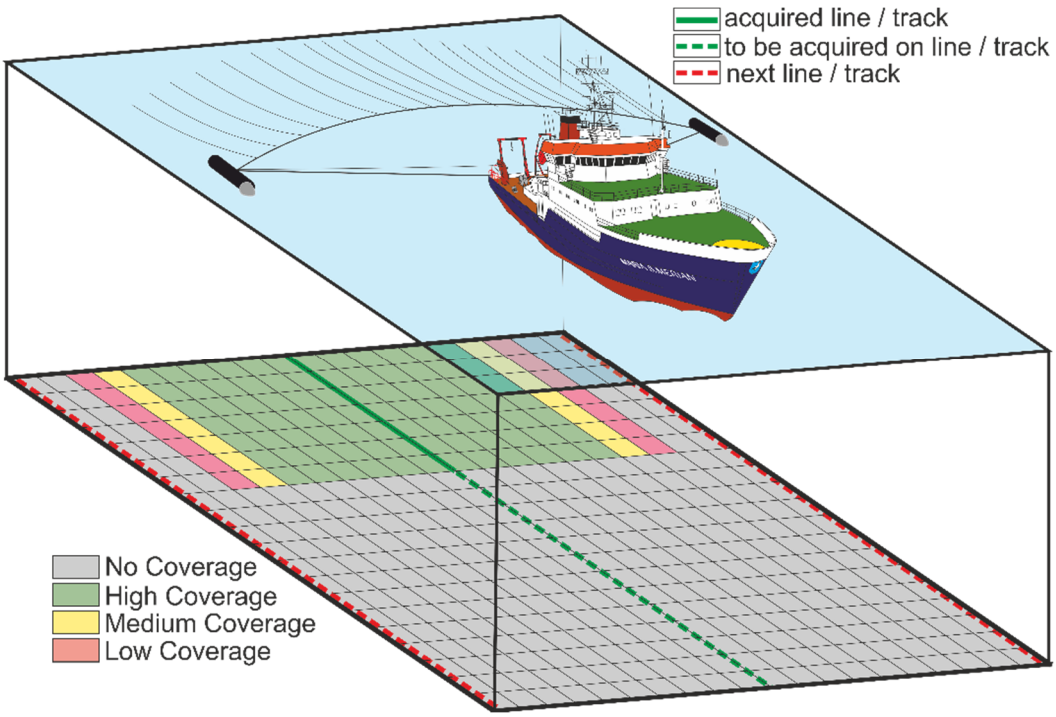

Figure 17: Schematic drawing of the P-Cable and its subsurface coverage. The coverage is a result of: cruise speed, # Channels, # Streamer Segments, length of cross-cables between Streamer Segments, Track spacing

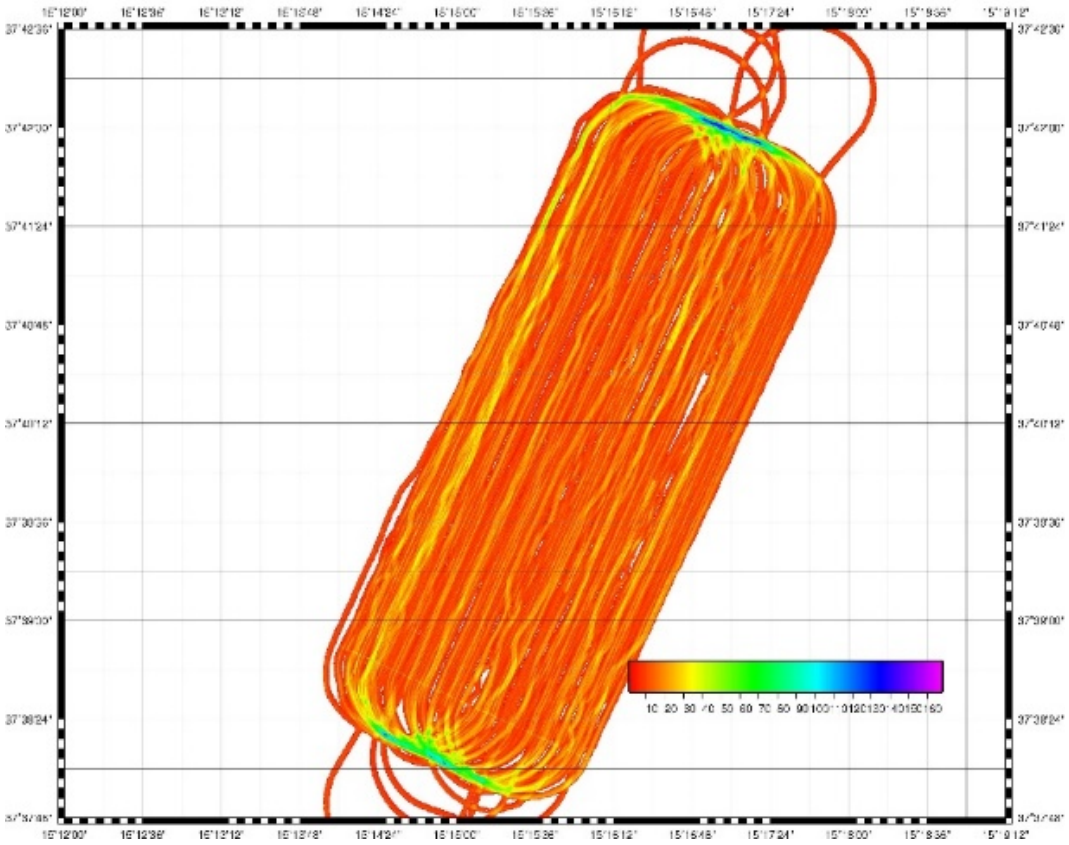

Figure 18: Coverage map short before the 3D acquisition was terminated. The coverage map was generated with a bin size of 12.5 m. The colour scale interprets the fold in each bin of the 3D area. Due to multiple coverage, the coverage in the turns is highest. Bin without coverage are left white. Undulations along the sides of white stripes indicate deviations from the track line during data acquisition *[Krastel et al. 2014].*

As the acquired 3D seismic cube might show gaps in the data record (Fig. 18), an interpolation of these gaps is calculated. Empirical knowledge shows that the best interpolation of 3D seismic data gaps can be carried out by time-slice interpolation, which is applied to each sampling depth (in our dataset 1 ms). This interpolation is done by using the Generic Mapping Tool (GMT). Each Inline and Crossline are then generated from the interpolated depth / time slices. The frequency filtering of P-Cable seismic data is an important process for noise elimination, as the CDP fold of this system is relatively small, compared to large 3D systems or the 2D reflection seismic data shown in this thesis (Fig. 18). The most important filtering algorithm is the Band-Pass filter in which the frequencies of the wavelet are passed and frequencies outside this range are attenuated. This filter is applied iteratively until the best-fit is established. Also F-K filters, radon filters can be applied to the dataset but were rejected due to negative interference during seismic processing of the M86/2 dataset. Due to the complexity of a real 3D data migration, the M86/2 dataset was migrated by applying a Stolt-Migration in In- and Crossline direction. Detailed information about parameters of the M86/2 3D cube can be found in Table 2.

Next to seismic amplitude analysis in IHS KingdomSuite, additional seismic attributes were generated by using the open source software OpendTect. For this thesis, especially the similarity attribute, which is the coherency attribute in the software package of OpendTect, was calculated and analyzed. The similarity attribute was calculated by using a +-28 ms time window. The created cube was exported from OpendTect and imported to IHS KingdomSuite. All Interpretation and graphical processing was carried out with IHS KingdomSuite 8.8 and 2015.

Table 2: Parameters of the final M86/2 3D Cube offshore Mt Etna used for this work

Parameter	Value
3D Volume Size:	3325 m x 8000 m, 26.6 km^2
Bin Size / CDP Grid:	5 m x 5 m
Depth Range:	500 ms – 2000 ms
Inlines:	665 (4420 – 5085)
Crosslines:	1600 (4850 – 6450)
Coordinates (Corners)	Inline 4420 / Crossline 4850: 37°37.46 , 15°15.50
	Inline 4420 / Crossline 6450: 37°41.42 , 15°18.06
	Inline 5085 / Crossline 6450: 37°42.27 , 15°16.03
Fold:	1-3
Interpolated:	yes, with time slices by using GMT and interpolation grid of 10 m
Band Pass Filter:	20, 55, 200, 400
Sampling Rate:	1 ms
Migration:	Stolt Migration, const. vel. 1500 m/s

3.5 Multi-Beam Bathymetry and PARASOUND Echo-Sounder data Acquisition and Processing

During Cruise M86/2, bathymetric data was acquired by using RV Meteor's hull mounted Kongsberg Simrad EM122 and Kongsberg EM710 multi-beam sounders. Whereas the EM122 is a full ocean depth covering mutli-beam, which can be used from depth of 20 m up to 11000 m, the EM710 is designed for shallow water conditions of less than ~2000 m water depth.

The systems were operating during the entire cruise. They were used next to seismic profiling and additional hydro-acoustic surveys during seismic system maintenance and evaluation of sediment sampling sites. The acquired data was processed using the open source software MB System (David W. Caress, Monterey Bay Acquarium Reseach Institute and Dale N. Chayes, Lamont-Doherty Earth Observatory, Columbia University). The presented bathymetric grid in this thesis shows a combination of the bathymetric data, acquired during the MaGIC project of our cooperation partner Francesco Latino Chiocci from La Sapienza University of Rome *[Chiocci and Ridente 2011]*, and the newly acquired M86/2 dataset. The presented grid has a cell size of 30x30 m.

For high resolution echo-sounder data acquisition, the RV Meteor's hull-mounted Atlas Hydrographic PARASOUND P70 was used. The PARASOUND P70 provides high-resolution echo-sounder data with up to 100 m sediment penetration. In comparison to conventional 3.5 kHz echo-sounders, the system works as a parametric echo sounder by using primary frequencies of 18 (Primary High Frequency PHF) and adjustable 18.5 – 28 kHz. From these primary frequencies, the parametric secondary frequencies in the ranges of 0.5 – 10 kHz (Secondary Low Frequency SLF) and 36,5 – 48 kHz (Secondary High Frequency SHF) are generated by the nonlinear acoustic interaction of the primary waves at high signal amplitudes, which occurs in the emission cone of the high-frequency. In the Atlas Hydrographic PARASOUND P70, the emission cone is limited to an aperture angle of 4°, which is the result of the array's architecture by featuring 128 transducers arranged on a rectangular plate of ~1 m^2. This architecture enables a footprint size of ~7% of the water column, which makes it a significant improvement, compared to conventional 3.5 KHz echo-sounder systems. The System was operated during the entire cruise M86/2 next to 2D / 3D seismic profiling and multi-beam echo-sounder mapping. Furthermore, the PARASOUND system was used to locate and evaluate possible sites for gravity- and box coring. All acquired data was converted from the *.ps3 format into the *.sgy format by using the custom tool ps32sgy (Hanno Keil, University of Bremen). For further interpretation, the data was then loaded into IHS KingdomSuite.

References

Biondi, B., 2006. 3D seismic imaging. Tulsa, Okla: Society of Exploration Geophysicists, Investigations in geophysics series 14. ISBN: 1-56080-137-9

Chiocci, F.L., Ridente, D., 2011. Regional-scale seafloor mapping and geohazard assessment. The experience from the Italian project MaGIC (Marine Geohazards along the Italian Coasts). Marine Geophysical Research 32. 13–23. DOI:10.1007/s11001-011-9120-6.

Elger, J., Berndt, C., Krastel, S., Piper, D. J. W., Gross, F., Spielhagen, R. F., Meyer, S., 2014. The Fram Slide off Svalbard: a submarine landslide on a low-sedimentation-rate glacial continental margin. Journal of the Geological Society. DOI:10.1144/jgs2014-055.

Krastel, S. and cruise participants, 2014. Seismogenic faults, landslides, and associated tsunamis off southern Italy. Cruise No. M86/2 – November 21, 2011 – January 17, 2012 – Cartagena (Spain) – Brindisi (Italy). METEOR-Berichte. M86/2. 49 pp. DFG-Senatskommission für Ozeanographie, DOI:10.2312/cr_m86_2.

Planke, S., Eriksen, F.N., Berndt, C., Mienert, J., and Masson, D.G., 2009, P-Cable High-resolution 3D Seismic. Oceanography 22, 81.

Vermeer, G.J.O., Beasley, C.J., 2012. 3D seismic survey design. Second edition. Geophysical references series, no. 12.

4 MANUSCRIPT I

The limits of seaward spreading and slope instability at the continental margin offshore Mt Etna, imaged by high-resolution 2D seismic data

Felix Gross, Sebastian Krastel, Jacob Geersen, Jan-Hinrich Behrmann, Domenico Ridente, Francesco Latino Chiocci, Jörg Bialas , Cord Papenberg, Deniz Cukur, Morelia Urlaub and Aaron Micallef

In Review, submitted on 12.02.2015 to:

Tectonophysics

Abstract

Mount Etna is the largest active volcano in Europe. Instability of the eastern flank is well documented onshore, and continuously monitored by geodetic and InSAR measurements. Little is known, however, about the offshore extension of the eastern volcano flank, defining a serious shortcoming in stability models. In order to better constrain the active tectonics of the continental margin offshore the eastern flank of the volcano, we acquired a new high-resolution 2D reflection seismic dataset. The data provide new insights into the heterogeneous geology and tectonics at the continental margin offshore Mt Etna. The submarine realm is characterized by different blocks, which are controlled by local- and regional tectonics. A compressional regime is found at the toe of the continental margin, which is bound to a complex basin system affecting the eastward movement of the flank. Both, the clear link between on- and offshore tectonic structures as well as the compressional regime at the easternmost flank edge, indicate a continental margin gravitational collapse as well as spreading to be present at Mt Etna. Moreover, we find evidence for the offshore southern boundary of the moving flank, which is identified as a right lateral oblique fault north of Catania Canyon. Our findings suggest a coupled volcano edifice and continental margin instability at Mt Etna, demonstrating first order linkage between on- and offshore tectonic processes.

1 Introduction

1.1 Tectonic setting of Mt Etna

Mt Etna, Europe's largest volcano, rises to a height of 3323 m (Fig. MI-1). The composite volcanic edifice sitting on top of continental crust *[Gvirtzman and Nur 1999]* is highly active with an eruption history of ~500 kyr *[Branca and Del Carlo 2004; Branca et al. 2004]*. Its recent volcanic unrest is documented by several eruptions per year during the last decades *[Branca and Del Carlo 2004]*.

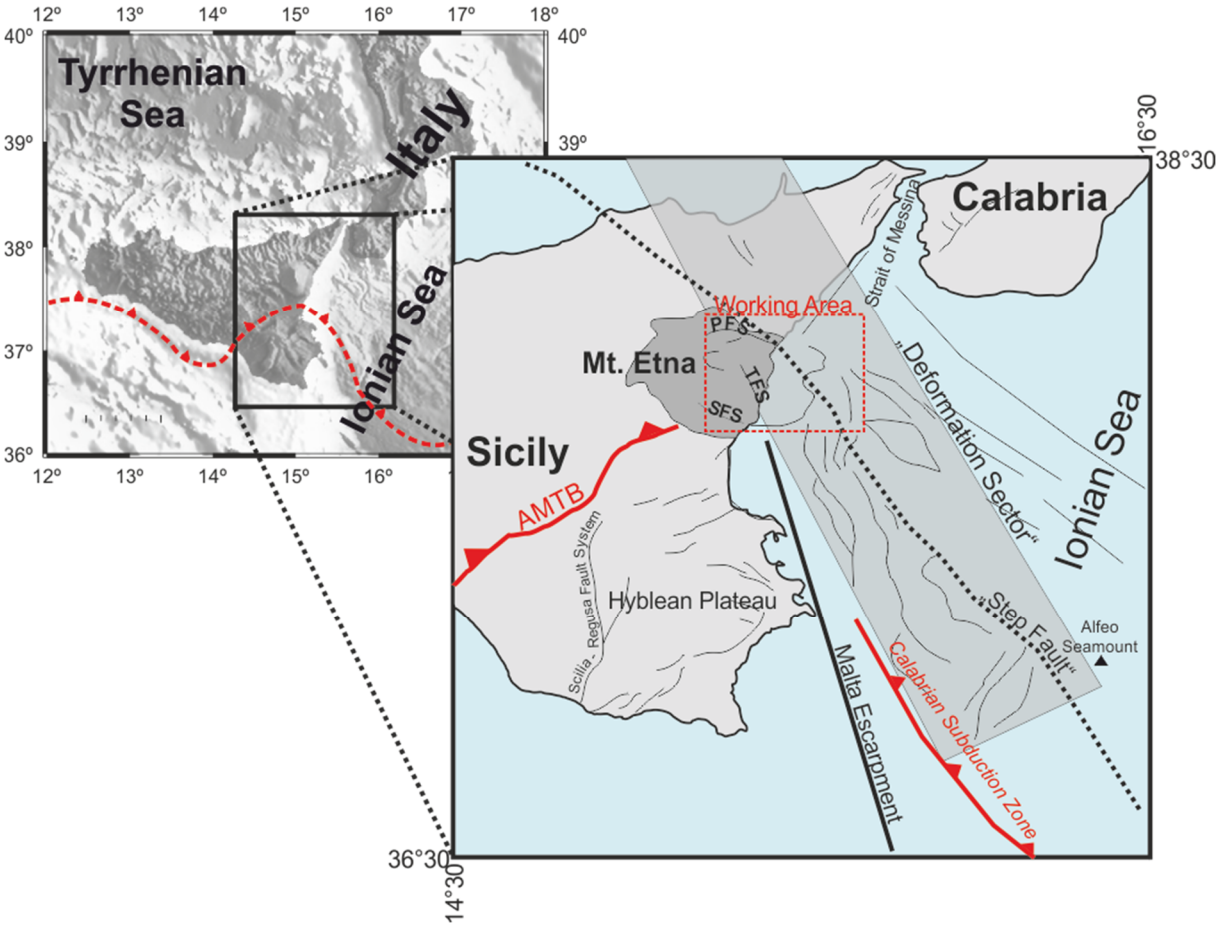

Figure MI-1: Overview map of the geographical setting of Sicily and Tectonic map of East Sicily modified after *Argnani [2014]*. Sicily is separated from the Italian mainland by the Strait of Messina, which opens towards the Ionian Sea east of Sicily. PFS=Pernicana-Provenzana-Fault-System, TFS=Timpe-Fault-System, SFS=Southern-Fault-System, AMTB=Appenine-Maghrebian Fold and Thrust Belt. The working area is marked by a red box.

Mt Etna's geological setting is characterized by the complex compressional tectonics of the Appenine-Maghrebian Fold and Thrust Belt to the south (Fig. MI-1), and the northwest dipping Calabrian subduction zone to the southeast *[e.g. Doglioni et al. 2001]*. The Malta Escarpment (Fig. MI-1), a large

northward trending crustal discontinuity between eastern Sicily's continental crust and the oceanic crust making up the Ionian Sea, is a prominent morphological feature at the seafloor. It can be traced southward and passes east of the Maltese Islands *[Lentini et al. 2006; Argnani and Bonazzi 2005]*, thereby affecting the subduction regime underneath Calabria (Fig. MI-1) *[e.g. Gvirtzman and Nur 1999; Argnani and Bonazzi 2005]*. Because of its regional importance as a deep-seated fault, a link between the Malta Escarpment and Mt Etna's edifice has been proposed *[Rust and Kershaw 2000]*. However, the complex structure and morphology of the Timpe Plateau (see Fig. MI-2) makes it difficult to trace the Malta Escarpment as far north as Mt Etna's coastal offshore extension, and into the onshore volcanic edifice *[Argnani and Bonazzi 2005; Nicolich et al. 2000]*.

The NNE trending right-lateral Scilia-Regusa fault system, heading towards Mt Etna at the western boundary of the Hyblean Plateau (Fig. MI-1), was also invoked to explain the location of Mt Etna *[e.g. Lo Guidice and Rasà, 1992]*. Furthermore, recent interpretations based on refraction and reflection seismic data favor the existence of a distinct southeast trending Subduction Transform Edge Propagator Fault (STEP-Fault), passing by Mt Etna's northern flank (Fig. MI-1) *[Polonia et al. 2012; Gallais et al. 2013; Gallais et al. 2014; Musumeci et al. 2014]*. Such a fault is required to delimit the retreating Calabrian subduction front towards the southwest, and to open an asthenospheric window at sub-lithosphere depths. The proposed STEP-fault is somewhat oblique to the Malta Escarpment (Fig. MI-1) *[Gallais et al. 2013; Musumeci et al. 2014]*. *Argnani [2014]*, however, does not find indications for a distinct near-surface STEP-fault in a dense grid of seismic lines from offshore eastern Sicily. Instead, he suggests a 20-30 km wide corridor of SSE trending faults (Fig. MI-1) affecting the entire area from Alfeo Seamount to Sicily to be the surface expression of a deep crustal-scale structure controlling the regional tectonics in this area. *Argnani [2014]* bases his interpretation on a series of asymmetric half-grabens, bound to eastward dipping normal faults *[Hirn et al. 1997; Nicolich et al. 2000; Bianca et al. 1999; Argnani and Bonazzi 2005]*. These normal faults are proposed to have generated earthquakes like the 1693 Catania event *[Bianca et al. 1999; Argnani et al. 2012]*.

The entire region around Mt Etna is seismically highly active. Large earthquakes like the disastrous Messina 1908 event *[e.g. Pino et al. 2009]* occurred in the Strait of Messina north of Mt Etna. Furthermore, deep (20-30 km) compressive earthquakes, probably related to thrusting in the Appennine-Maghrebian Thrust Belt, have been recorded close to the volcano *[Lavecchia et al. 2007]*. Another set of seismic events (hypocenter depths <10km) were observed underneath the eastern flank of Mt Etna. This small scale variation in location and kinematics of seismic events leads to the interpretation that the stress field underneath Mt Etna is highly heterogeneous *[Cocina et al. 1997]*.

1.2 Mt Etna's eastern flank and its slope instability

Large volcano edifices are well known for their hazardous potential due to gradual volcano spreading *[van Wyk de Vries and Francis 1997]*. In comparison to other large volcano edifice instabilities, such as the Hawaiian Islands *[e.g. Nakamura 1980; Moore et al. 1989; Borgia and Treves 1992]* and the Canary Islands *[Krastel et al. 2001; Masson et al. 2002]*, the setting at Mt Etna differs dramatically, as the volcano edifice builds upon continental crust, creating a volcano flank- and continental margin instability. The volcano flank gravitational instability *[e.g. Firth et al. 1996]* is considered to creep on a weak substratum-décollement like a pre-Etnean landslide deposit *[Nicolosi et al. 2014]* or a dipping weak clay-rich layer or substratum *[e.g. Delcamp et al. 2008]*.

Mt Etna's flank instability, first described as gravitational spreading by *Borgia et al. [1992]*, is one of the best-monitored and studied examples for volcano flank instability around the world. Evidence for both, episodic and continuous flank movement, was reported *[e.g. Froger et al. 2001; Acocella et al. 2003; Bonforte and Puglisi 2003]*. By a dense network of GPS and geodetic stations *[Lundgren et al. 2003; Puglisi et al. 2008; Bonforte et al. 2009; Neri et al. 2009]*, gas monitoring *[Neri et al. 2007; Bonforte et al. 2013]*, and geologic fieldwork *[Groppelli and Tibaldi 1999; Neri et al. 2004]*, it was possible to locate and characterize the instability of Mt Etna's eastern flank.

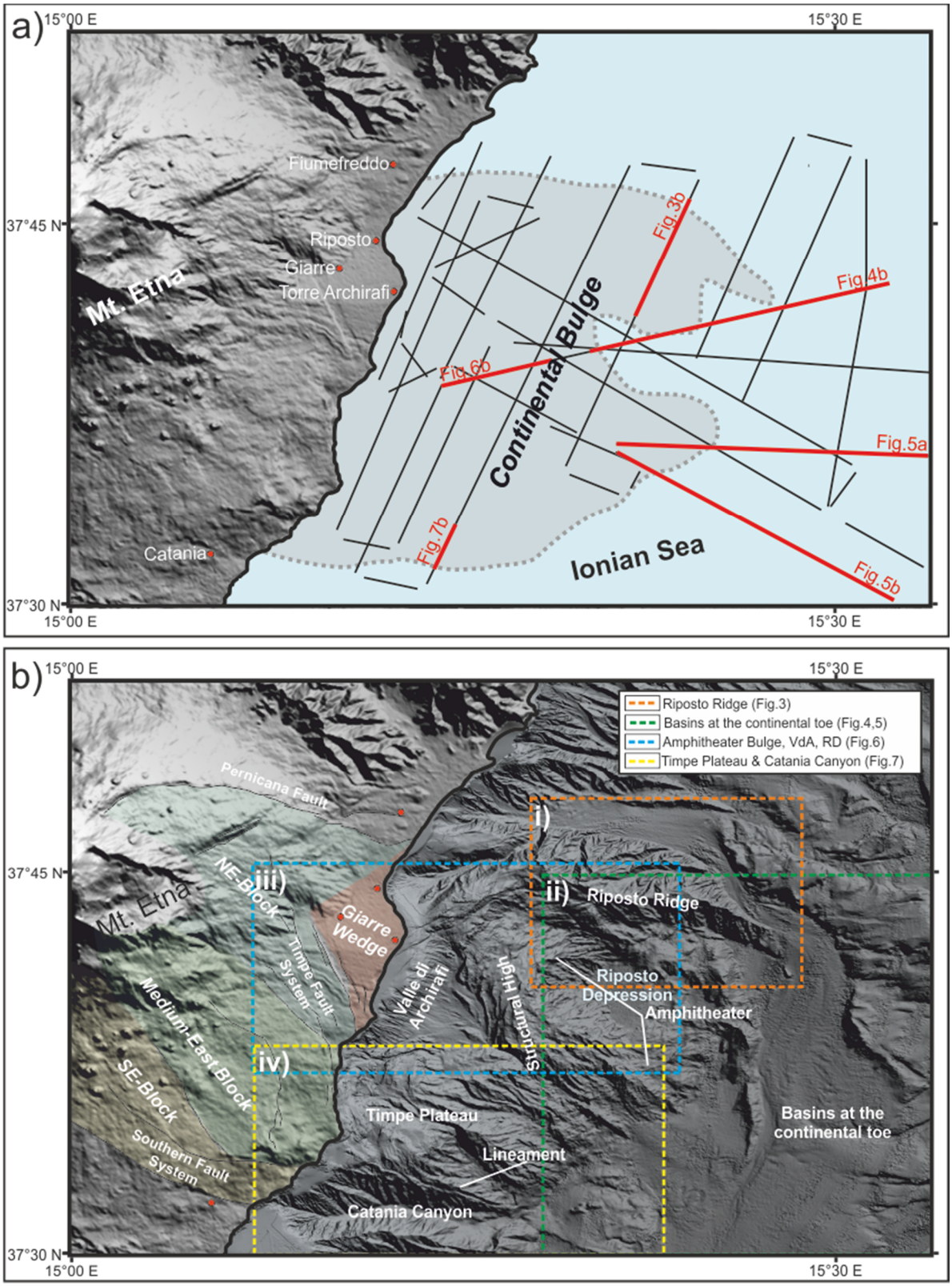

Figure MI-2: a) Grid of high-resolution 2D seismic lines acquired during M86/2 cruise offshore Mt Etna. Red lines are the seismic profiles shown in this work. b) Bathymetric and topographic map from the eastern flank of Mt Etna (See Fig. MI-1 for location). Bathymetric data is a combination of the dataset presented by *Chiocci et al. [2011]* and M86/2 Data. The onshore Digital Elevation Model is the SRTM90 dataset *[Farr et al. 2007]*. Onshore structures and kinematic domains are after *Bonforte et al. [2011]*. Colored boxes indicate the four different morphologic areas discussed below.

The northern boundary of the moving flank is described as the left lateral Pernicana-Provenzana Fault (Figs. MI-1, MI-2) with a continuous horizontal displacement of ~2.8 cm/yr *[Bonforte and Puglisi 2003]* that may accelerate during volcanic activity *[Bonforte et al. 2007]*. The Timpe Fault System (Figs. MI-1, MI-2) separates the NE-Block to the Medium East Block (Fig. MI-2). The southern boundary (Fig. 2) of the moving flank, which can be related to the Southern Fault System (Fig. MI-2) is only constrained by InSAR measurements and Soil Gas emissions *[Froger et al. 2001; Bonforte et al. 2013]*.

In contrast to the well-studied onshore part, little information is available concerning the topography and structure of the offshore flank of Mt Etna, and the transition towards the continental margin. *Marani et al. [2004]* presented the first multi-beam bathymetric map of the area, imaging the major morphological features offshore Mt. Etna. *Chiocci et al. [2011]* acquired and used a high-resolution bathymetry for a first interpretation on the continental margin offshore Mt Etna.

Chiocci et al. [2011] proposed the idea of an upslope propagating instability, caused by a large-scale mass wasting event offshore Mt Etna, creating a prominent amphitheater-like structure offshore the village of Riposto (Fig. MI-2). Furthermore, the multi-beam bathymetric map shows a WNW trending lineament at the seafloor at a location which may coincides with an offshore continuation of the suggested terrestrial boundary of the southern fault system *[Chiocci et al. 2011]*. Reflection seismic data indicate that the offshore area around the volcano is dominated by extensional faulting, with only a few isolated thrust faults close to the coast at Riposto Ridge *[Argnani et al. 2013]*. So far, it was not possible to determine the exact northern and southern boundaries of the moving flank in the marine realm *[Argnani et al. 2013]*. The instability of Mt Etna's continental margin is documented by large scale submarine mass wasting deposits *[Pareschi et al. 2006]* and small / medium scale debris deposits *[Gross et al. 2014 – this thesis]*.

1.3 Objectives

We collected a high-resolution acoustic dataset including multi-beam bathymetry and 2D seismic reflection lines in order to investigate the tectonic setting of the continental margin offshore Mt Etna and its linkage to onshore volcanic and tectonic processes. The main objective of this manuscript is to link tectonic features and processes between the on- and offshore area around the volcano with special emphasis on evaluating the impact of offshore processes, such as the continental margin instability, on Mt Etna's flank instability. On a long-term perspective, the results may contribute an improved hazard assessment for the entire on- and offshore system consisting of the onshore eastern volcanic flank and the continental margin off Mt Etna.

2 Methods

During RV Meteor Cruise M86/2 from December 2011 – January 2012, a new seismic and hydro-acoustic dataset was acquired offshore Mt Etna. Recording of 2D seismic signals was realized by using a 104-channel GEOMETRICS GeoEel digital streamer with a group interval of 1.56 m.

A 1.7 l GI Gun was operated at ~200 bar in harmonic mode with a shot interval of 4 s, resulting in an average shot-spacing of ~8 m, and achieved a general sub-bottom penetration of up to 1 s TWT. A dense grid of 2D reflection seismic profiles offshore Mt Etna was collected with this system (Fig. MI-2a).

The seismic profiles were processed using the commercial software package Gedco Vista Seismic Processing. Processing including a 20/40/200/400 Hz band pass filter, despiking, CMP-binning, Normal-Move-Out Correction and debias-filtering. The CMP bin size was set to 2 m, which resulted in an average fold of 14. Due to the limited offset range of the relatively short streamer, Normal-Move-Out is not sensitive to a dedicated velocity analysis. Therefore, a constant velocity of 1500 m/s was applied to the dataset. All data were time-migrated by using the software's finite difference migration method with a constant velocity of 1500 m/s.

Bathymetric data were acquired with a hull-mounted Kongsberg EM122 mutlibeam-echosounder. The presented bathymetric grid in this work has a cell size of 30x30m and represents a combination of the bathymetric data presented by *Chiocci et al. [2011]*, and the new acquired M86/2 dataset.

3 Results

To account for the complex morphology offshore Mt Etna *[Chiocci et al. 2011; Argnani et al. 2013; Gross et al. 2014 – this thesis]*, we divided the study area off Mt Etna's eastern flank into four different morphological domains (coloured boxes in Fig. MI-2):

i) Riposto Ridge

ii) Basins at the toe of the continental margin

iii) The Amphitheatre, the adjacent Valle Di Archirafi and the Riposto Depression

iv) Timpe Plateau and the southern boundary of the moving flank

These individual domains will be described separately before being combined in a general discussion of the regional tectonics.

3.1 Riposto Ridge

Riposto Ridge (RR) is a prominent W-E trending, ~22 km long and up to ~6 km wide ridge, that rises up to 700 m above the surrounding seafloor (Fig. MI-3). Its southern flank has slope gradients of up to 30°, whereas the northern flank is characterized by slope gradients of ~10-20°. The ridge is shaped by multiple gullies and channels with an increase in channel density at the northern flank where they cut up to ~150 m into the subsurface (Fig. MI-3). From its morphological and internal structure, the ridge can be divided into three major domains.

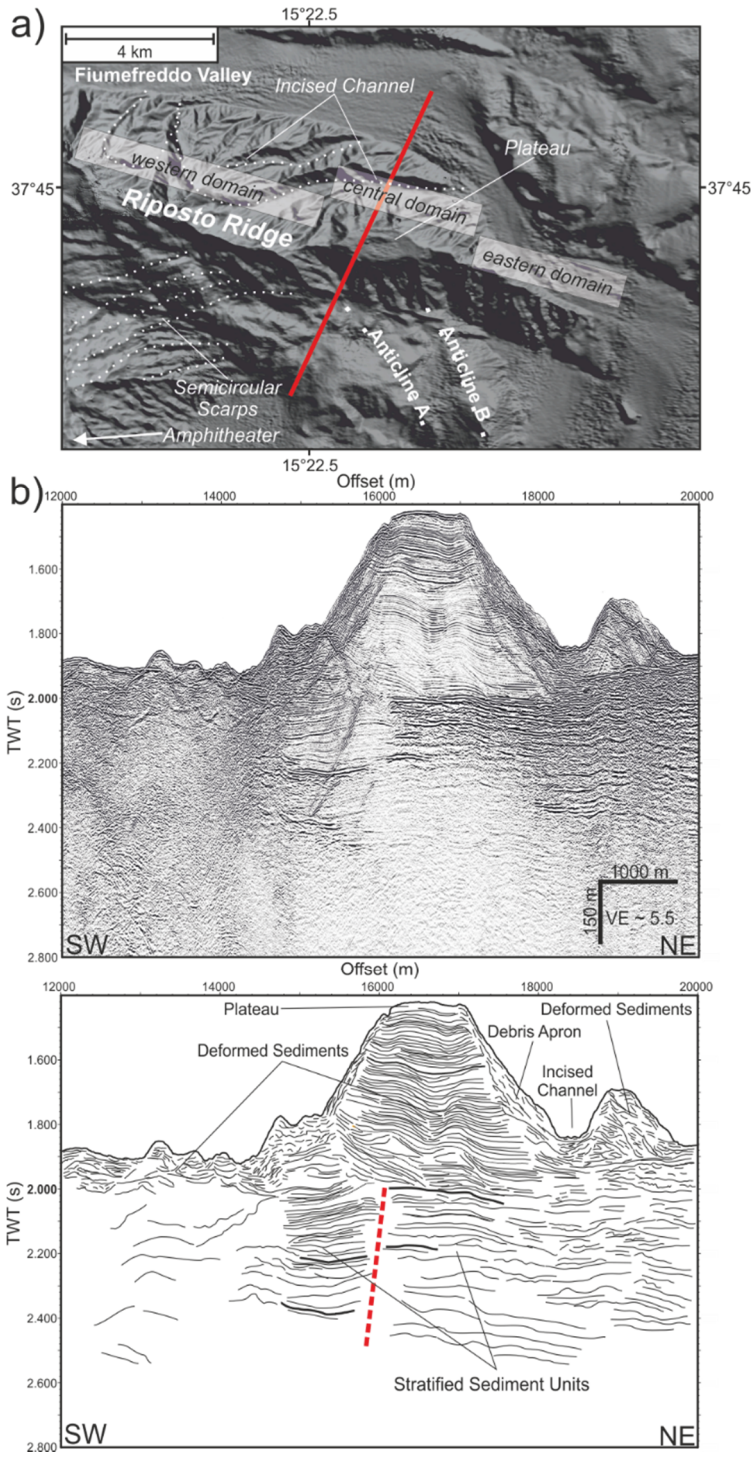

Figure MI-3: a) Morphology of Riposto Ridge (RR) and its surroundings. RR is a prominent elongated ridge at the northern boundary of Mt Etna's moving flank. The northern realm of RR is characterized by two E-W trending incised channels, which are overprinted by gullies and channels. The location of the map is shown as orange dashed box on Fig. MI-2b) SW-NE trending seismic profile M86-2-248 crossing the central domain of RR (See Fig. MI-3a for location). The ridge is highly deformed in its upper units and is underlain by undisturbed well-stratified sedimentary units. A steep normal fault, marked as dashed red line, is imaged underneath the deformed strata. Mass movements such as debris flows are seen on the flanks of the ridge. The upper surface of RR appears as flat plateau-like feature. Overall, RR represents a highly heterogeneous, tectonically controlled feature offshore Mt Etna.

The western domain is characterized by a morphological connection to the amphitheater structure (see below) and reveals semicircular scarps at its southern flank that can be traced into the crest of the amphitheater structure (Figs. MI-2, MI-3). In the central domain (Fig. MI-3), deeply incised channels are imaged at the northern side of the ridge. Here, deformed sediments can be observed in the upper ~300 m (~0.4 s TWT) of sediments, which are underlain by a package of high amplitude continuous reflections; these high amplitude continuous reflectors can be traced towards the northern end of the seismic line shown on Fig. MI-3b. The seafloor expression shows a plateau at this part of the ridge (Fig. MI-3). A southward dipping normal fault is found at a depth of ~1500 m (2 s TWT), and can be traced to a depth of ~1950 m (~2.6 s TWT). This fault shows a vertical displacement of ~150 m (~200 ms TWT). The eastern domain of the ridge includes the tip of the ridge, which is bent towards the south (Fig. MI-3). An apron of high amplitude and discontinuous reflections surrounds RR on the northern and southern flanks (Fig. MI-3).

3.2 Basins at the toe of the continental margin

Three sedimentary basins, the West, Central and East Basins (Fig. MI-4), are observed offshore Mt Etna at the toe of the continental margin. All basins widen towards the south (Figs. MI-2, MI-4). They are separated from each other by two buried anticlines (A and B in Figs. MI-4 and MI-5). This basin system is bounded to the east by the limb of a rollover-anticline (Figs. MI-4, MI-5). Anticlines A and B have a clear surface expression in the northern and central part of the working area, but plunge beneath the sedimentary basin fill towards the south, where no seafloor expression is visible. The general attitude of the hinge lines of the anticlines is convex with respect to the continental toe (Fig. MI-4). The anticlines have a thin sedimentary cover which does not exceed ~100 ms TWT (~75 m) (Figs. MI-4, MI-5). The anticlines host a seismic facies with low amplitudes, but continuous reflectors defining an upright fold with an axial plane steeply dipping to the west (Fig. MI-5). The rollover-anticline towards the east has no distinct surface expression, except for an uplift of strata around the axis of the fold (Figs. MI-4, MI-5).

The large East Basin shows maximum widths of ~12 km and sediment thicknesses of up to ~750 m (1000 ms TWT) (Fig. MI-4). The seafloor is inclined towards the south (Fig. MI-4). The northernmost tip of East Basin lies south of RR. East Basin can generally be described as an asymmetric half-graben, limited by a westward dipping growth fault in the west and the limb of a buried anticline in the East (Fig. MI-4a). This basin can be traced towards the south where it does not show indications for an anticline west of its growth fault *[Bianca et al. 1999; Nicolich et al. 2000; Argnani and Bonazzi 2005]*.

Based on a seismic facies characterization, the sediment infill of East Basin subdivides into four major seismic units (Fig. MI-4, MI-5):

- Unit-A: The lowermost seismic unit (Figs. MI-4, MI-5) is characterized by low amplitude, continuous reflectors that dip to the west. Strata have uniform thicknesses and show little internal deformation. The seismic facies of Unit A is similar to the shallow sub-surface sediments to the east of the East Basin, indicating the spatial continuity of Unit A into this area (Figs. MI-4, MI-5).

- Unit-B: The boundary zone between Unit A and Unit C is characterized by a seismic unit, which thickens towards the south (Fig. MI-5). Acoustically, Unit B is characterized by moderate amplitude, chaotic reflectors.

- Unit-C: The central Unit C is characterized by high-amplitude continuous reflectors, pinching out towards the east (Figs. MI-4, MI-5). In the eastern part of East Basin, uplift of strata is visible, whereas the western boundary of the basin is marked by a growth fault and subsidence.

- Unit-D: The uppermost Unit D (Fig. MI-4, MI-5) is characterized by sub-horizontal reflectors with almost no internal deformation. Towards Anticline B (Figs. MI-4, MI-5), the uppermost strata form a moat, whereas towards the east they form part of the rollover-anticline described above (Fig. MI-5).

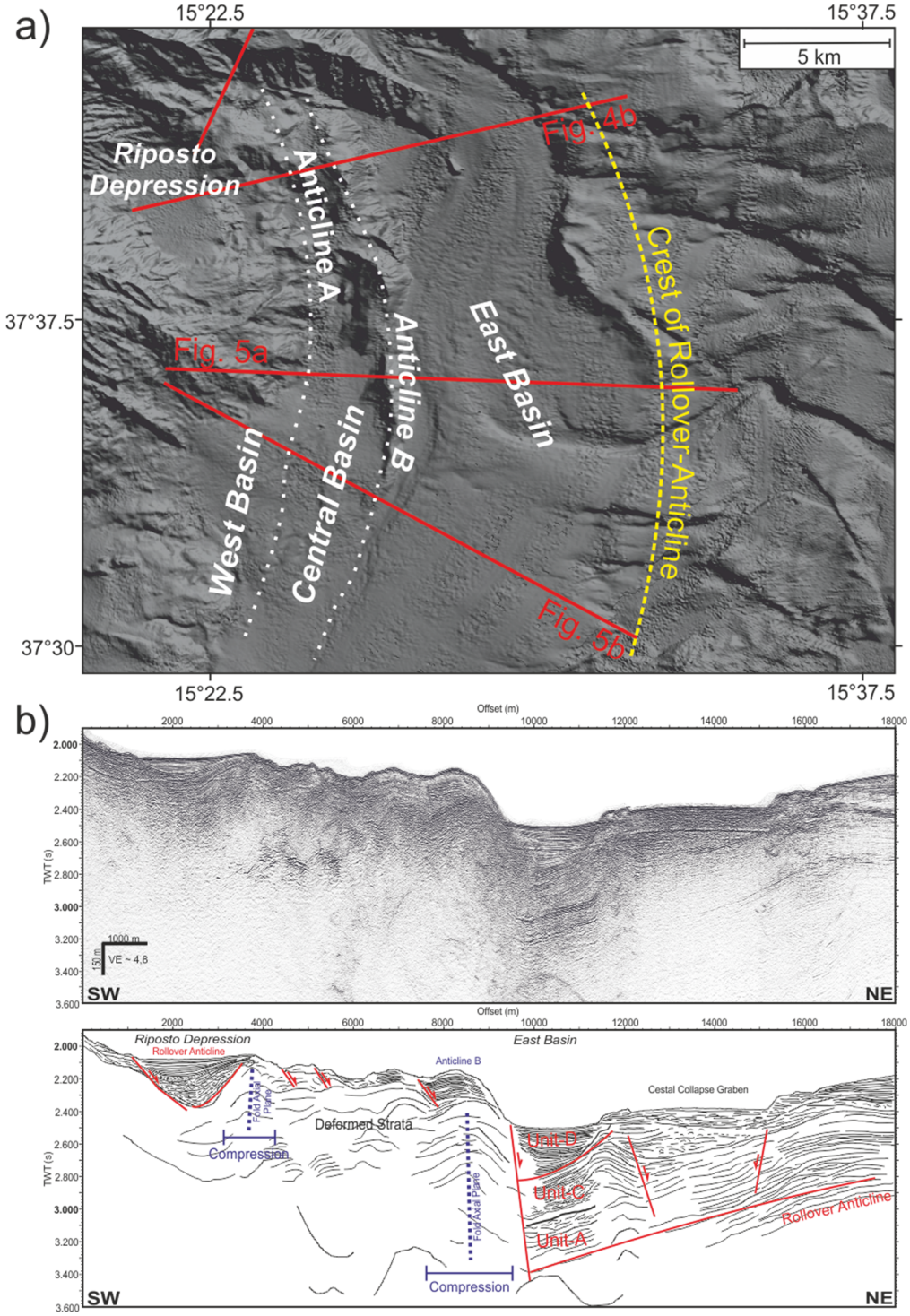

Figure MI-4: a) Bathymetry of West Basin, Central Basin and East Basin. Red lines are seismic profiles, shown in this work. The basins reveal a general southward dip and widen towards the South. The three basins are bound by anticlines, which host surface expressions in the northern and central regions of the working area. See green dashed box in Fig. 2 for location of map. b) Seismic profile M86-2-p243 and its interpretation (See Fig. 4a for location of profile).The profile presents the northernmost tip of the half-graben shaping East Basin, which is bound by a steep growth fault and a rollover anticline. The central part of the profile is dominated by deformed sedimentary units, which are affected by the Anticlines A and B. The southwestern part of the seismic profile images Riposto Depression, which is a sedimentary basin at the toe of the steep Amphitheater headwall (see below). Similar to East Basin, it is bound by a growth fault in the southwest and characterized by a rollover-anticline.

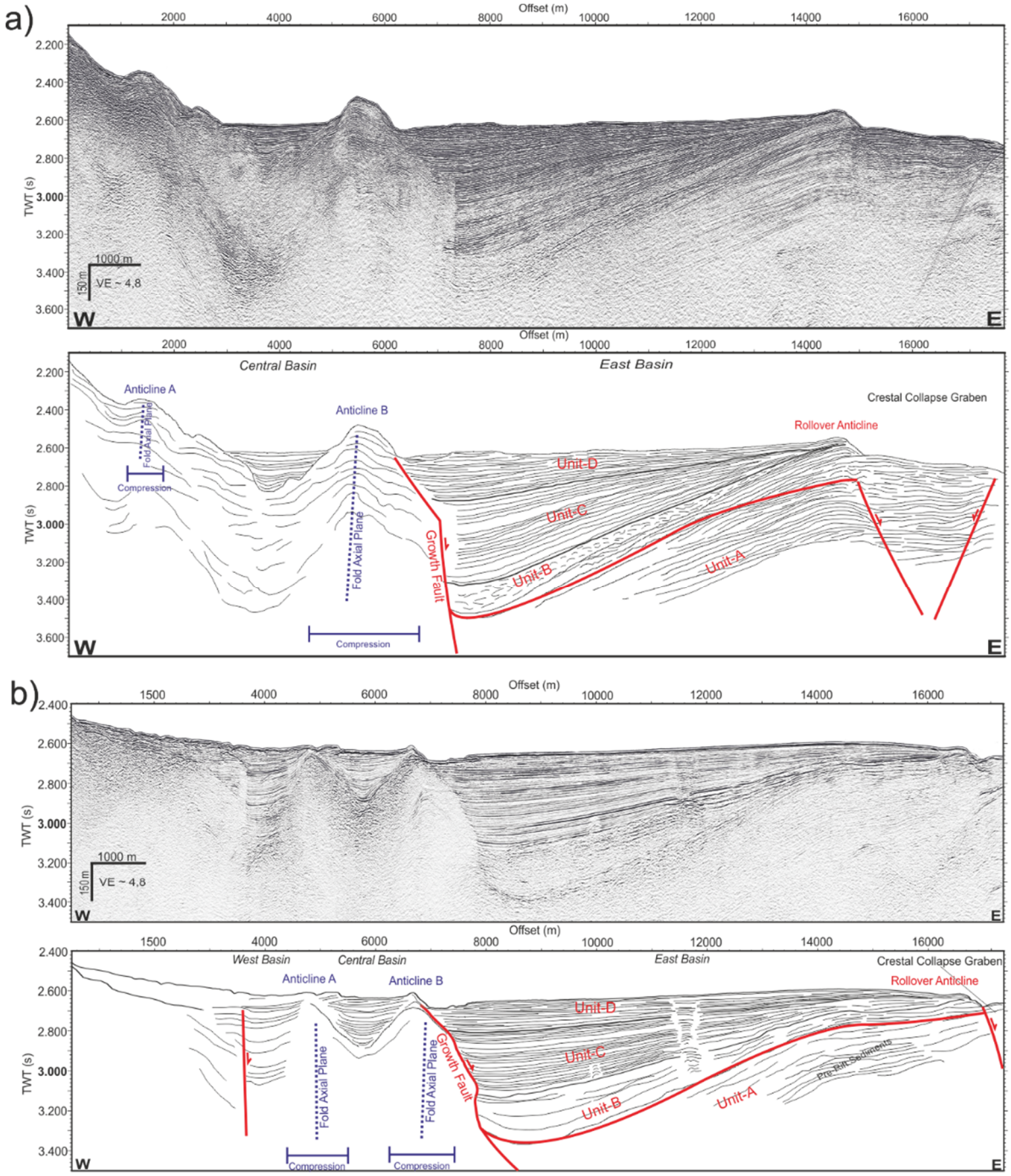

Figure MI-5: a) W-E striking seismic profile M86-2-p703 crossing the central footwall sedimentary basins and interpretation (See Fig. 4a for location). East Basin appears to form a half-graben filled by pre-rift and syn-rift sediments. To the west, it is bound by a growth fault, which is adjacent to Anticline B. The entire Basin is affected by a rollover-anticline; the crest of the rollover-anticline is adjacent to a crestal collapse graben. The westernmost Central basin is characterized as a graben, bound by Anticline A in the west and Anticline B towards the east. b) Southernmost seismic profile M86-2-p704, crossing the sedimentary basins at the toe of the continental margin (See Fig. 4a for location). West Basin and Central Basin are sedimentary basins, confined by the continental margin towards the west and Anticline A and Anticline B towards the east. East Basin is a half-graben, bound by an eastward dipping growth fault towards the west; it is underlain by the rollover-anticline; the crest of this rollover-anticline is outcropping in the east. The onset of a crestal collapse graben is visible in the east.

Central Basin (Fig. MI-2, MI-4a) shows a maximum width of ~3000 m and reveals a sediment infill of ~150 m (200 ms TWT). It is separated from the East Basin (Fig. MI-4) by Anticline B and towards the West by Anticline A. It reveals well-stratified, high amplitude, continuous reflectors, which terminate at the flank of Anticline A and Anticline B (Fig. MI-5).

Farther towards the toe of the continental margin, West Basin lies adjacent to Mt Etna's eastern flank (Fig. MI-2, MI-4a). It is only present in the southernmost profiles across the sedimentary basins, and seafloor morphology suggests that it continues farther to the south (Fig. MI-4a, MI-5b). Its boundary is defined by Anticline A (Fig. MI-4a, MI-5b), separating it from the Central Basin (Fig. MI-4). It reveals widths of up to 4000 m, whereas its sedimentary infill extends up to ~490 m (~650 ms TWT) (Fig. MI-5). Its internal structure is dominated by westward dipping high amplitude reflectors, terminating in the East against Anticline B (Fig. MI-5). To the west, West Basin is constrained by the continental margin and an adjacent shallow dipping fault (Fig. MI-5).

3.3 The Amphitheatre and the Valle Di Archirafi

South of RR, the massive amphitheater-like structure with an estimated headwall length of ~20 km represents one of the most prominent seafloor features offshore Mt Etna *[Chiocci et al. 2011; Gross et al. 2014 – this thesis]* (Fig. MI-6a). The amphitheater encloses the Riposto Depression, a small basin with a lateral extent of ~ 13.5 km2 (Fig. MI-6a). Seismic reflection data and high resolution PARASOUND echo sounder data across Riposto Depression reveal an internal seismic facies, dominated by high amplitude reflectors intersected by localized chaotic seismic units that are interpreted as mass transport deposits *[Gross et. al 2014 – this thesis]*. The amphitheater headwall is located at the eastern section of a structural high, expressed by the topographic structural high in Fig. MI-6a. Prominent northward trending ridges with lengths between 2500 and 5500 m, and heights of up to 60 m are present on the western part of the seismic profile shown on Fig. MI-6a. The morphological expression of these ridges vanishes towards the southern flank of Riposto Ridge. The Valle Di Archirafi (VdA) is located west of the amphitheater's headwall and the prominent structural high (Fig. MI-6a). This funnel-shaped sedimentary system covers an area of ~55 km^2 and is characterized by multiple small WNW-striking gullies and channels cutting into the deposits close to the coastline.

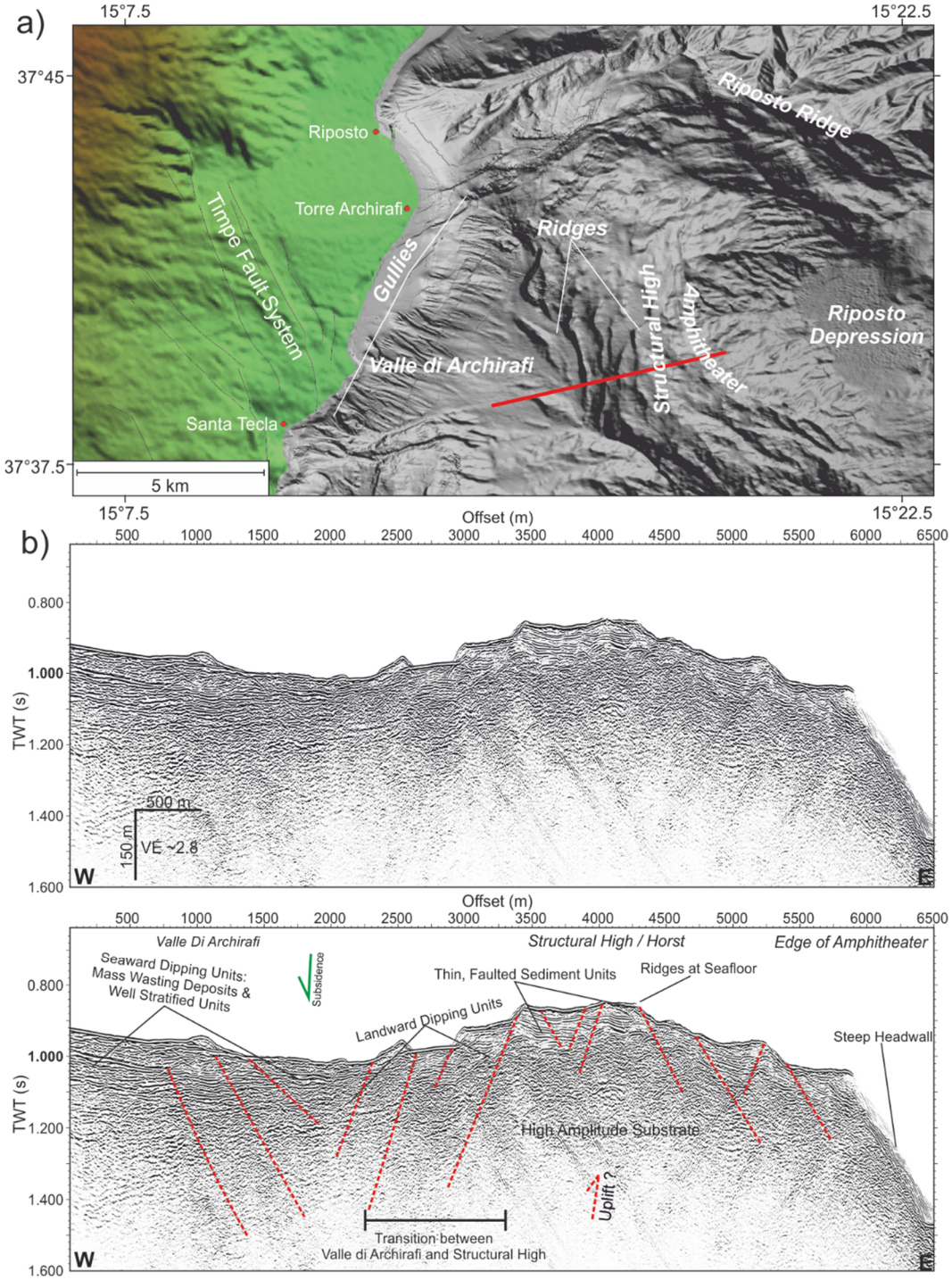

Figure MI-6: a) Bathymetry of the amphitheater and its adjacent funnel shaped Valle di Archirafi (VdA). The morphology hosts a variety of incised gullies at the proximal areas of VdA, whereas the transition to the structural high at the amphitheater headwall is dominated by N-S ridges. Onshore Tectonics after *Bonforte et al. [2011]*. See dashed blue box on Fig. 2 for location of map.b) Reflection seismic profile M86-2-p243 and its interpretation across VdA, the structural high at the amphitheater and the steep headwall of the amphitheater (See Fig. 6a for location. The western part of the profile shows the eastward dipping sedimentary infill of the VdA, which comprises some eastward dipping normal faults. The transition towards the local structural high / horst is characterized by an abrupt change in seismic facies and the onset of westward dipping sedimentary units. The onset of westward dipping normal faults is imaged. Within the first 200 ms TWT, the structural high/horst features westward dipping normal faults in its western realm, whereas the eastern realm, close to the amphitheater headwall, is characterized by eastward dipping normal faults. Except for a thin well stratified sedimentary drape on top of the structural high/horst, the internal structure is dominated by a high amplitude, low coherent substrate.

The internal sedimentary architecture of VdA exhibits seaward dipping units, that abut against the structural high (Fig. MI-6b, MI-6c). They are characterized by well-stratified continuous seismic reflector packages interlayered with chaotic to transparent sections. Some reflectors in the lower part of the section indicate diverging reflection pattern towards the west. Towards the structural high, east-dipping normal faults appear to produce small displacements in the lower part of the strata. Sediments of VdA are separated from the structural high to the east by a set of westward dipping normal faults and a change in seismic facies. The structural high is characterized as a horst close to the edge of the amphitheater headwall (Fig. MI-6). The internal seismic facies is dominated by high-amplitude units, which reveal a low coherency. The structural high is draped by a thin sedimentary cover with a thickness of ~150 ms TWT and can be separated into two major domains (Fig. MI-6b). The western domain is characterized by west-dipping normal faults, whereas the eastern domain is characterized by east-dipping normal faults. The surface expression of all faults observed in the seismic lines correlates with topographic lows in the pattern of the north-south trending ridges described above (Fig. MI-6a).

3.4 Timpe Plateau and Catania Canyon

The Timpe Plateau (TP) comprises the southern sector of Mt Etna´s offshore bulge (Fig. MI-7). Its morphological expression is dominated by east-southeast trending channel- and gully systems cutting up to 60 m into the underlying strata (Fig. MI-7a). The older sedimentary units making up the TP have a thin (up to 0.25 s TWT) undisturbed cover. The southern boundary of TP is marked by the incision of the Catania Canyon (CC) (Fig. MI-7a). The topographic ridge immediately north of CC hosts a lineament at its crest with a 292° strike direction (Fig. MI-7a). This lineament can be traced over a distance of ~9.5 km down to the depositional basin at the toe of the continental slope. It forms a morphological depression about 20 m deep. The depression is about ~850 m wide close to the coastal zone and narrows down to ~200 m at the eastern, seaward end.

High-resolution reflection seismic data show a set of faults just south of the topographic depression, and on the northern flanks of Catania Canyon (Fig. MI-7b). Fault attitudes and offsets point towards a positive flower structure with only a few meters of vertical displacement of the strata in the seismic section (Fig. MI-7c). Positive flower structures owe their geometry to transpressive movements across a strike-slip fault. The geomorphic expression of the fault system is restricted because of the high slope gradients and indications for a strong overprint by submarine mass movement events and bottom current activity *[Gross et al. 2014 – this thesis]*.

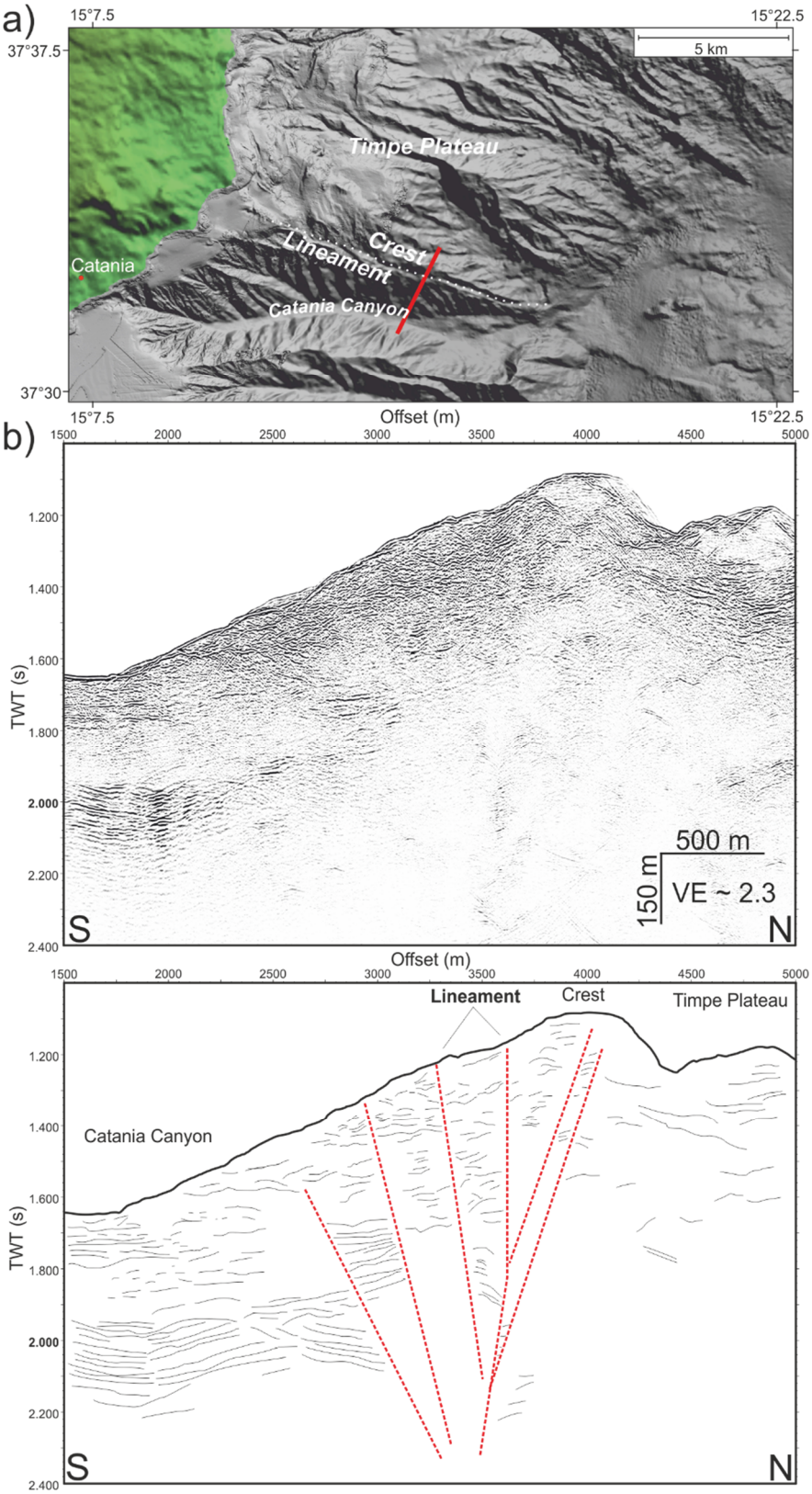

Figure MI-7: a) Bathymetry of the proposed southern boundary of Mt Etna's moving flank. *Chiocci et al. [2011]* described the 292° striking lineament at the crest north of Catania Canyon as an indicator for the outcropping boundary fault of the moving flank. Location of map is shown as dashed yellow box in Fig. 2. b) Seismic Profile M86-2-p246 crossing Catania Canyon and the northern ridge showing the subsurface structure of the lineament mentioned above (See Fig. MI-7a **for location). The profile shows a positive flower structure with faults outcropping underneath the observed lineament.**

4 Discussion

4.1 The architecture and limits of the continental margin

Mt Etna is located adjacent to the coast of eastern Sicily. For a comprehensive understanding of the tectonic setting of the volcano it is therefore inevitable to include offshore structures and morphologies and their link to onshore processes. The area affected by the build-up of Mt Etna can generally be subdivided into three major regimes (Fig. MI-8). The volcanic edifice of Mt Etna that cover the entire onshore part of the volcano but also extend into the shallow marine realm formed as a result of repeated volcanic activities during the last ~500 kyr *[Branca et al. 2011]*. The upper and middle parts of the eastern continental margin of Sicily form the immediate foundation of the volcano and are described as the continental margin regime. The morphology here is characterized by an east oriented convex bulge that hosts high slope gradients of up to 25°, as well as multiple deeply incised gullies and channels between the cities of Catania and Fiumefreddo *[Chiocci et al. 2011]* (Fig. MI-8). This bulge may display a response of magmatic inflation *[Chiocci et al. 2011]* or the result of thrust faulting *[Argnani et al. 2013]*. The third tectonic regime is the toe of the continental margin with a relatively flat morphology and several sedimentary basins, accumulating the sediments transported eastward over the slopes of the continental margin, and sediments with a northern provenance channelized through the Strait of Messina (Fig. MI-8).

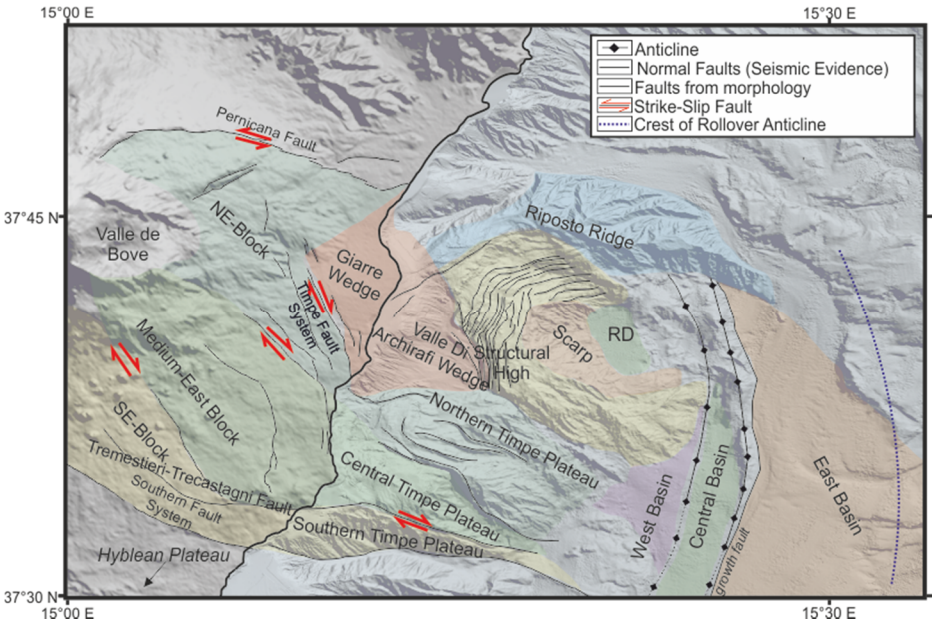

Figure MI-8: New tectonic map including high-resolution bathymetry and traced tectonic features. The offshore structures were derived from our new reflection seismic dataset. Onshore information was taken from *Bonforte et al. [2011]*.

The tectonic systems, confining the onshore volcano flank movements, are well documented *[e.g. Bonforte et al. 2011]* (Fig. MI-8). Hence, we will here concentrate on the offshore realm, mostly expressed by the continental margin off East Sicily. The bulge can be subdivided into 7 different blocks (Fig. MI-8), which are defined by their morphological expression or their tectonic origin; these blocks are discussed in the following.

Riposto Ridge is located at the expected seaward extension of the left-lateral Pernicana-Provenzana Fault System (PFS). PFS is supposed to display the northern boundary of Mt Etna's moving flank *[Bonforte and Puglisi, 2003; Bonforte and Puglisi 2006; Bonforte et al. 2007]* (Fig. MI-8). Riposto Ridge was postulated to be a submarine extension of the thrust of the Appennine Chain, which was confined by dredging of hard rocks at the northern flank of Riposto Ridge *[Gabbianelli et al. 1995; Bousquet et al. 1998]*. In contrast to the brittle deforming PFS onshore, Riposto Ridge is affected by a diffuse grade of internal deformation *[Argnani et al. 2013]* (Fig. MI-3). Riposto Ridge thus likely represents the northern boundary of Mt Etna's continental margin slope instability. Due to a lack of high-resolution data, its exact role in the geodynamic context is still to evaluate.

The Timpe Plateau (Figs. MI-8, MI-9) is considered as the seaward extension of the Hyblean Plateau *[Argnani et al. 2013]* and is dominated, as the entire bulge, by seaward oriented gullies and channels (Fig. 8). *Chiocci et al. [2011]* considered the ESE lineament at the seafloor as the surface expression of the offshore extension of the Tremestieri-Trecastagni Fault System, which was mapped by InSAR measurements onshore *[Froger et al. 2001]* and is considered as the southern boundary of the moving flank *[e.g. Bonforte et al. 2011]* (Fig. MI-8). The seismically imaged positive flower structure underlying the ESE seafloor lineaments (Fig. MI-7) strongly supports the interpretation of a transpressional regime underneath the ESE lineament. Considering the slip motion of the onshore fault, this fault likely represents a right lateral transpressive fault. Farther to the south, the seismic facies of Catania Canyon implies a major tectonic discontinuity in this area (Fig. MI-7).

The central realm of the offshore continental margin bulge is described by the Valle Di Archirafi and its adjacent local structural high (Figs. MI-8, MI-9). Whereas the structural high is characterized by a substrate underneath a thin sedimentary drape of up to ~150 m, Valle Di Archirafi (VdA) hosts major seaward dipping mass transport units, which are confined towards the structural high (Figs. MI-6). Based on a seismic facies analysis, VdA likely represents an accommodation basin that catches debris from onshore sector collapses and submarine mass wasting events. The entire area is dominated by normal faulting leading to overall subsidence of the VdA in respect to the structural high (Fig. MI-6).

The amphitheater is a semi-circular structure enclosing Riposto Depression (Fig. MI-8). It is characterized by extensional tectonics towards the steep headwalls (Fig. MI-6). We consider it as an ancient structure, which is strongly overprinted by recent tectonic events such as the formation of the

adjacent structural high and a possible rotation of the entire continental margin in a counter-clockwise rotation at its southern boundary (Figs. MI-8, MI-9). Minor failures occurred at the steep slopes of the amphitheater, creating small-scale mass transport deposits in Riposto Depression and its adjacent sedimentary systems. The small-scale mass transport deposits can be traced within upper first ~100 m of the sedimentary record *[Gross et al. 2014 – this thesis]*. As it is still unclear, whether a large scale mass wasting event, the tectonic setting of the continental margin or a combination of both has formed this semi-circular amphitheater: Further investigations have to be carried out in this area.

Anticlines A and B are open upright folds, which are located in concave-shape in front of the continental bulge (Fig. MI-8, MI-9). The anticlines are only overlain by a thin sedimentary cover, attesting to young or active processes of deformation. Both appear to be deep-seated compressive structures indicating an east-west shortening of the sediments making up the continental toe off eastern Sicily. It is not entirely resolved if these anticlines are rollover structures of a larger extensional detachment system. However, the detachment would have to be relatively shallow given the small wavelength of the structures, and should be imaged in our seismic sections if present. The West- and Central Basins (Figs. MI-4, MI-5) are small basins, which act as sediment traps behind the evolving anticlines. The concave shape of the anticline's fold axial plane in front of the continental margin indicates a compressional regime at the toe of the continental margin. Its semi-circular westward opening arrangement stands in strong contrast to the eastward opening semi-circular structures, which can be observed on- and offshore. As these anticlines at the toe of the continental margin are not traceable south and north off Mt Etna, we consider these structures to be bound to the presence of Mt Etna.

4.2 Coupling of volcano flank gliding and continental margin spreading

As observed at passive continental margins, gravity gliding, gravitational collapse as well as spreading play an important role at continental margins *[e.g. Morley et al. 2011; Peel 2014]*. As the continental margin displays a bulge, which is only observed in front of Mt Etna's edifice offshore east Sicily, we consider a strong connection of processes leading to volcano buildup and bulging at the continental margin. The origin of the bulge is still debated. *Chiocci et al. [2011]* suggest an intrusive inflation of the bulge related to Mt Etna's magmatic feeder, whereas *Argnani et al. [2013]* interpret it as a response to thrusting. Our new data show extensional structures within the upper ~500 m of the sedimentary cover at the continental margin bulge which are displayed as normal faults (Figs. MI-8, MI-9). Furthermore, the entire bulge is affected by a high grade of denudation. As the observed fault systems display seaward and landward dipping fault planes, we consider a gravitational collapse and spreading rather than a pure gliding to be present at the continental margin (Figs. MI-8, MI-9). The anticlines at the toe of the

continental margin indicate contraction, off the eastern flank of Mt Etna. We interpret these anticlines as the eastern limit of the observed continental margin instability (Fig. MI-9). The anticlines show highest level of compression and more distinct seafloor expressions in their Northern- and Central parts (compare Figs. MI-5a and MI-5b). This is most likely a result of higher flank movement rates at the Northern and Central blocks of the volcano edifice (Fig. MI-8), which is in good agreement with onshore observations by *Acocella and Puglisi [2013]*. Furthermore, we see clear implications for a coupled gravitational instability of the volcano edifice and the continental margin, which could be the result of a dipping substrate-décollement *[Wooller et al. 2004]*, as the southern flank boundary can be traced over the volcano edifice at the Tremestieri-Trecastagni Fault System into the offshore realm to the lineament at the continental margin (Fig. MI-9). The coupled edifice- and continental margin instability is limited towards the north by the Pernicana-Provenzana Fault and Riposto Ridge and towards the south by the Tremestieri-Trecastagni Fault System and its offshore continuation, north of Catania Canyon (Fig. MI-9). The continental margin instability extends down to the continental toe, were the two concave anticlines display the eastern limit of the moving system (Fig. MI-9).

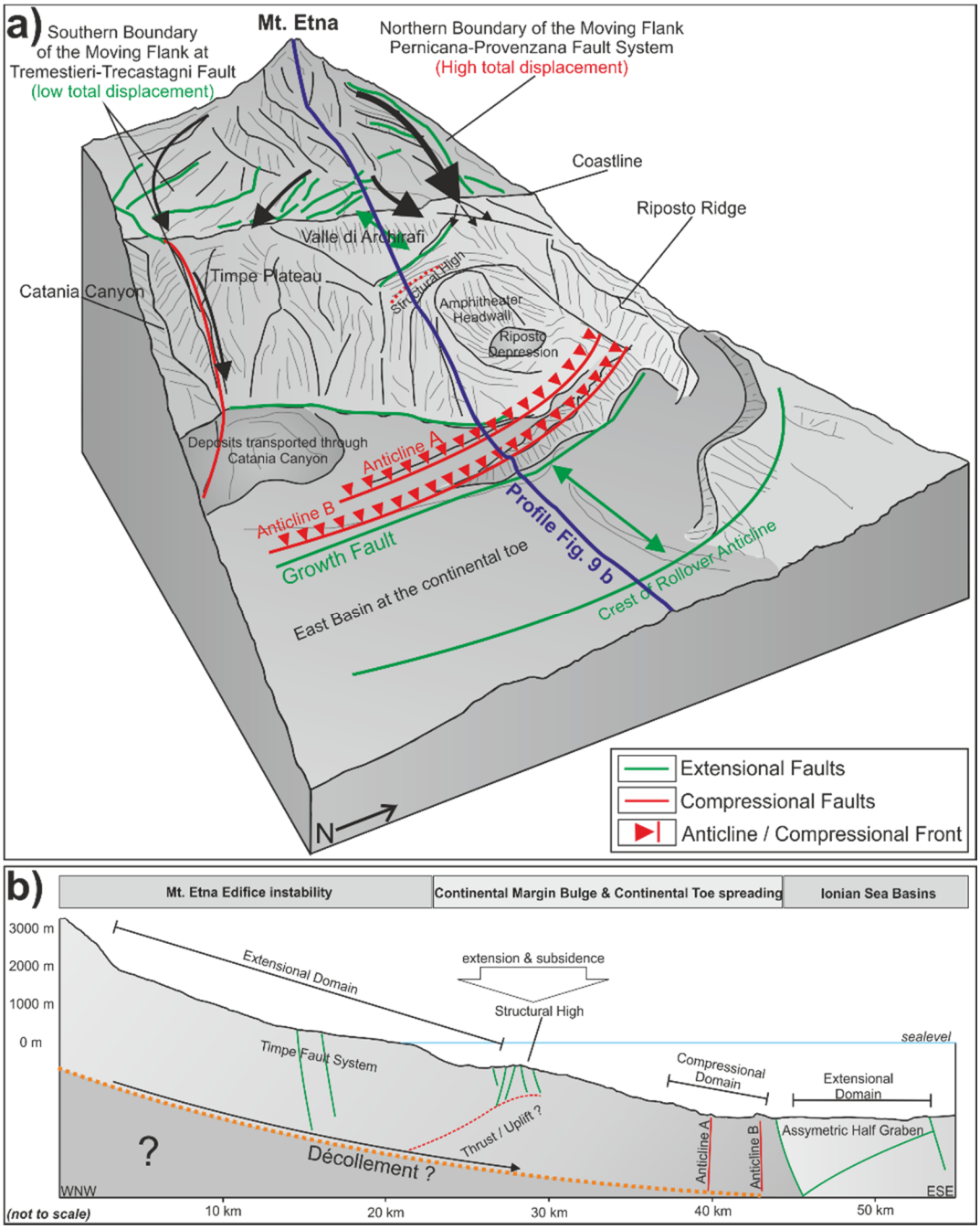

Figure MI-9: a) Model for the volcano edifice and continental margin instability. The limits of the moving flanks are described as two anticlines indicating shortening in this regime. The prominent half graben observed in front of the continental slope is a pre-Etnean feature, which can be traced south of the prominent continental bulge and is only partially influenced by the instability observed at the volcano and its adjacent continental margin. b) Sketch (not to scale) across the Volcano Edifice, the continental margin and the sedimentary basins in the Ionian Sea. The entire volcano flank is bound by the Pernicana-Fault System in the north and the Tremestieri-Trecastagni Fault System in the south. The volcano edifice is dominated by seaward dipping normal faults like the Timpe Fault System, but landward dipping faults can be traced at the continental margin as well. This implies a gravitational collapse and spreading at the continental margin off Mt Etna's edifice. As some of the faults like the Tremestieri-Trecastagni Fault System can be traced from the volcano edifice over the continental margin, we interpret the entire system as a coupled volcano edifice- and continental margin instability. The coupled instability is limited at two concave anticlines, which are located in front of the continental toe. The basin east of the anticline is bound by a growth fault and is rather related to the regional tectonic setting, as it can be traced further to south in continental margin areas not affected by Mt Etna. Based on our data, we cannot decide, if the entire system is underlain by a constant décollement or decoupled.

4.3 Sedimentary- and tectonic systems at the toe of the continental margin

East Basin with its distinct growth fault reveals fault displacements of up to 550 m (-0.75 s TWT) in the upper 1 s TWT; it is located east of the two anticlines (Figs. MI-4, MI-5, MI-8). This asymmetric half graben is one of the graben systems, which can be traced farther south to an area east of the Malta Escarpment *[Hirn et al. 1997; Bianca et al. 1999; Nicolich et al. 2000; Argnani and Bonazzi, 2005]*. Several authors suggest that the growth faults play an important role in generation of hazardous earthquakes like the 1693 Catania Earthquake *[Bianca et al. 1999; Argnani et al. 2012]*.

In contrast to deep reflection/refraction seismic data, our high resolution dataset only images the upper 1000 ms TWT (~750 m) of the sedimentary succession, making it impossible to constrain deep tectonic features. Therefore, we do not have the ability to image and analyses deep tectonic features in the working area. Additional deep seismic data and related high-resolution seismic datasets are necessary to evaluate the trend of a possible STEP fault (Fig. MI-1) *[Polonia et al. 2012; Gallais et al. 2013: Argnani 2014]* in this area and to investigate if a distinct surface feature matches with this postulated crustal scale tectonic feature.

5 Conclusions

We analyzed new high-resolution seismic dataset in order to investigate near surface processes offshore Mount Etna, which are controlled by deep tectonic features as well as regional tectonic regimes.

- In front of the toe of the continental margin, two vertical concave anticlines result from ongoing seaward migrating gravitational spreading of the continental margin. In contrast, normal faults suggest an extensional regime for the upper continental margin.

- The southern boundary of Mt Etna's moving flank is most likely located north of Catania Canyon. The entire area is underlain by a positive flower structure, indicating a transpressional regime in this area. The mapped fault system is the prolongation of onshore-observed fault movements. The exact location of the northern boundary of the moving flank is still to evaluate, as Riposto Ridge shows rather defuse deformation, then a distinct boundary fault.

- The structural high west of the amphitheater headwall is characterized by prominent ridges, which are the surface expression of a normal fault system.

- The sedimentary basins at the toe of Mt Etna's continental margin have to be addressed to a pre-Etnean genesis.

All findings show that the continental margin offshore Mt. Etna's edifice is strongly overprinted by recent tectonic activity. We consider a coupled volcano edifice / continental margin instability to be present, which can be traced from the toe of the continental margin towards the volcano edifice. As most of the models for Mt Etna's flank instability base on onshore observed and monitored data, we emphasize the need of advanced models, in which the continental margin spreading is addressed.

6 Literature

Acocella, V., Behncke, B., Neri, M., D'Amico, S., 2003. Link between major flank slip and 2002–2003 eruption at Mt. Etna (Italy). Geophysical Research Letters 30. 2286. DOI:10.1029/2003GL018642

Acocella, V., Puglisi, G., 2013. How to cope with volcano flank dynamics? A conceptual model behind possible scenarios for Mt. Etna. Journal of Volcanology and Geothermal Research 251. 137–148. DOI:10.1016/j.jvolgeores.2012.06.016

Argnani, A., Bonazzi, C., 2005. Malta Escarpment fault zone offshore eastern Sicily: Pliocene-Quaternary tectonic evolution based on new multichannel seismic data. Tectonics 24. DOI:10.1029/2004TC001656

Argnani, A., Armigliato, A., Pagnoni, G., Zaniboni, F., Tinti, S., Bonazzi, C., 2012. Active tectonics along the submarine slope of south-eastern Sicily and the source of the 11 January 1693 earthquake and tsunami. Natural Hazards Earth System Sciences 12. 1311–1319. DOI:10.5194/nhess-12-1311-2012

Argnani, A., Mazzarini, F., Bonazzi, C., Bisson, M., Isola, I., 2013. The deformation offshore of Mount Etna as imaged by multichannel seismic reflection profiles. Journal of Volcanology and Geothermal Research 251. 50–64. DOI:10.1016/j.jvolgeores.2012.04.016

Argnani, A., 2014. Comment on the article "Propagation of a lithospheric tear fault (STEP) through the western boundary of the Calabrian accretionary wedge offshore eastern Sicily (Southern Italy)" by Gallais et al., 2013 Tectonophysics. Tectonophysics 610. 195–199. DOI:10.1016/j.tecto.2013.06.035

Bianca, M., Monaco, C., Tortorici, L., Cernobori, L., 1999. Quaternary normal faulting in southeastern Sicily (Italy): a seismic source for the 1693 large earthquake. Geophysical Journal International 139. 370–394. DOI:10.1046/j.1365-246x.1999.00942.x

Bonforte, A., Puglisi, G., 2003. Magma uprising and flank dynamics on Mount Etna volcano, studied using GPS data (1994–1995). Journal of Geophysical Research 108. 2153. DOI:10.1029/2002JB001845

Bonforte, A., Puglisi, G., 2006. Dynamics of the eastern flank of Mt. Etna volcano (Italy) investigated by a dense GPS network. Journal of Volcanology and Geothermal Research 153. 357–369. DOI:10.1016/j.jvolgeores.2005.12.005

Bonforte, A., Branca, S., Palano, M., 2007. Geometric and kinematic variations along the active Pernicana fault: Implication for the dynamics of Mount Etna NE flank (Italy). Journal of Volcanology and Geothermal Research 160. 210–222. DOI:10.1016/j.jvolgeores.2006.08.009.

Bonforte, A., Gambino, S., Neri, M., 2009. Intrusion of eccentric dikes: The case of the 2001 eruption and its role in the dynamics of Mt. Etna volcano. Tectonophysics 471. 78–86. DOI:10.1016/j.tecto.2008.09.028

Bonforte, A., Guglielmino, F., Coltelli, M., Ferretti, A., Puglisi, G., 2011. Structural assessment of Mount Etna volcano from Permanent Scatterers analysis. Geochemistry Geophysics Geosystems 12. DOI:10.1029/2010GC003213.

Bonforte, A., Federico, C., Giammanco, S., Guglielmino, F., Liuzzo, M., Neri, M., 2013. Soil gases and SAR measurements reveal hidden faults on the sliding flank of Mt. Etna (Italy). Journal of Volcanology and Geothermal Research 251. 27–40. DOI:10.1016/j.jvolgeores.2012.08.010

Borgia, A., Ferrari, L., Pasquarè, G., 1992. Importance of gravitational spreading in the tectonic and volcanic evolution of Mount Etna. Nature 357. 231–235. DOI:10.1038/357231a0

Borgia, A., Treves, B., 1992. Volcanic plates overriding the ocean crust: structure and dynamics of Hawaiian volcanoes.Geological Society, London, Special Publications 60. 277–299. DOI:10.1144/GSL.SP.1992.060.01.18

Bousquet,J.C., Gabbianelli,G., Lanzafame,G., Sartori,R., 1998. Evolution volcanotectonique de l'Etna (Sicilie): nouvelles données de géologie marine et terrestre. Rapport de la Commission Internationale pour l'Exploration Scientifique de la Mer Méditerranee, 35. 56–57

Branca, S., Del Carlo, P., 2004. Eruptions of Mt Etna during the past 3,200 years: a revised compilation integrating the historical and stratigraphic records. In:Bonaccorso, A., Calvari, S., Coltelli, M., Del Negro, C., Falsaperla, S. (Eds.), Mt. Etna: Volcano Laboratory. Geophysical Monograph Series 143. American Geophysical Union, Washington, D.C..1–27.

Branca, S., Coltelli, M., Groppelli, G., 2004. Geological evolution of Etna volcano. In: Bonaccorso, A., Calvari, S., Coltelli, M., Del Negro, C., Falsaperla, S. (Eds.), Mt. Etna: Volcano Laboratory. Geophysical Monograph Series, 143. American Geophysical Union, Washington, D.C.. 49–63.

Branca, S., Coltelli M., Groppelli G., Lentini F., 2011. Geological map of Etna volcano, 1: 50,000 scale. Italian Journal of Geosciences 130. 265-291. DOI:10.3301/IJG.2011.15

Chiocci, F. L., Coltelli, M., Bosman, A., Cavallaro, D., 2011. Continental margin large-scale instability controlling the flank sliding of Etna volcano. Earth and Planetary Science Letters 305. 57–64. DOI:10.1016/j.epsl.2011.02.040

Cocina, O., Neri, G., Privitera, E., Spampinato, S., 1997. Stress tensor computations in theMount Etna area (Southern Italy) and tectonic implications. Journal of Geodynamics 23. 109–127. DOI:10.1016/S0264-3707(96)00027-0

Delcamp, A., van Wyk de Vries, B., James, M.R., 2008. The influence of edifice slope and substrata on volcano spreading. Journal of Volcanology and Geothermal Research 177. 925–943. DOI:10.1016/j.jvolgeores.2008.07.014

Doglioni, C., Innocenti, F., Mariotti, G., 2001. Why Mt Etna?. Terra Nova 13. 25–31. DOI:10.1046/j.1365-3121.2001.00301.x

Farr, T.G., Rosen, A., Caro, E., Crippen, R., Duren, R., Hensley, S., Kobrick, S., Rodriguez, E., Roth, L., Seal, D., Shaffer, S., Shimada, J., Umland, J., Werner, M., Oskin, M., Burbank, D., Alsdorf, D., 2007. The Shuttle Radar Topography Mission. Reviews of Geophysics 45. DOI:10.1029/2005RG000183

Firth, C., Stewart, I., McGuire, W.J., Kershaw, S., Vita-Finzi, C., 1996. Coastal elevation changes in eastern Sicily: implications for volcano instability at Mount Etna. Geological Society, London, Special Publications 110. 153–167. DOI:10.1144/GSL.SP.1996.110.01.12

Froger, J.L., Merle, O., Briole, P., 2001. Active spreading and regional extension at Mount Etna imaged by SAR interferometry. Earth and Planetary Science Letters 187. 245–258. DOI:10.1016/S0012-821X(01)00290-4

Gabbianelli, G., Lanzafame, G., Lucchini, F., Pompilio, M., Rossi, L.P., Sartori, R., 1995. Indagini di geologia marina alla base orientale dell'Etna. In: Ferrucci, F., Innocenti, F. (Eds.), Progetto Etna 1993–95: Giardini, Pisa, Italy. 79–84.

Gallais, F., Graindorge, D., Gutscher, M.A., Klaeschen, D., 2013. Propagation of a lithospheric tear fault (STEP) through the western boundary of the Calabrian accretionary wedge offshore eastern Sicily (Southern Italy). Tectonophysics 602. 141–152. DOI:10.1016/j.tecto.2012.12.026

Gallais, F., Graindorge, D., Gutscher, M.A., 2014. Reply to comment on the article "Propagation of a lithospheric tear fault (STEP) through the western boundary of the Calabrian accretionary wedge offshore eastern Sicily (Southern Italy)" by Gallais et al., 2013 Tectonophysics. Tectonophysics 610. 200–203. DOI:10.1016/j.tecto.2013.10.012

Groppelli, G., Tibaldi, A., 1999. Control of rock rheology of deformation style and sliprate along the active Pernicana fault, Mt. Etna, Italy. Tectonophysics 305. 521–537. DOI:10.1016/S0040-1951(99)00035-9

Gross, F., Krastel, S., Chiocci, F.L., Ridente, D., Bialas, J., Schwab, J., Beier, J., Cukur, D., Winkelmann, D., 2014. Evidence for Submarine Landslides Offshore Mt. Etna, Italy. S. Krastel (Eds.), Submarine Mass Movements and Their Consequences, Bd. 37. 307–316. DOI:10.1007/978-3-319-00972-8_27

Gvirtzman, Z., Nur, A., 1999. The formation of Mount Etna as the consequence of slab rollback. Nature 401. 782–785. DOI:10.1038/44555

Hirn, A., Nicolich, R., Gallart, J., Laigle, M., Cernobori, L., ETNASEIS Scientific Group, 1997. Roots of Etna volcano in faults of great earthquakes. Earth and Planetary Science Letters 148. 171–191. DOI:10.1016/S0012-821X(97)00023-X

Krastel, S., Schmincke, H., Jacobs, C.L., Rihm, R., Le Bas, T.P., Alibés, B., 2001. Submarine landslides around the Canary Islands. Journal Geophysical Research. 106. DOI:10.1029/2000JB900413.

Lavecchia, G., Ferrarini, F., De Nardis, R., Visini, F., Barbano,M.S., 2007. Active thrusting as a possible seismogenic source in Sicily (sourthern Italy). Some insights from integrated structural-kinematic and seismological data. Tectonophysics 445. 145–167. DOI:10.1016/j.tecto.2007.07.007

Lentini, F., Carbone, S., Guarnieri, P., 2006. Collisional and postcollisional tectonics of the Apenninic-Maghrebian orogen (southern Italy). Dilek, Y., Pavlides, S. (Eds.), Postcollisional Tectonics and Magmatism in the Mediterranean Region and Asia. Special Paper - Geological Society of America 409. 57–81. DOI:10.1130/2006.2409(04)

Lo Giudice, E., Rasà, R., 1992. Very shallow earthquakes and brittle deformation in active volcanic areas: the Eatnean region as an example. Tectonophysics 202,. 257–268

Lundgren, P., Berardino, P., Coltelli, M., Fornaro, G., Lanari, R., Puglisi, G., Sansosti, E., Tesauro, M., 2003. Coupled magma chamber inflation and sector collapse slip observed with synthetic aperture radar interferometry on Mt. Etna volcano. Journal of Geophysical Research 108. 2247. DOI:10.1029/2001JB000657.

Marani, M.P., Gamberi, F., Bortoluzzi, G., Carrara, G., Ligi, M., Penitenti, D., 2004. Seafloor bathymetry of the Ionian Sea. In: Marani, M.P., Gamberi, F., Bonatti, E. (Eds.), From Seafloor to Deep Mantle: Architecture of the Tyrrhenian Backarc Basin: Memorie Descrittive della Carta Geologica d'Italia 44. Plate 3. Roma, System Cart.

Masson, D.G., Watts, A.B., Gee, M.J.R., Urgeles, R., Mitchell, N.C., Le-Bas, T.P., Canals, M., 2002. Slope failures on the flanks of the western Canary Islands. Earth-Science Review 57. 1-35. DOIi:10.1016/S0012-8252(01)00069-1

Moore, J.G., Clague, D.A., Holcomb, R.T., Lipman, P.W., Normark, W.R., Torresan, M.E., 1989. Prodigious submarine landslides on the Hawaiian Ridge, Journal of Geophysical Research 94. 17. 465-484.

Morley, C.K., King, R., Hillis, R., Tingay, M., Backe, G., 2011. Deepwater fold and thrust belt classification, tectonics, structure and hydrocarbon prospectivity: A review. Earth-Science Reviews 104. 41–91. DOI:10.1016/j.earscirev.2010.09.010

Musumeci, C., Scarfì, L., Palano, M., Patanè, D., 2014. Foreland segmentation along an active convergent margin: New constraints in southeastern Sicily (Italy) from seismic and geodetic observations. Tectonophysics 630. 137–149. DOI:10.1016/j.tecto.2014.05.017

Nakamura K., 1980. How do long rift zones develop in Hawaiian volcanoes?—A possible role of thick oceanic sediments. Bulletin of the Volcanological Society of Japan 25. 255–269.

Neri, M., Acocella, V., Behncke, B., 2004. The role of the Pernicana Fault System in thespreading of Mt. Etna (Italy) during the 2002–2003 eruption. Bulletin of Volcanology 66. 417–430. DOI:10.1007/s00445-003-0322-x

Neri, M., Guglielmino, F., Rust, D., 2007. Flank instability on Mount Etna: radon, radar interferometry and geodetic data from the southern boundary of the unstable sector. Journal of Geophysical Research 112. DOI:10.1029/2006JB004756

Neri, M., Casu, F., Acocella, V., Solaro, G., Pepe, S., Berardino, P., Sansosti, E., Caltabiano,T., Lundgren, P., Lanari, E., 2009. Deformation and eruptions at Mt. Etna (Italy): alesson from 15 years of observations. Geophysical Research Letters 36. L02309, DOI:10.1029/2008GL036151

Nicolich, R., Laigle, M., Hirn, A., Cernobori, L., Gallart, J., 2000. Crustal structure of the Ionian margin of Sicily: Etna volcano in the frame of regional evolution. Tectonophysics 329. 121–139. DOI:10.1016/S0040-1951(00)00192-X

Nicolosi, I., D'Ajello Caracciolo, F., Branca, S., Ventura, G., Chiappini, M., 2014. Volcanic conduit migration over a basement landslide at Mount Etna (Italy). Scientific Reports 4. DOI:10.1038/srep05293.

Pareschi, M.T., Boschi, E., Mazzarini, F., Favalli, M., 2006. Large submarine landslides offshore Mt. Etna. Geophysical Research Letters 33. DOI:10.1029/2006GL026064.

Peel, F.J., 2014. The engines of gravity-driven movement on passive margins: Quantifying the relative contribution of spreading vs. gravity sliding mechanisms. Tectonophysics 633. 126–142. DOI:10.1016/j.tecto.2014.06.023

Pino, N.A., Piatanesi, A., Valensise, G., Boschi, E., 2009. The 28 December 1908 MessinaStraits earthquake (Mw 7.1): a great earthquake throughout a century of seismology. Seismological Research Letters 80. 243–259. DOI:10.1785/gssrl.80.2.243

Polonia, A., Torelli, L., Gasperini, L., Mussoni, P., 2012. Active faults and historical earthquakes in the Messina Straits area (Ionian Sea). Natural Hazards and Earth System Sciences 12. 2311-2328. DOI:10.5194/nhess-12-2311-2012

Puglisi, G., Bonforte, A., Ferretti, A., Guglielmino, F., Palano, M., Prati, C., 2008. Dynamicsof Mount Etna before, during, and after the July–August 2001 eruption inferred from GPS and differential synthetic aperture radar interferometry data. Journal of Geophysical Research 113. B06405. DOI:10.1029/2006JB004811

Rust, D., Kershaw, S., 2000. Holocene tectonic uplift patterns in northeastern Sicily: evidence from marine notches in coastal outcrops. Marine Geology 167. 105–126. DOI:10.1016/S0025-3227(00)00019-0

van Wyk de Vries, B., Francis, P.W., 1997. Catastrophic collapse at stratovolcanoes induced by gradual volcano spreading. Nature 387, 387–390. DOI:10.1038/387387a0

Wooller, L., van Wyk de Vries, B., Murray, J.B., Rymer, H., Meyer, S., 2004. Volcano spreading controlled by dipping substrata. Geology 32. 573. DOI:10.1130/G20472.1

5 MANUSCRIPT II

High-Resolution 3D seismic imaging of spreading and gravitational instability next to a giant amphitheater headwall at the continental margin offshore Mt Etna, Italy

Felix Gross, Sebastian Krastel, Cord Papenberg, Jacob Geersen, Jörg Bialas, Federica Maisto, Jan-Hinrich Behrmann, Morelia Urlaub, Deniz Cukur, Stephanie Koch, Gareth Crutchley , Aaron Micallef, Domenico Ridente and Francesco Latino Chiocci

Draft

Planned submission to:

Geochemistry, Geophysics and Geosystems

Abstract

Flank instability of onshore Mt Etna is a well-known phenomenon which is investigated and monitored by means of geodetic stations and InSAR measurements. In contrast, little is known about the continental margin, affected by the buildup of Mt Etna, offshore the coast of East Sicily though extensional and compressional tectonic features imaged by bathymetric and seismic data suggest a strong connection of volcano flank instability and continental margin instability. We acquired a new high-resolution P-Cable 3D reflection seismic cube during RV Meteor cruise M86/2 in order to investigate tectonic controls for postulated spreading and gravitational instability at the submarine continental margin east of Mt Etna. The 3D cube is located at the transition between the funnel shaped depositional system of the Valle di Archirafi and the steep headwalls of an amphitheater structure observed offshore Mt Etna. The steep headwall of the amphitheater is directly located east of a structural high, which is strongly overprinted by a normal fault-controlled block system dipping towards the scarp of the amphitheater. Valle di Archirafi shows indications for repeated mass transport deposits but is tectonically less overprinted. The transition between the structural high and the Valle di Archirafi shows a strong heterogeneity of its morphological and internal structures. A negative flower structure suggests a right-lateral transtensional regime for this area. Our findings indicate that the central part of the submarine continental margin east of Mt Etna is strongly influenced by gravitational collapse and spreading as expressed by intense normal- and transtensional faulting. As this tectonic system seems to be highly active and directly adjacent to a massive amphitheater headwall, we consider the system as prone to future catastrophic slope failures.

1 Introduction

Mt Etna, Europe's largest volcano, rises to a height of 3323 m (Fig. MII-1). The composite volcanic edifice sitting on top of continental crust *[Gvirtzman and Nur 1999]* is highly active with an eruption history of ~500 ka *[Branca and Del Carlo 2004; Branca et al. 2004]*. Its recent volcanic unrest is documented by several eruptions per year during the past decades *[Branca and Del Carlo 2004]*. Mt Etna's geological setting is characterized by the complex compressional tectonics of the Appenine-Maghrebian Fold and Thrust Belt to the south (Fig. MII-1), and the northwest dipping Calabrian subduction zone to the southeast *[e.g. Doglioni et al. 2001]*. The Malta Escarpment (Fig. MII-1), a large northward trending crustal discontinuity between eastern Sicily's continental crust and the oceanic crust making up the Ionian Sea, is a prominent morphological feature at the seafloor. It can be traced southward and passes east of the Maltese Islands *[Lentini et al. 2006; Argnani and Bonazzi 2005]*, thereby affecting the subduction regime underneath Calabria (Fig. MII-1) *[e.g. Gvirtzman and Nur 1999; Argnani and Bonazzi 2005]*. Due to its regional importance as a deep-seated fault, a link between the Malta Escarpment and Mt Etna's edifice has been proposed *[Rust and Kershaw 2000]*. However, the complex structure and morphology of the Timpe Plateau (Fig. MII-1) makes it difficult to trace the Malta Escarpment as far north as Mt Etna's coastal offshore extension, and into the onshore volcanic edifice *[Argnani and Bonazzi 2005; Nicolich et al. 2000]*.

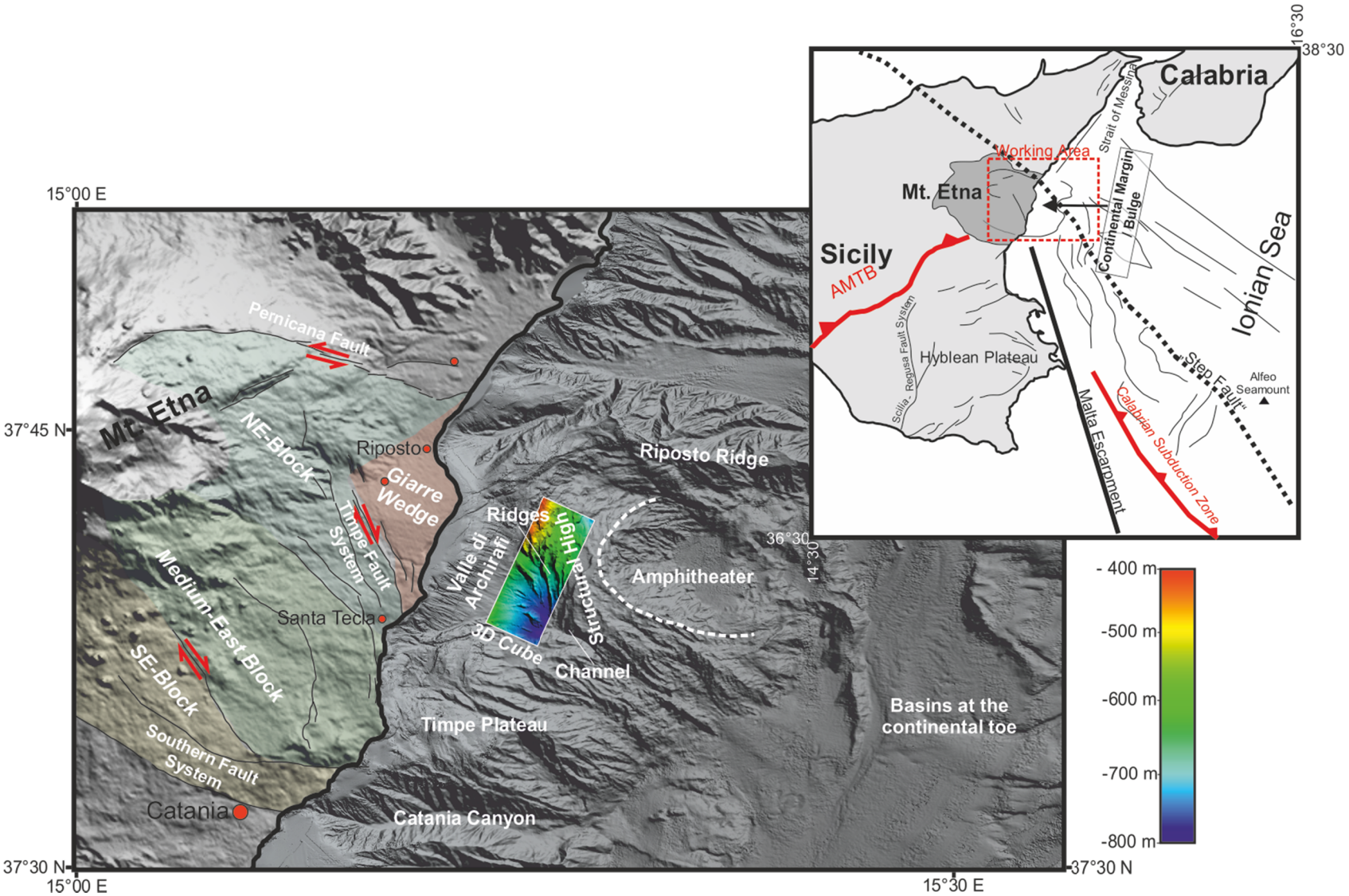

Figure MII-1: Right: General overview map of the working area with most important tectonic features. (AMTB = Appennine Maghrebian Fold and Thrust Belt). Left: Overview map of regional/local tectonic features on the subaerial/submarine flank east of Mt Etna *[modified after Argnani [2014]*. The location and surface morphology of the acquired 3D seismic cube is shaded using the same scheme as in Fig.2. The bathymetric data is combination of the map shown *by Chiocci et al. [2011] and Gross et al. [2014]*. The onshore digital elevation model is taken from *Farr et al. [2007]*. The onshore faults are taken from *[Bonforte et al. 2011]*.

Mt Etna shows clear signs of gravitational instability at its eastern and southern flank, which was first described by *Borgia et al. [1992]*. Today, Mt Etna's unstable flank is one of the best-monitored and studied examples for volcano flank instability, worldwide *(e.g. Bonforte et al. 2011)*. Evidences for both, episodic and continuous flank movements, were reported *[e.g. Froger et al. 2001; Acocella et al. 2003; Bonforte and Puglisi 2003]*. Explaining flank instability of Mt Etna is particularly challenging as deformation due to magma overpressure reaches its maximum at the summit, whereas the larger subsidence and seaward movements are recorded along the coast *[Acocella and Puglisi 2013]*. Moreover, displacement measurements are yet limited to the onshore volcano flank. The volcanic flank does not have a significant offshore continuation east of the main edifice but it is proposed that the offshore continental margin east of Mt Etna is strongly affected by the volcano buildup *[Chiocci et al. 2011; Argnani et al. 2013]*.

In contrast to the well-studied volcano edifice of Mt Etna *[e.g. Branca et al. 2011]*, only few information is available about the offshore continental margin east of Mt Etna. A first multi-beam bathymetric map showed several prominent morphologic features in the area off Mt Etna *[Marani et al. 2004]*, but the first detailed interpretation of high-resolution bathymetric data was carried out by *Chiocci et al. [2011]*. *Chiocci et al. [2011]* described intense bulging of the continental margin in front of Mt Etna's edifice, which could not be mapped further north towards the Strait of Messina and further south, next to the prominent Malta Escarpment (Fig. MII-1).

Chiocci et al. [2011] interpret the bulge to be a response to intrusive inflation of a pre-Etnean continental margin. Furthermore, *Chiocci et al. [2011]* proposed the idea of an upslope propagating instability, caused by a large scale mass wasting event offshore Mt Etna, which created a prominent amphitheater (Fig. MII-1) offshore the village of Riposto (Fig. MII-1). *Argnani et al. [2013]* interpreted the bulge at the continental margin as the northernmost extent of the Hyblean Foreland, as reflection seismic data indicate that the offshore area around the volcano is dominated by extensional faulting with thrust faults close to the coast and towards the distal extent of the continental margin. Therefore, *Argnani et al. [2013]* interpret the bulge rather to be generated by thrusting than by simple inflation due to magmatic intrusion related to volcanic activity of Mt Etna. The limits of the continental margin are described by *Gross et al. [2014 - This Thesis]*.

The semi-circular amphitheater is one of the most prominent structural expressions at the continental margin off Mt Etna (Fig. MII-1) *[Chiocci et al. 2011; Gross et al. 2014 – this thesis]*. It is a semi-circular, concave shaped feature opening towards the east, which is clearly visible on bathymetric data (Fig. 1) *[Chiocci et al. 2011]*. The crest of amphitheater is dominated by bended ridges (Fig. MII-1), which strike in the same direction as the steep concave amphitheater headwall *[Gross et al. 2014 – this thesis]*. The area east of the headwall can be described as a local structural high, as it reveals significant

higher altitudes than its surroundings (Fig. MII-1). *Chiocci et al. [2011]* proposed the amphitheater to be the remnant of an ancient slope failure, as such semi-circular scarps are known as typical headwalls of submarine mass transport events at volcanic slopes *[e.g. Moore et al. 1989; Whelan and Kelletat 2003]* and continental margins *[e.g. Lindberg et al. 2004; Vanneste et al. 2006]*. Towards the north, the amphitheater is restricted by the E-W striking anticline of Riposto Ridge, which most likely is a remnant of the Apennine Orogeny *[Bousquet et al. 1998]* (Fig. MII-1). Towards the south, it is confined by a W-E channel adjacent to the Timpe Plateau (Fig. MII-1). The western edge of the rim of the amphitheater is characterized by a sharp boundary towards the Valle Di Archirafi (Fig. MII-1). Valle di Archirafi is a funnel shaped depositional system offshore Mt Etna and opens up between the villages of Santa Tecla and Riposto directly at the shoreline of the Giarre Wedge (Fig. MII-1) *[Bonforte et al. 2011]*, which is one of Mt Etna's moving blocks and is limited towards the west by the prominent Time Fault System (Fig. MII-1). Valle di Archirafi covers an area of ~55 km^2 (Fig. MII-1). At its proximal parts, Valle di Archirafi is dominated by SE-ward trending gullies cutting into the seafloor, whereas its distal parts are characterized by elongated SE-ward trending ridges (Figs. MII-1, MII-2). The continental margin is not only known for its bulging and instability; furthermore, mass transport deposits were mapped at the continental slope and the continental toe *[Pareschi et al. 2006; Chiocci et al. 2011; Gross et al. 2014 – this thesis]*.

Especially the transition from the Valle di Archirafi towards the steep headwall of the amphitheater structure and its adjacent structural high reveals a striking seafloor morphology (Fig. MII-1). In order to investigate this remarkable system, a new high-resolution 3D reflection seismic volume was acquired. This study aims to describe and characterize the origin of this eye-catching area at the central part of the continental margin, as the entire morphology of the Valle di Archirafi and the amphitheater headwall seems to be strongly overprinted by recent tectonic activity. The obtained tectonic and structural implications will be used to present insights to continental margin deformation and spreading offshore Mt Etna.

2 Methods: 3D Seismic Acquisition and Processing

During RV Meteor Cruise M86/2 from December 2011 – January 2012, a new seismic and hydro-acoustic dataset was acquired offshore Mt Etna *[Krastel et al. 2014]*. For 3D seismic acquisition, the so called P-Cable system *[Planke et al. 2009; Petersen et al. 2010]* was used to image subsurface features in the working area offshore Mt Etna with high resolution. The system has been successfully used for a comparable geological setting at Montserrat *[Crutchley et al. 2013]*. The P-Cable system was configured with 13 streamers; each streamer was a 12.5 m-long 8-channel streamer. The streamers were towed between two paravanes behind the vessel at a distance slightly less than 10 m between the streamers. A single 1.7 l GI Gun was operated at ~200 bar and a shot interval of 4 s resulting in a shot point spacing of ~ 6 m at 3 knots. Sub-bottom penetration was up to ~0.5 s TWT (Two-Way-Travel-Time) (~375 m). With the help of this system, it was possible to acquire a high-resolution 3D seismic cube with a coverage of 26.6 km^2, offshore Mt Etna (Fig. MII-1). A bin size of 5 m with an average fold of 2-3 was achieved during 3D seismic processing, resulting in 665 seismic inlines and 1600 seismic crosslines. As the P-Cable System operates with numerous short streamers, it is not capable of a dedicated velocity analysis. Therefore a constant velocity of 1500 $m*s^{-1}$ was applied to the dataset during Normal-Move-Out corrections and migration. Data interpretation was carried out by using the commercial software IHS KingdomSuite.

During seismic attribute analysis, the similarity attribute was calculated for the 3D cube by using the open source software OpendTect. A time window of +-28 ms was chosen, to generate a similarity cube, which was then loaded into IHS KingdomSuite. By means of similarity attribute mapping, it is possible to show time slices, which illustrate the coherency of selected areas. This coherency / similarity mapping is a common tool to carry out facies- and / or fault mapping. The similarity / coherency is defined by a specific point in the dataset, which is then compared with its neighboring data points. High similarity can be observed at continuous seismic facies like laminated sediments. Low similarities show a high grade of discrepancy of coherency of the neighboring data points. This can be the result of disturbed sediments or fault offsets. This statistical approach is then carried out for specific depths over the entire dataset (Fig. MII-3).

3 Results

3.1 Seafloor Morphology of the 3D Cube Area

The 3D seismic reflection cube is located at the transition between the funnel shaped Valle di Archirafi and the steep headwall of the amphitheater-like structure at the continental margin offshore Mt Etna (Figs. MII-1, MII-2). Although covering an area of only 26.6 km², the seafloor morphology in the 3D cube area displays a strong heterogeneity (Fig. MII-2). The western region of the 3D cube comprises the easternmost extent of the Valle di Archirafi, a basin, which can be traced towards the shore of eastern Sicily (Figs. MII-1, MII-2). Valle di Archirafi hosts an eastward inclined seafloor with dip angles <10°, which is further characterized by positive elevated flute shaped features at its seafloor (Fig. MII-2). The seafloor in the central area of the 3D cube is dominated by S-N striking asymmetric ridges, featuring steep slope gradients of up to 30° at their western- and up to 10° at their eastern slopes.

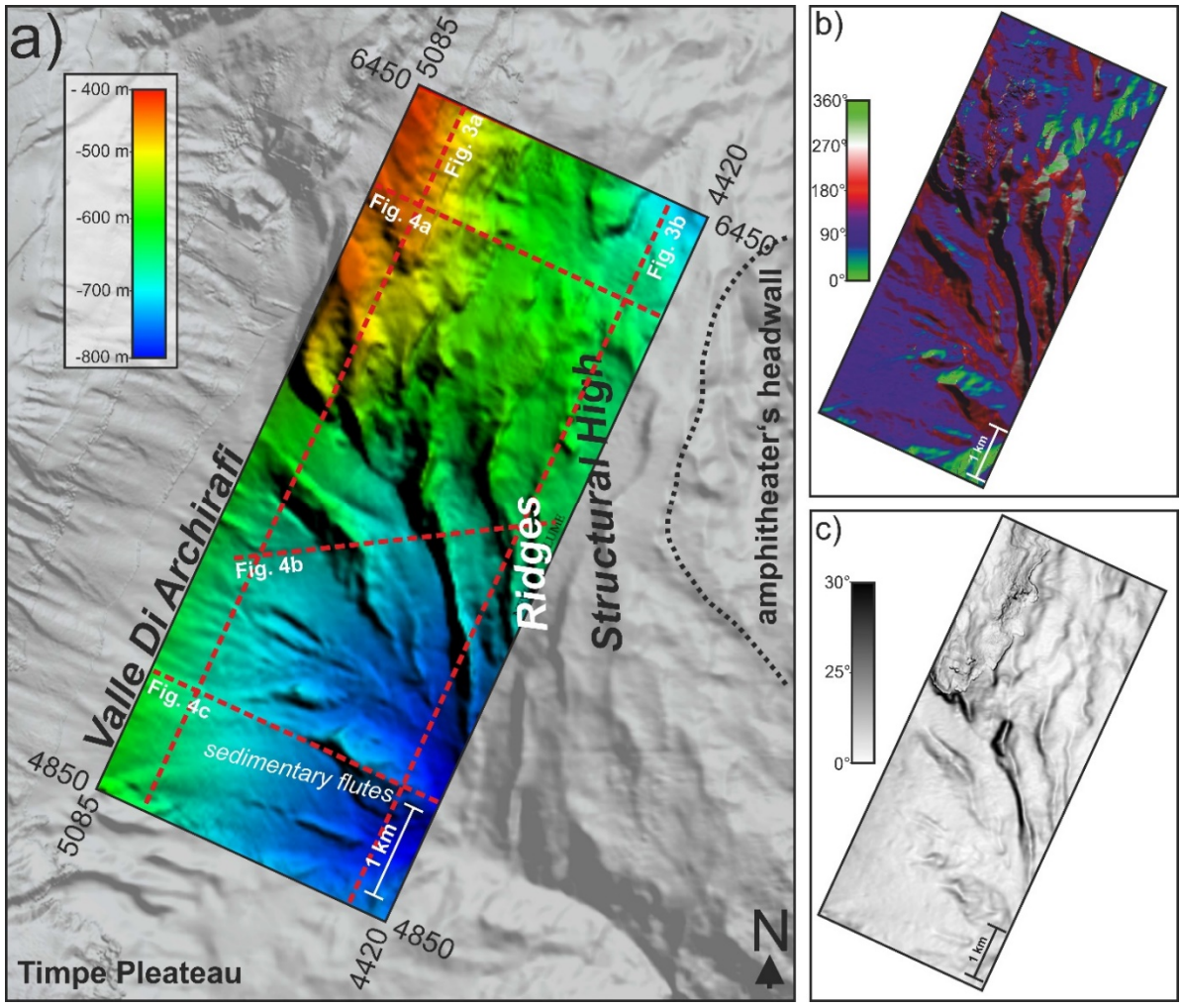

Figure MII-2: a) Bathymetric map of the 3D seismic reflection cube area (colored) and the surrounding seafloor (grey shaded). Location of seismic profiles shown in this manuscript are marked as dashed red lines. b) Slope aspect map of the seafloor in the area covered by the 3D cube. c) Slope gradient map of the seafloor in the area covered by the 3D cube

To the east of these prominent asymmetric ridges, the onset of a structural high is visible, which lies adjacent to the steep headwall of the amphitheater-like structure. The structural high towers above the Valle di Archirafi for up to 175 m (Fig. MII-2). Seafloor morphology of the structural high is dominated by less continuous NE striking ridges, which are subparallel to the headwall of the amphitheater (Figs. MII-1, MII-2).

3.2 Sub-seafloor structure in the area covered by the 3D Cube

The heterogeneous surface morphology of the area covered by the 3D cube continues into the sub-surface (Fig. MII-3). A shallow onset of high amplitude reflectors, here referred to as the substrate, reduces the penetration of the seismic signals dramatically. This seismic unit was identified before by *Argnani et al. [2013]* and *Gross et al. [2014 – this thesis]*; it is described in more detail at a later point in this study.

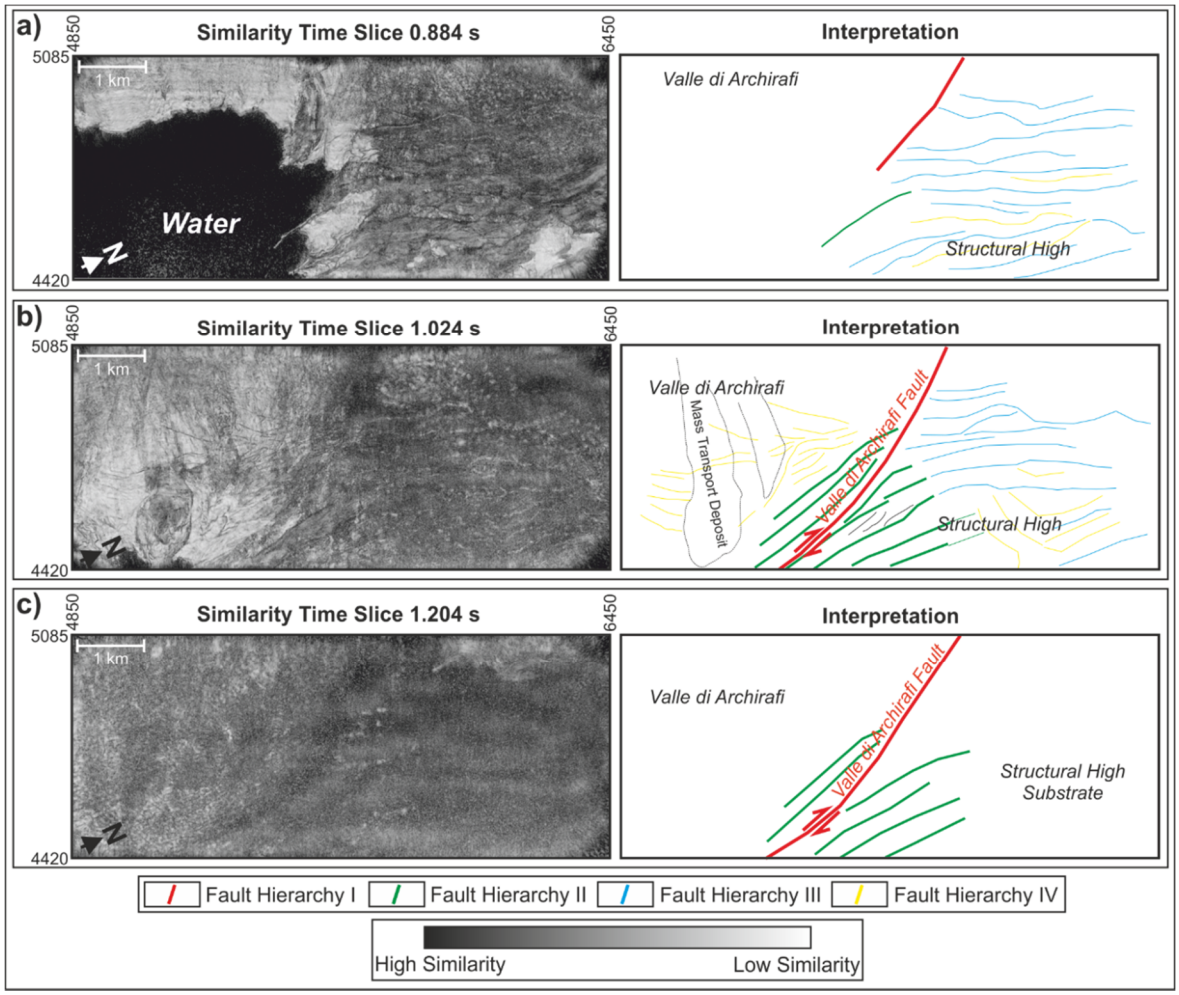

Figure MII-3: Similarity Attribute time slices of the 3D volume and their interpretation. Similarity attributes show the fault strike and seismic facies homogeneity/heterogeneity at a specific depth. 0.884 s, 1.024 and 1.204 s were chosen as representative depths. A clear separation based on similarities exists between the Valle di Archirafi and the structural high. The transition is characterized by deeper-rooted faults, which are the expression of a flower structure bound to the Valle Di Archirafi Fault. The faults are colored according to their Fault Hierarchy – see text for further description of Fault Hierarchies.

Seismic similarity attribute maps show a strong heterogeneity of the subsurface structures (Fig. MII-3). Furthermore, the entire 3D cube is dominated by a heterogeneous set of faults. For better comparison, we subdivide the individual faults into different hierarchies (Figs. MII-3 and following). Hierarchy I faults host the highest vertical offsets and show a deep-rooted origin. With the help of our high-resolution 3D cube, an offset calculation is impossible, as the hanging- and footwall show high discrepancies in their seismic facies. Hierarchy II faults are branches of Hierarchy I faults or faults, which can be traced deep into the substrate. Hierarchy III faults are shallow faults with indications for deeper-rooted structures and are mostly visible in the sedimentary drape of the structural high. Hierarchy IV faults are shallow faults, which only affect the upper ~0.2 s TWT sub-seafloor depth and reveal small vertical displacements of less than 10 m; they cannot be traced into the seismic facies of the substrate.

As already observed in bathymetric data, also the similarity attribute map (Fig. MII-3) and seismic profiles (Fig. MII-4) show significant differences between the Valle di Archirafi, the transition between the Valle di Archirafi and the structural high, as well as the structural high itself.

The Valle di Archirafi region shows only few shallow normal faults, which are arranged perpendicular to the slope gradient of the funnel-shaped basin (Fig. MII-3). The entire basin of Valle di Archirafi shows wedges characterized by a chaotic seismic facies, which are typically interpreted as submarine mass wasting deposits. The transition between Valle di Archirafi and the onset of the structural high is characterized by a sharp boundary, illustrated by an abrupt increase in similarity, indicating the onset of a different seismic facies. The onset of northwards striking faults that dip both, east- and westwards (Figs. MII-3, MII-4) can be observed in this area. These faults correlate with the asymmetric seafloor ridges (Figs. MII-2, MII-6). These ridges and their connected faults are the surface expression of a negative flower structure (Figs. MII-4b, MII-6). The negative flower structure is bound to a deep-rooted normal fault, which can be traced into the substrate. This fault is referred to as the Valle di Archirafi Fault in the following (Figs. MII-3, MII-4). The structural high is characterized by a set of normal faults, intersecting the well-stratified drape on top of the substrate. The faults are imaged as a fault set, which is dipping towards the steep headwall of the amphitheater (Fig. MII-3). Some of the faults can be traced into the substrate, which is underlying the well-stratified sedimentary drape on top of the structural high (Figs. MII-3, MII-4). The individual areas of the 3D-cube are described in more detail in the following.

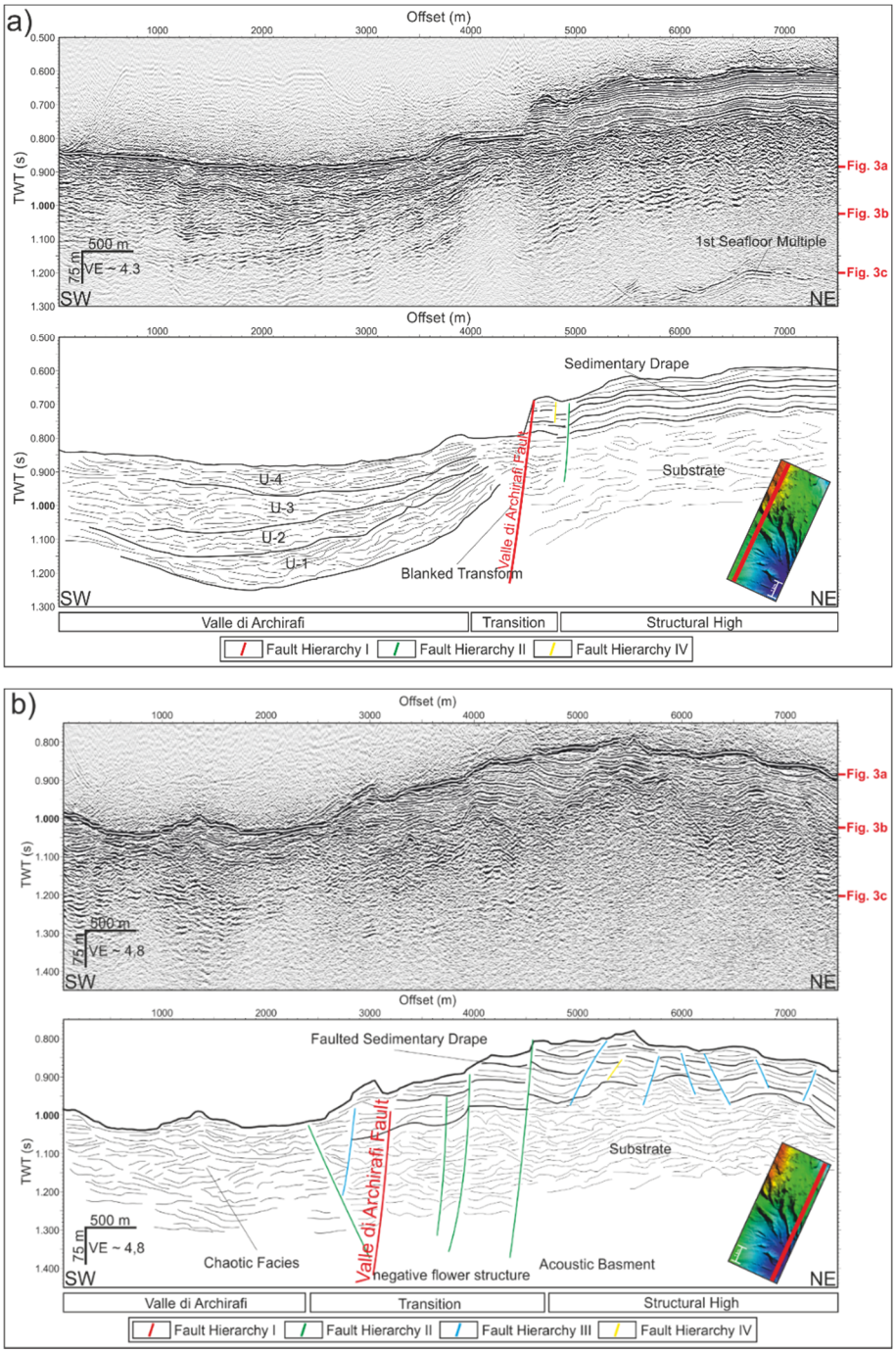

Figure MII-4: a) Seismic Inline 4995 of the 3D Volume and interpretation. The southwestern part of the profile shows the deposits in the Valle di Archirafi, which are subdivided into four units U-1 – U-4. The units display a chaotic to transparent seismic facies, which are separated by high amplitude continuous reflectors. The structural high west of the amphitheater is visible in the northeastern part of the profile. It is characterized by a thin well-stratified sedimentary drape. The sediment drape is underlain by high amplitude chaotic seismic facies, which is referred to as the substrate. The transition between Valle di Archirafi and the structural high is marked by normal faulting and a blanking of reflectors towards the southwest. b) Seismic Inline 4515 of the 3D volume and interpretation. A chaotic seismic facies is imaged in the distal parts of the Valle di Archirafi (southwestern part of profile). The transition between Valle di Archirafi and the structural high is marked by a negative flower structure, the branches of which are striking-out close to the seafloor. In the northeastern part of the profile, the structural high displays a sediment drape above the high amplitude, low coherent substrate. The realm of the structural high is strongly overprinted by normal faulting. The seafloor expressions of these faults are asymmetric ridges visible on bathymetric data. The faults are colored according to their Fault Hierarchy – see text for further description of Fault Hierarchies.

3.3 The Valle di Archirafi

Four seismic units with a chaotic to transparent seismic facies (U-1 to U-4, Figs. MII-4, MII-5) can be observed in Valle di Archirafi. They are interbedded by high-amplitude continuous reflector packages (Fig. MII-5). These units can also be observed in the seismic similarity maps and can be classified as submarine mass transport deposits (Fig. MII-3). Thicknesses of the individual seismic units decrease towards distal parts of Valle di Archirafi and the dip direction of the unit boundaries changes from seaward- to landward dipping units with increasing distance to the coast (Fig. MII-5). Internal deformation in all units increases in the distal parts of Valle di Archirafi, making it harder to differentiate between the individual units (Figs. MII-4, MII-5). In comparison to the proximal areas close to the coast (Fig. MII-1), the distal parts of Valle di Archirafi are overprinted by positive flute-shape sedimentary bodies, which can be observed within the first 0.1 s TWT of the seismic record (Figs. MII-4, MII-5). Due to limited penetration of the seismic signals, the base of Valle di Archirafi is not resolved (Fig. MII-5).

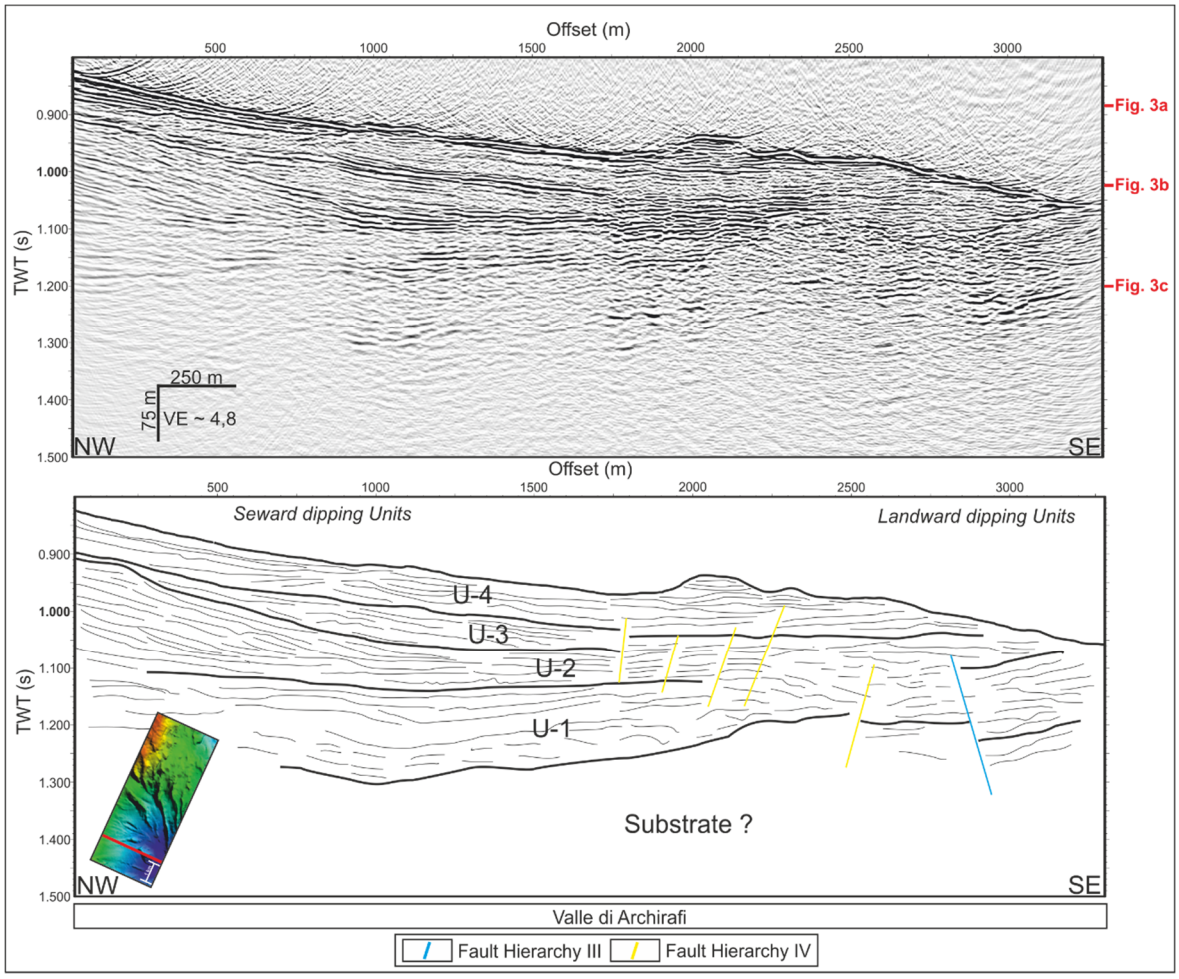

Figure MII-5: Seismic Crossline 5155 crossing the SE part of the 3D volume and interpretation. The profile images the Valle di Archirafi sediments, which are characterized by major chaotic seismic units separated by high amplitude reflectors with high coherency. The faults are colored according to their Fault Hierarchy – see text for further description of Fault Hierarchies.

3.4 The transition of Valle di Archirafi towards the structural high

The transition of Valle Di Archirafi towards the structural high represents the central part of the 3D cube (Figs. MII-2, MII-4, MII-6). Whereas the Valle die Archirafi shows a few buried eastward dipping faults, the transition towards the structural high shows westward dipping faults, which are connected to the westward dipping steep escarpments of the S-N-orientated asymmetric ridges (Figs. MII-2, MII-6). The internal seismic facies of these asymmetric ridges show a thin sedimentary drape of ~0.2 s TWT above the high amplitude, low coherency substrate (Figs. MII-4, MII-6). Seismic profiles show the major (Fault Hierarchy I) Valle di Archirafi fault (Figs. MII-3, MII-4, MII-6) at the transition of Valle di Archirafi towards the structural high. Whereas the Valle di Archirafi fault seems to propagate deeply into the substrate (Fig. MII-3), the branches (Fault Hierarchy II) of this fault are connected to the asymmetric ridges at the seafloor east of this fault (Figs. MII-3, MII-6). In general, a clustering of normal faults close to the Valle di Archirafi fault can be observed; these faults feature only small values of vertical displacement (Fig. MII-6). The general fault pattern suggests a negative flower structure and we consider the Valle di Archirafi fault as master fault of this negative flower structure, dominating the entire transition from the Valle di Archirafi towards the structural high (Fig. MII-3, MII-4, MII-6).

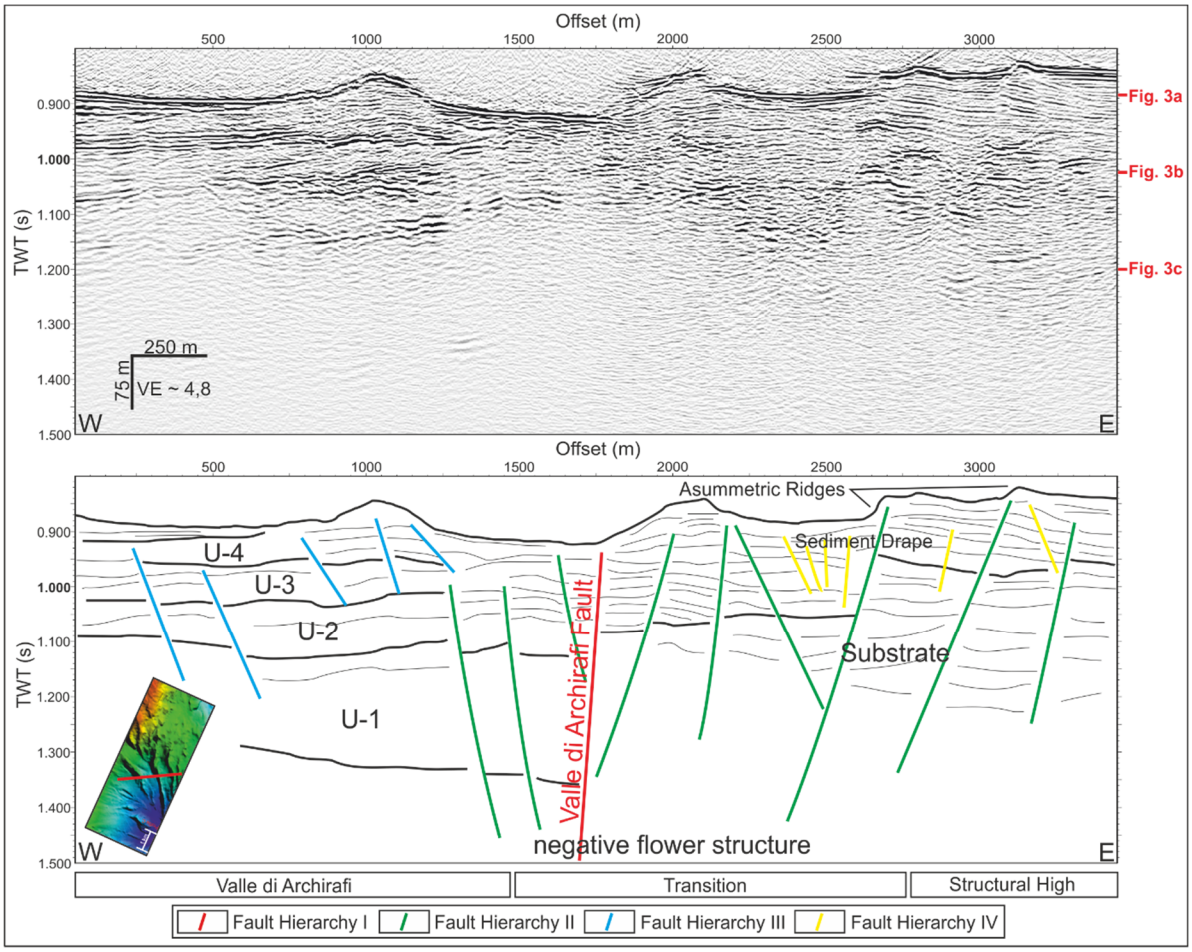

Figure MII-6: Arbitrary line through the transition between Valle di Archirafi and structural high and interpretation. A clear presence of eastward and westward dipping faults can be recognized. The uppermost 0.2 s TWT of the section is dominated by well-bedded, medium coherent units, which are underlain by a high amplitude reflector masking most of the structures beneath. The transition between Valle di Archirafi and the structural high is marked by a prominent negative flower structure. The master fault of this system is the Valle di Archirafi fault, which is also observed in the similarity time slices (Fig. MII-3). The faults are colored according to their Fault Hierarchy – see text for further description of Fault Hierarchies.

3.5 The structural high and the adjacent steep headwall of the amphitheater

The structural high is located directly adjacent to the prominent headwall of the amphitheater (Figs. MII-1, MII-2). Seismic data illustrate a well-stratified, high amplitude sedimentary unit with a thickness of ~0.2 s TWT, overlaying a low coherent substrate (Figs. MII-3, MII-4a). The onset of the substrate is marked by a high amplitude reflector (Fig. MII-7).

As observed in similarity attribute maps (Fig. MII-3), the entire structural high is strongly overprinted by a set of normal faults (Fault Hierarchy III), dipping towards the steep headwall of the amphitheater-like structure. These faults are connected to deeper faults in the substrate, which host nearly sub-vertical dip angles. As these deep fault segments can be traced towards the negative flower structure at the

transition of the Valle di Archirafi towards the structural high (Figs. MII-3, MII-6), they are classified as Fault Hierarchy II faults (Fig. 7). Some of these faults show a distinct surface expression, as they are outcropping at morphological escarpments at the seafloor (Fig. MII-7). The internal structure of the sedimentary drape is heavily deformed and rotated by these faults, which is expressed by elongated domino-style arranged blocks on the structural high (Figs. MII-3, MII-7). Undisturbed sediments can be observed in the western part of the structural high; these undisturbed sediments are underlain by Fault Hierarchy III faults, which have not propagated through the sediment drape (Fig. MII-7).

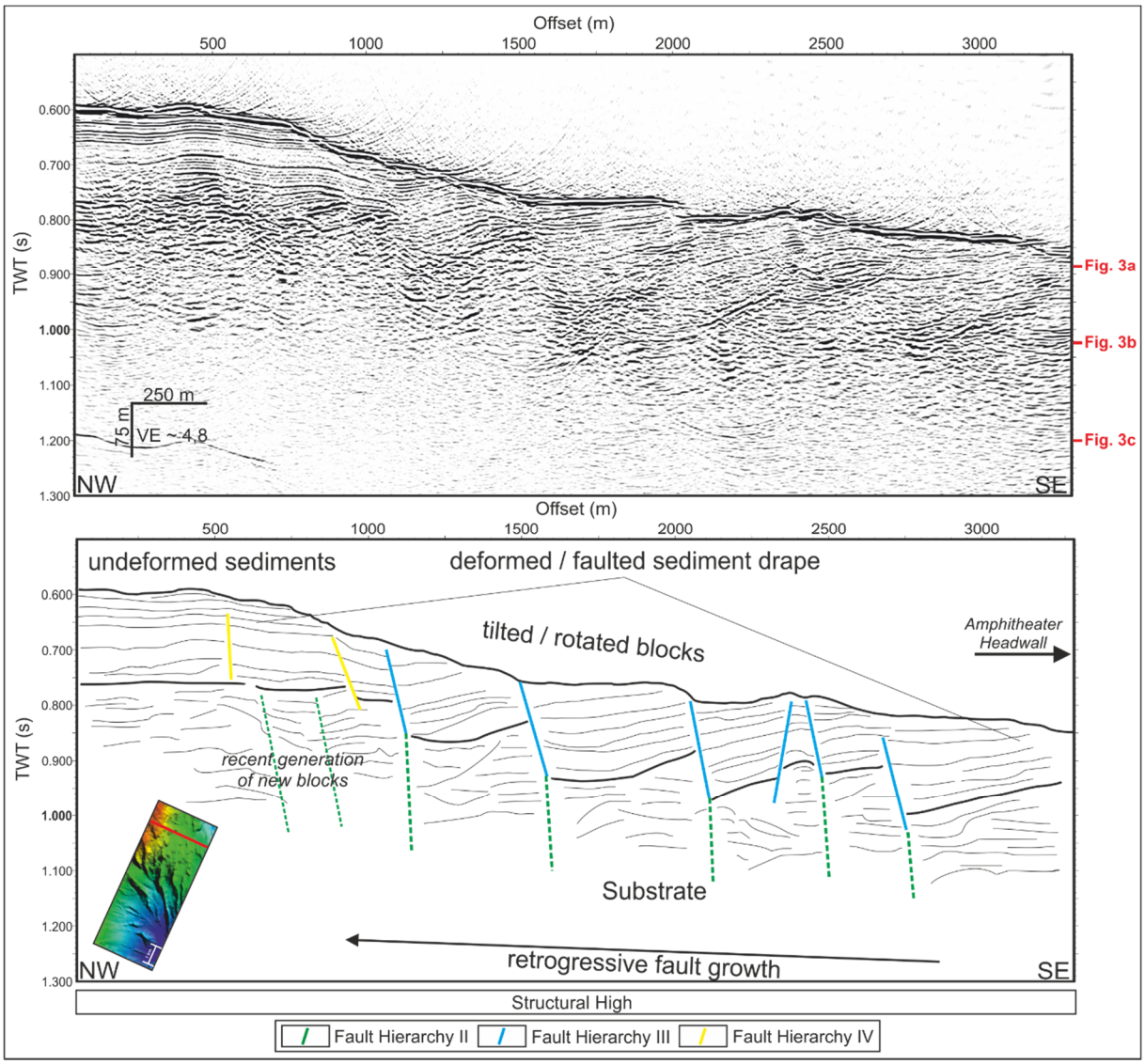

Figure MII-7: Seismic Crossline 6155 crossing the NE part of the 3D volume and interpretation. The profile shows eastward dipping normal faults resulting in domino-style arranged rotated blocks. The faults are colored according to their Fault Hierarchy – see text for further description of Fault Hierarchies.

3.6 The substrate at the structural high

The substrate underneath the structural high is characterized by a seismic facies of high-amplitude and low coherency reflectors. The morphology of the substrate's onset is dramatically deformed and bound to faults (Figs. MII-4, MII-7), which can be observed in the sedimentary drape, too (Figs. MII-4, MII-7). The sedimentary drape on top of the substrate shows thicknesses between ~25 m and ~175 m assuming a sediment sound velocity of 1500 m/s. Highest sediment thicknesses of ~175 m are observed at the un-deformed section of the drape in the northwestern part of the 3D volume, whereas the tilted and rotated blocks reveal a strong heterogeneity of sediment thicknesses of ~150 and ~25 m (Fig. MII-9).

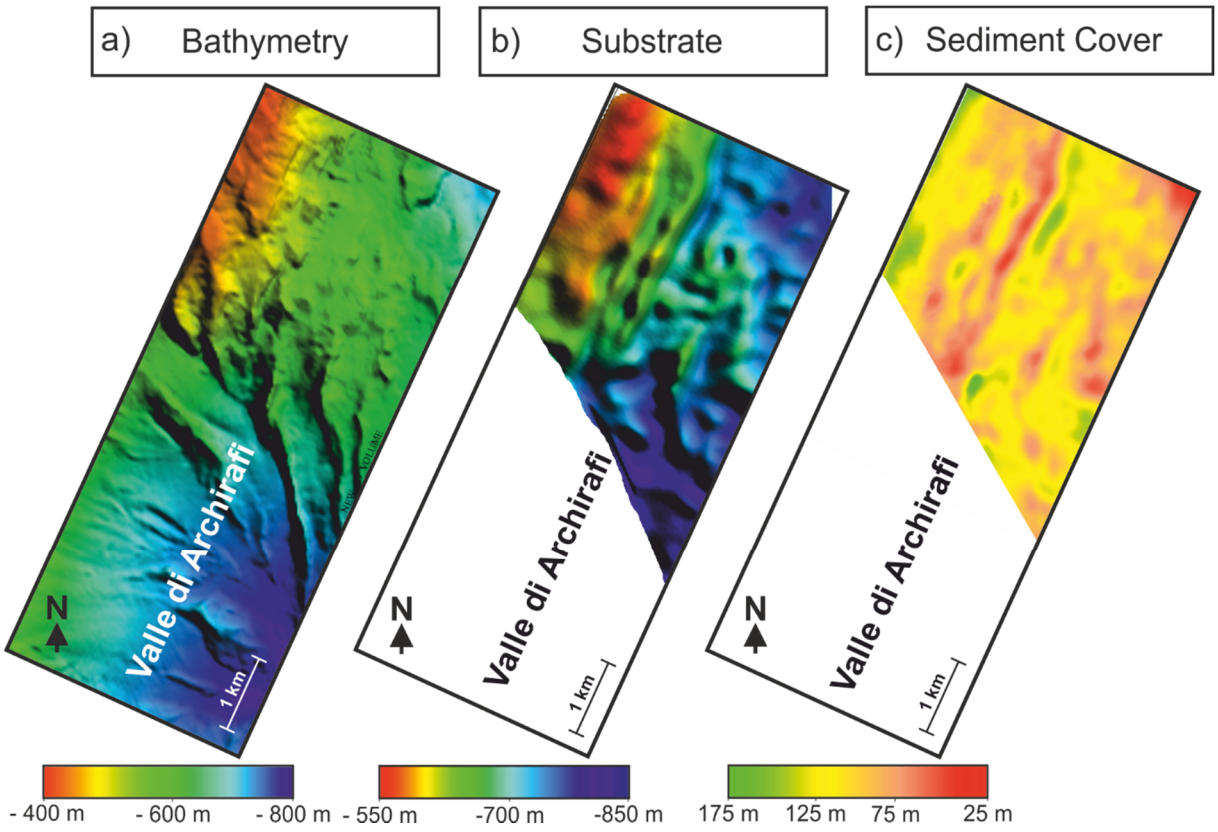

Figure MII-8: a) Bathymetry of the 3D cube b) Depth map of the substrate calculated with a sound velocity of 1500 m/s c) Sedimentary drape on top of the substrate calculated with a sound velocity of 1500 m/s.

4 Discussion

The new high-resolution 3D reflection seismic dataset at the continental margin offshore Mt Etna images the transition from the sedimentary conduit and depositional system of Valle di Archirafi towards a structural high, which is located directly adjacent to the massive amphitheater structure described offshore Mt Etna. As the morphology and the tectonic regime changes dramatically within a few kilometers, we consider this region as a highly remarkable site at the continental margin offshore Mt Etna.

4.1 Sediment and debris deposition

Valle di Archirafi hosts major mass transport deposits, which built up most of the bulk composition of the sedimentary basin (Units U-1 to U-4, Figs. MII-4, MII-5). The undisturbed high amplitude reflectors between the disturbed units may represent the background sedimentation in Valle di Archirafi including tephra layers related to volcano eruptions of Mt Etna and hemi-pelagic / terrestrial sediments. As the basin is directly adjacent to the onshore Giarre Wedge and the edifice of Mt Etna (Fig. MII-1), we consider the basin to be a conduit and depositional system for periodic debris and mass movement deposits, generated during volcano buildup and related sector collapses. This type of sediment input dominates and overprints the hemi-pelagic background sedimentation. Seafloor morphology, seismic facies mapping and fault patterns imply a strong differentiation between the sedimentary basin of the Valle di Archirafi and the structural high (Fig. MII-9). The structural high is covered by a thin sedimentary unit, which is up to ~175 m thick and reveals well-stratified sediments indicating continuous hemi-pelagic sedimentation without any major mass transport deposits. The entire structural high is overprinted by ongoing extensional deformation resulting in a set of normal faults (Fig. MII-7). Whereas Valle di Archirafi shows a strong seafloor reflector, which was impossible to penetrate with gravity corers (Fig. MII-APPENDIX-2). The structural high was easy to sample during gravity coring *[Gross et al. 2014 – this thesis]*. Due to the seismic facies discrimination of the two systems, we consider Valle di Archirafi and the structural high as two different sedimentary systems.

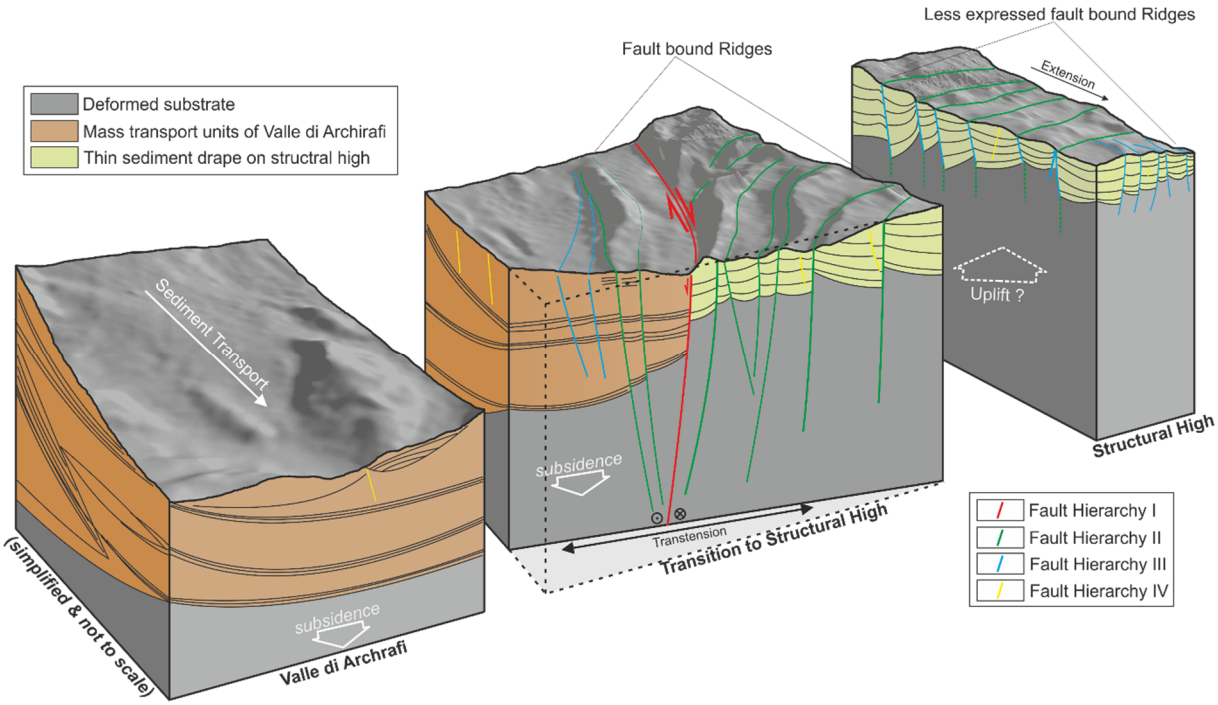

Figure MII-9: Schematic sketch of the 3D volume divided into the three regions of the Valle di Archirafi, the transition towards the structural high with its fault bound ridges, and the structural high. Valle di Archirafi is characterized by a depositional system, catching debris from mass wasting events from on- and offshore. The transition towards the structural high is marked by a thin sedimentary drape, which reveals a high grade of internal deformation caused by normal faulting. The structural high reveals a homogenous sedimentary drape and is characterized by well-stratified seismic units. The entire structural high is overprinted by a set of normal faults, creating a domino-style imbricated block system. The faults, dividing the blocks from each other, show increased fault dips at the onset to the substrate. These deeper faults are connectable to the Hierarchy II faults, which are branches of the negative flower structure, forming the prominent ridges at the transition between the Valle di Archirafi and the structural high. Seismic evidence for a sedimentary discrimination between Valle di Archirafi and the structural high is given by the low coherency between these two systems.

4.2 Tectonic controls on the Valle di Archirafi and the structural high

The Valle di Archirafi is only affected by shallow normal faulting. The onset of intense normal faulting is observed at the transition of the Valle di Archirafi towards the structural high. This region shows a negative flower structure; the fault planes are coherent with the steep western slopes of the asymmetric ridges exposed at the seafloor (Figs. MII-2, MII-6, MII-9). We consider this negative flower structure to be bound to a growth fault resulting in the subsidence of the basin in relation to the structural high. The fault geometry of eastward bending fault planes at the onset of the structural high implies this negative flower structure to be the surface expression of the deeply rooted Valle di Archirafi transtensional fault (Figs. MII-3, MII-6, MII-9). We consider this transtensional fault system as right-lateral, as the faults at the structural high show clear lateral displacements towards the amphitheater's headwall (Figs. MII-3, MII-7, MII-9). As most of the fault planes of the negative flower structure are continuous and are expressed by prominent asymmetric ridges at the seafloor, we consider this fault to

be highly active and growing faster than the sedimentary deposition. Due to relative subsidence Valle di Archirafi can be considered as an import sediment / debris conduit / catcher in the area offshore of the Mt Etna edifice (Figs. MII-3, MII-4, MII-5, MII-9). The structural high is affected by a strong overprint of extension and consequent normal faulting. The location of the structural high at the amphitheater headwall and its relative positive elevation in comparison to its surroundings may imply that the structural high i) represents an ancient horst, which is less affected by subsidence and spreading, or ii) is an area, which is affected by a deep thrust fault leading to the relative uplift of the area (Fig. MII-9). As the bounding faults of the blocks at the structural high reveal higher fault dips at the onset of the substrate, we consider the entire system to be the surface expression of deeper-rooted sub-vertical faults; these deeper-rooted faults, however, are not resolved by our high-resolution 3D seismic system due to limited penetration.

The surveyed area at the structural high reveals a lateral extension of up to 340 m (Fig. MII-APPENDIX-1), which is oriented towards the amphitheater's headwall in the east and the distal parts of Valle di Archirafi towards the south. This measured extension only includes the spreading caused by the fault system imaged in the upper sedimentary drape. As the observed sedimentary drape hosts indications for internal deformation and thinning (Fig. MII-7), we consider even higher values for total lateral extension at the structural high area. The substrate at the western edge of the structural high is cut by faults, which do not propagate trough the sediment drape, but show ductile deformation at the upper strata (Fig. MII-7). Hence, we consider the fault system to evolve retrogressively upslope. This implies a recent activity of the fault system, which may lead to future slope instability at the structural high close to the amphitheater's headwall (Fig. MII-1, MII-10). However, the uppermost ~200 m of sediments of the structural high display extensional processes, which are not consistent in direction. The northern section of the structural high exhibits an eastward dipping normal fault system, whereas the central section is strongly influenced by the transtensional Valle di Archirafi Fault (Fig. MII-10). The strike slip movement along the Valle di Archirafi Fault bends the faults and related blocks towards the south, leading to a westward dip of associated faults.

These insights to the central part of the continental margin offshore Mt Etna imply a strong extensional tectonic overprint in the near surface, resulting in spreading of the continental margin. Extension and spreading is not the only process present towards the amphitheater's headwall and the continental toe; furthermore westward dipping normal faults and right-lateral transtensional faults display the heterogeneous stress regime in this area. In comparison to the overall gravitational spreading, which affects the volcano flank *[e.g. Borgia et al. 1992]* and the continental margin *[Chiocci et al. 2011, Gross et al. 2014 - this thesis]*, the new 3D seismic data implies a coherent smaller spreading system to be present. These findings imply the overprint of a secondary spreading center at the structural high, directly at the steep amphitheater's headwall. This gravitational instability and spreading is effecting the

central part of the continental margin and leads to the high heterogeneity of the offshore realm of Mt Etna.

4.3 Relevance of the Valle di Archirafi and the structural high in the regional tectonic context

Mt Etna's eastern onshore slope is strongly overprinted by volcano-tectonic processes, creating prominent blocks as a result of its flank instability (Fig. MII-1). These blocks are bound by faults controlling different movements *[Bonforte et al. 2011]*. The Timpe Fault System is one of the most prominent fault systems dividing the central-block from the Giarre Wedge at the center of the slope (Figs. MII-1, MII-10). The Timpe Fault System features the same strike direction as the Malta Escarpment, which is observed in the Ionian Sea south of the volcano edifice of Mt Etna *[Argnani and Bonazzi 2005]* (Fig. MII-1). *Chiocci et al. [2011]* interpret the Timpe Fault System to be a near-surface tectonic expression of a tectonic basement fault that developed as a response to a steep slope. Analogue modelling studies by *Le Corvec et al. [2014]* suggest the interplay of the Timpe Fault System and potential thrust faulting offshore Mt Etna during and after magmatic intrusions at Mt Etna.

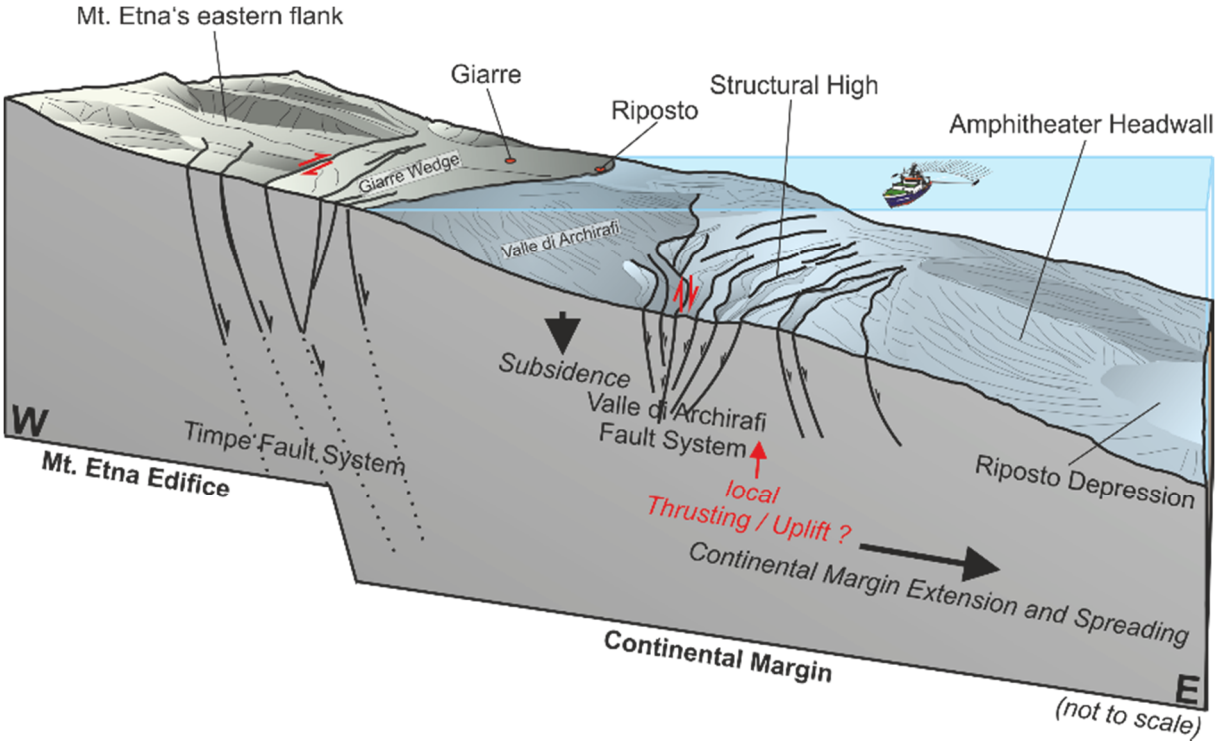

Figure MII-10: Schematic Model for the Timpe Fault System in relation to the offshore Valle di Archirafi Fault System. The Timpe Fault System reveals an eastward dip, whereas the deeper rooted structures of the structural high show westward dips. The Timpe Fault System and the Valle di Archirafi Fault generate a basin, which is described as the onshore Giarre Wedge and the offshore Valle di Archirafi block.

Our new data shows that the Valle di Archirafi and the structural high close to the amphitheater's headwall are strongly overprinted by a negative flower structure, which strikes in the same directions as the Timpe Fault System. Hence, we consider a connection between the Timpe Fault System and the Valle di Archirafi Fault as likely though our data does not provide direct proof for this hypothesis because of the limited penetration (Fig. MII-10). The Timpe Fault system and the Valle di Archirafi Fault system might be responsible for the movement of the Giarre / Valle di Archirafi block (Fig. MII-10) due to a pull-apart like opening. The growth faults of this basin are described by the Timpe Fault System towards the west and the Valle di Archirafi Fault towards the east (Fig. MII-10). The resulting basin implies strong extensional domains at the near surface, which are controlling the continental margin off Mt Etna. As *Le Corvec et al. [2014]* proposes a possible thrust fault at the location of the structural high, the structural high might display the uplifted response of this thrust fault. Due to the lack of a deep penetration of the used seismic system, we are not able to display the deeper parts of the structural high and a possible thrust fault in this region. Nevertheless, landward dipping reflectors in the distal parts of Valle di Archirafi (Fig. MII-5) might be related to a deep thrust *[Argnani et al. 2013]* or magmatic inflation of the continental bulge *[Chiocci et al. 2011]*. Both processes would lead to an uplift of the structural high and subsidence of Valle di Archirafi, respectively (Figs. MII-9, MII-10).

The substrate displayed in our data shows low coherency, which is an indicator for a high grade of disintegration. This disintegration can be caused either by intense faulting or may display an ancient mass transport deposit. *Nicolosi et al. [2014]* shows implications for a pre-Etnean basement landslide underneath Mt Etna's edifice, which is promoting the edifice's movement towards the east. As the observed substrate features high amplitudes and low coherency in stratification, this unit may display the distal extends of such a pre-Etnean mass wasting deposit, which is strongly overprinted by recent tectonic activities. However, we would like to point out that other processes, such as tectonic deformation or small-scale landsliding may generate a similar seismic facies of the substrate.

4.4 Hazard potential of the observed extension and resulting instability

The entire submarine continental margin off Mt Etna is considered to be highly overprinted by extensional faults *[Chiocci et al. 2011; Argnani et al. 2013]* and submarine mass transport deposits *[Pareschi et al. 2006; Gross et al. 2014 – this thesis]*. Our new high-resolution 3D seismic data suggests recent extension affecting near surface sediments, which points to ongoing tectonic activity, especially at the headwall of the amphitheater structure. We also see a connection between features formed by volcano tectonic processes like the Timpe Fault System and offshore continental margin tectonic processes at the Valle di Archirafi and the structural high. This tectonic setting implies a strong impact of volcano tectonics on the adjacent continental margin of the Ionian Sea east of Mt Etna's edifice. Our

new data show faulted blocks immediately upslope of the headwall of the amphitheater structure, which may be potentially unstable and could fail in the future. Possible triggers for such a failure include regional seismic activity *[e.g. Orecchio et al. 2014]* or seismicity related to volcanic processes *[Lo Giudice et al. 1992; Hirn et al. 1997]*.

The combination of Mt Etna's well-documented onshore eastward and southward migrating slope movement *[e.g. Bonforte et al. 2011]* and the observed recent fault activity at the submarine continental margin directly east of Mt Etna's edifice imply a generally instable system extending from the toe of the continental margin *[Chiocci et al. 2011]* up to the crest of Mt Etna's edifice *[e.g. Borgia et al. 1992]*. This instability is documented by extensional fault systems outcropping at the seafloor and at the onshore volcano flank. Therefore, we do see a potential hazard for submarine mass wasting events at the continental margin east of Mt Etna, which could also affect the onshore realm of Mt Etna.

5 Conclusions

New high resolution 3D seismic data show that the structural high at the amphitheater offshore Mt Etna is separated from the depositional basin of Valle di Archirafi by an active fault system. Several asymmetric ridges at the seafloor are the surface expression of this fault system. This fault system is not only controlling the subsidence of the Valle di Archirafi in respect to the structural high; furthermore it shows a right-lateral transtension, leading to eastward and westward spreading at the submarine central continental margin east of Mt Etna. The structural high is draped by a thin sedimentary layer featuring a domino style, imbricated fault system dipping towards the steep amphitheater headwall. This fault system indicates recent activity at the prominent escarpment of the amphitheater headwall and may represent a precursor for potential slope failures at the continental margin offshore Mt Etna. Valle di Archirafi is a conduit and depositional system, catching debris and mass transport deposits from on- and offshore. As the eastern growth fault of Valle di Archirafi exhibits the same strike direction as the Timpe Fault System onshore, we see indications for a coupled tectonic system creating the Giarre / Valle di Archirafi basin. This implies a strong connection between tectonics observed at the onshore volcano flank and the continental margin offshore Mt Etna. Furthermore, we consider the structural high at the amphitheater's headwall to display a secondary spreading center at Mt Etna's continental margin, which contributes to the overall gravitational instability observed at the volcano edifice onshore and the continental margin, offshore.

As the region at Mt Etna is seismically highly active due to regional tectonics and the volcano buildup, we consider the hazard potential for submarine mass wasting as relatively high. In order to evaluate this hazard and related risks, further studies like marine geodetic measurements need to be carried out in the future.

6 References

Acocella, V., Behncke, B., Neri, M., D'Amico, S., 2003. Link between major flank slip and 2002–2003 eruption at Mt. Etna (Italy). Geophysical Research Letters 30. 2286. DOI:10.1029/2003GL018642

Acocella, V., Puglisi, G., 2013. How to cope with volcano flank dynamics? A conceptual model behind possible scenarios for Mt. Etna. Journal of Volcanology and Geothermal Research 251. 137–148. DOI:10.1016/j.jvolgeores.2012.06.016

Argnani, A., Bonazzi, C., 2005. Malta Escarpment fault zone offshore eastern Sicily: Pliocene-Quaternary tectonic evolution based on new multichannel seismic data. Tectonics 24. DOI:10.1029/2004TC001656

Argnani, A., Mazzarini, F., Bonazzi, C., Bisson, M., Isola, I., 2013. The deformation offshore of Mount Etna as imaged by multichannel seismic reflection profiles. Journal of Volcanology and Geothermal Research 251. 50–64. DOI:10.1016/j.jvolgeores.2012.04.016

Argnani, A., 2014. Comment on the article "Propagation of a lithospheric tear fault (STEP) through the western boundary of the Calabrian accretionary wedge offshore eastern Sicily (Southern Italy)" by Gallais et al., 2013 Tectonophysics. Tectonophysics 610. 195–199. DOI:10.1016/j.tecto.2013.06.035

Bonforte, A., Puglisi, G., 2003. Magma uprising and flank dynamics on Mount Etna volcano, studied using GPS data (1994–1995). Journal of Geophysical Research 108. 2153. DOI:10.1029/2002JB001845

Bonforte, A., Guglielmino, F., Coltelli, M., Ferretti, A., Puglisi, G., 2011. Structural assessment of Mount Etna volcano from Permanent Scatterers analysis. Geochemistry Geophysics Geosystems 12. DOI:10.1029/2010GC003213

Borgia, A., Ferrari, L., Pasquarè, G., 1992. Importance of gravitational spreading in the tectonic and volcanic evolution of Mount Etna. Nature 357. 231–235. DOI:10.1038/357231a0

Bousquet,J.C., Gabbianelli,G., Lanzafame,G., Sartori,R., 1998. Evolution volcanotectonique de l'Etna (Sicilie): nouvelles données de géologie marine et terrestre. Rapport de la Commission Internationale pour l'Exploration Scientifique de la Mer Méditerranee 35. 56–57.

Branca, S., Del Carlo, P., 2004. Eruptions of Mt Etna during the past 3,200 years: a revised compilation integrating the historical and stratigraphic records. In:Bonaccorso, A., Calvari, S., Coltelli, M., Del Negro, C., Falsaperla, S. (Eds.), Mt. Etna: Volcano Laboratory. Geophysical Monograph Series 143. American Geophysical Union, Washington, D.C..1–27.

Branca, S., Coltelli, M., Groppelli, G., 2004. Geological evolution of Etna volcano. In: Bonaccorso, A., Calvari, S., Coltelli, M., Del Negro, C., Falsaperla, S. (Eds.), Mt. Etna: Volcano Laboratory. Geophysical Monograph Series, 143. American Geophysical Union, Washington, D.C.. 49–63.

Branca, S., Coltelli M., Groppelli G., Lentini F., 2011. Geological map of Etna volcano, 1: 50,000 scale. Italian Journal of Geosciences 130. 265-291. DOI:10.3301/IJG.2011.15

Chiocci, F.L., Coltelli, M., Bosman, A., Cavallaro, D., 2011. Continental margin large-scale instability controlling the flank sliding of Etna volcano. Earth and Planetary Science Letters 305. 57–64. DOI:10.1016/j.epsl.2011.02.040

Crutchley, G.J., Karstens, J., Berndt, C., Talling, P.J., Watt, S.F.L., Vardy, M.E., Hühnerbach, V., Urlaub, M., Sarkar, S., Klaeschen, D., Paulatto, M., Le Friant, A., Lebas, E., Maeno, F., 2013. Insights into the emplacement dynamics of volcanic landslides from high-resolution 3D seismic data acquired offshore Montserrat, Lesser Antilles. Marine Geology 335. 1–15. DOI: 10.1016/j.margeo.2012.10.004

Doglioni, C., Innocenti, F., Mariotti, G., 2001. Why Mt Etna?. Terra Nova 13. 25–31. DOI:10.1046/j.1365-3121.2001.00301.x

Farr, T. G., Rosen, A., Caro, E., Crippen, R., Duren, R., Hensley, S., Kobrick, S., Rodriguez, E., Roth, L., Seal, D., Shaffer, S., Shimada, J., Umland, J., Werner, M., Oskin, M., Burbank, D., Alsdorf, D., 2007. The Shuttle Radar Topography Mission. Reviews of Geophysics 45. DOI:10.1029/2005RG000183

Froger, J.L., Merle, O., Briole, P., 2001. Active spreading and regional extension at Mount Etna imaged by SAR interferometry. Earth and Planetary Science Letters 187. 245–258. DOI:10.1016/S0012-821X(01)00290-4

Gross, F., Krastel, S., Chiocci, F.L., Ridente, D., Bialas, J., Schwab, J., Beier, J., Cukur, D., Winkelmann, D., 2014 Evidence for Submarine Landslides Offshore Mt. Etna, Italy. S. Krastel (Eds.), Submarine Mass Movements and Their Consequences, Bd. 37. 307–316. DOI:10.1007/978-3-319-00972-8_27

Gvirtzman, Z., Nur, A., 1999. The formation of Mount Etna as the consequence of slab rollback. Nature 401. 782–785. DOI:10.1038/44555

Hirn, A., Nicolich, R., Gallart, J., Laigle, M., Cernobori, L., ETNASEIS Scientific Group, 1997. Roots of Etna volcano in faults of great earthquakes. Earth and Planetary Science Letters 148. 171–191. DOI:10.1016/S0012-821X(97)00023-X

Krastel, S. and cruise participants, 2014. Seismogenic faults, landslides, and associated tsunamis off southern Italy. Cruise No. M86/2 – November 21, 2011 – January 17, 2012 – Cartagena (Spain) – Brindisi (Italy). METEOR-Berichte, M86/2. 49 pp. DFG-Senatskommission für Ozeanographie, DOI: 10.2312/cr_m86_2

Le Corvec, N., Walter, T. R., Ruch, J., Bonforte, A., Puglisi, G., 2014. Experimental study of the interplay between magmatic rift intrusion and flank instability with application to the 2001 Mount Etna eruption. Journal of Geophyical Research Solid Earth. DOI: 10.1002/2014JB011224.

Lentini, F., Carbone, S., Guarnieri, P., 2006. Collisional and postcollisional tectonics of the Apenninic-Maghrebian orogen (southern Italy). Dilek, Y., Pavlides, S. (Eds.), Postcollisional Tectonics and Magmatism in the Mediterranean Region and Asia. Special Paper - Geological Society of America 409. 57–81. DOI:10.1130/2006.2409(04)

Lindberg, B., Laberg, J.S., Vorren, T.O., 2004. The Nyk Slide—morphology, progression, and age of a partly buried submarine slide offshore northern Norway. Marine Geology 213. 277–289. DOI: 10.1016/j.margeo.2004.10.010

Lo Giudice, E., Rasà, R., 1992. Very shallow earthquakes and brittle deformation in active volcanic areas: the Etnean region as an example. Tectonophysics 202. 257–268.

Marani, M.P., Gamberi, F., Bortoluzzi, G., Carrara, G., Ligi, M., Penitenti, D., 2004. Seafloor bathymetry of the Ionian Sea.Marani, M.P., Gamberi, F., Bonatti, E. (Eds.), From Seafloor to Deep Mantle: Architecture of the Tyrrhenian Backarc Basin. Memorie Descrittive della Carta Geologica d'Italia 44. Plate 3. Roma. System Cart.

Moore, J.G., Clague, D.A., Holcomb, R.T., Lipman, P.W., Normark, W.R., Torresan, M.E., 1989. Prodigious submarine landslides on the Hawaiian Ridge, Journal of Geophysical Research 94. 17. 465-484.

Nicolich, R., Laigle, M., Hirn, A., Cernobori, L., Gallart, J., 2000. Crustal structure of the Ionian margin of Sicily: Etna volcano in the frame of regional evolution. Tectonophysics 329. 121–139. DOI:10.1016/S0040-1951(00)00192-X

Nicolosi, I., D'Ajello Caracciolo, F., Branca, S., Ventura, G., Chiappini, M., 2014. Volcanic conduit migration over a basement landslide at Mount Etna (Italy). Scientific Reports 4. DOI:10.1038/srep05293

Orecchio, B., Presti, D., Totaro, C., Neri, G., 2014. What earthquakes say concerning residual subduction and STEP dynamics in the Calabrian Arc region, south Italy. Geophysical Journal International 199. 1929–1942. DOI: 10.1093/gji/ggu373

Pareschi, M. T., Boschi, E., Mazzarini, F., Favalli, M., 2006. Large submarine landslides offshore Mt. Etna. Geophysical Research Letters 33. DOI:10.1029/2006GL026064

Planke, S., Eriksen, F.N., Berndt, C., Mienert, J., and Masson, D.G., 2009. P-Cable High-resolution 3D Seismic. Oceanography 22. 81.

Petersen, C.J., Bünz, S., Hustoft, S., Mienert, J., Klaeschen, D., 2010. High-resolution P-Cable 3D seismic imaging of gas chimney structures in gas hydrated sediments of an Arcticsediment drift. Marine and Petroleum Geology 27. 1981–1994. DOI:10.1016/j.marpetgeo.2010.06.006

Rust, D., Kershaw, S., 2000. Holocene tectonic uplift patterns in northeastern Sicily: evidence from marine notches in coastal outcrops. Marine Geology 167. 105–126. DOI:10.1016/S0025-3227(00)00019-0.

Vannaste, M., Mienert, J., Bunz, S., 2006. The Hinlopen Slide: A giant, submarine slope failure on the northern Svalbard margin, Arctic Ocean. Earth and Planetary Science Letters 245. 373–388. DOI:10.1016/j.epsl.2006.02.045

Whelan, F., Kelletat, D., 2003. Submarine slides on volcanic islands – a source for mega-tsunamis in the Quaternary. Progress in Physical Geography 27. 198–216. DOI:10.1191/0309133303pp367ra.

7 Appendix

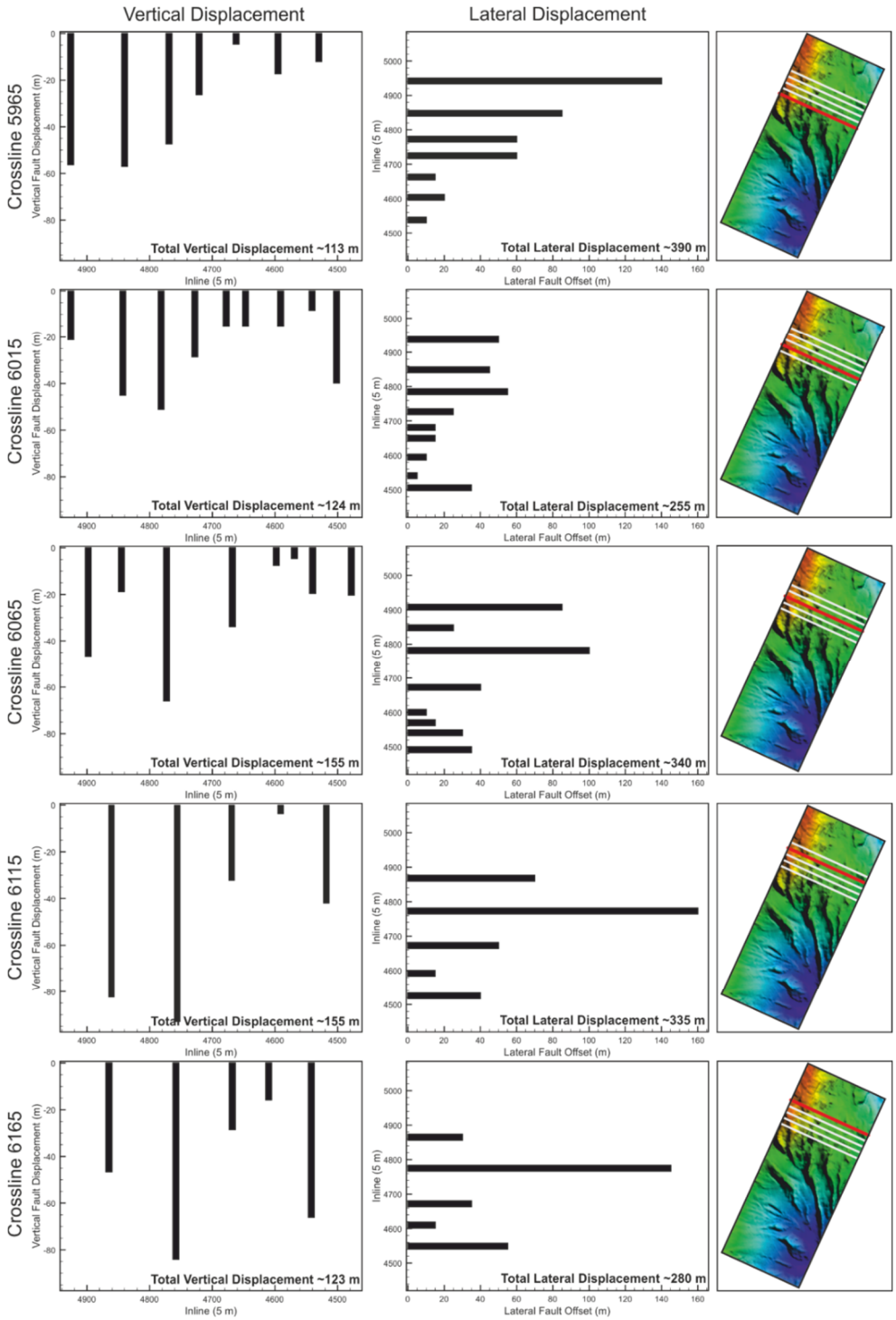

Figure MII-APPENDIX-1: Vertical fault displacement and lateral fault displacement in the sedimentary drape of the structural high. The vertical fault displacement of individual faults varies between ~3 to ~88 m assuming a sediment sound velocity of 1500 m/s. By measuring the lateral offset at the reference horizon at the structural, high values for lateral fault offset and coherent extension was measured between ~5 and ~150 m. The rates of total vertical and lateral displacements, measured at the reference crosslines 5965, 6015, 6065, 6115, 6165 at the onset of the structural high. The total lateral displacement varies between ~255 m and ~390 m.

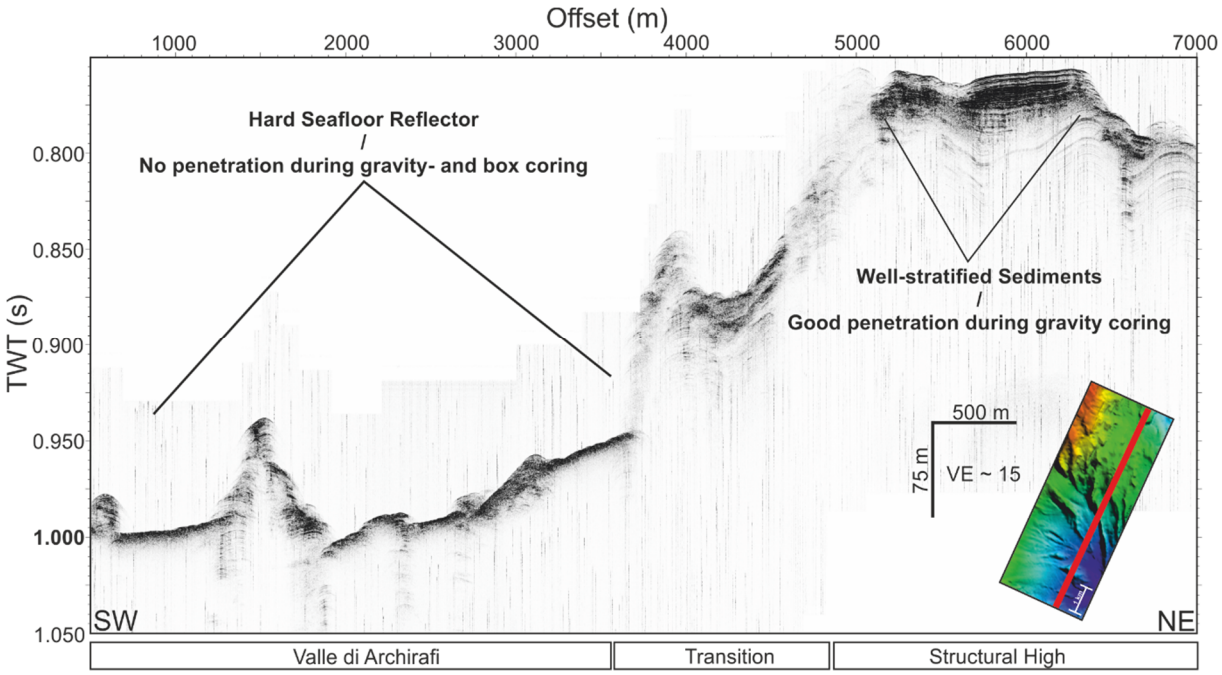

Figure MII-APPENDIX-2: PARASOUND line across the Valle di Archirafi, the transition and the structural high. Whereas Valle di Archirafi is characterized by a hard seafloor reflector with no signal penetration, the structural high shows well-stratified sediments. During gravity- and box coring it was not possible to penetrate Valle di Archirafi. Examples for cores from the structural high can be found in *Gross et al. [2014 – this thesis]*.

6 MANUSCRIPT III

Evidence for Submarine Landslides Offshore Mt. Etna, Italy

Felix Gross, Sebastian Krastel, Francesco Latino Chiocci, Dominico Ridente,

Jörg Bialas, Julia Schwab, Julio Beier, Deniz Cukur and Daniel Winkelmann

Published in: S. Krastel (Eds.), Submarine Mass Movements and Their Consequences, Bd. 37, Springer, 2014

DOI: 10.1007/978-3-319-00972-8_27

Chapter 27
Evidence for Submarine Landslides Offshore Mt. Etna, Italy

Felix Gross, Sebastian Krastel, Francesco Latino Chiocci, Dominico Ridente, Jörg Bialas, Julia Schwab, Julio Beier, Deniz Cukur, and Daniel Winkelmann

Abstract Mt. Etna is the largest and one of the best-studied volcanoes in Europe. It represents a highly active basaltic volcano on top of the active Apennine thrust belt. The instability of its eastern flank has been described as an important preconditioning factor for the occurrence of submarine mass wasting events. In order to better understand the processes that may cause submarine slope failures, a new dataset including seismic, hydroacoustic and core data was collected during RV Meteor cruise M86/2 from December 2011 to January 2012. Seismic profiles and sediment cores reveal repeated mass transport deposits (MTD), indicating a long history of landslides in the working area. Some of the sampled MTDs and their surrounding strata contain volcaniclastic debris, indicating that slope failures may be controlled by volcanic and non-volcanic processes. Several tephra layers directly cover MTDs, which is regarded as an indicator for the possibility that several flank failures occur immediately before or very early during an eruption.

Keywords Volcano flank • Mt. Etna • Submarine sliding • Slope instability • Tephra

F. Gross (✉) • J. Bialas • J. Schwab • D. Cukur • D. Winkelmann
GEOMAR Helmholtz Centre for Ocean Research Kiel, Wischhofstr. 1-3, 24148 Kiel, Germany
e-mail: fgross@geomar.de

S. Krastel • J. Beier
Institute of Geosciences, Christian-Albrechts-Universität zu Kiel, Kiel, Germany

F.L. Chiocci
Dip. Scienze della Terra, University "La Sapienza", Rome, Italy

D. Ridente
IGAG-CNR, National Research Council, Rome, Italy

S. Krastel et al. (eds.), *Submarine Mass Movements and Their Consequences*, Advances in Natural and Technological Hazards Research 37, DOI 10.1007/978-3-319-00972-8_27,

27.1 Introduction

Mt. Etna (Sicily, Italy) is known as the largest active volcano in Europe (Fig. 27.1) (Gvirtzman and Nur 1999). It represents a highly active basaltic volcano overlying the active plate boundary between the African and Eurasian Plate (Chiocci et al. 2011; Doglioni et al. 2001), and builds up on continental crust (Gvirtzman and Nur 1999).

The eastern flank of Mount Etna is well known for its instability (Branca and Ferrara 2013) and its ongoing deformation (Argnani et al. 2012), which is controlled by spreading of an extensional fault system (Borgia et al. 1992). Chiocci et al. (2011) consider this ongoing deformation as an important factor controlling subaerial and submarine mass wasting events. Pareschi et al. (2006) postulate a long-lasting history of mass movements after the built-up of Mt. Etna, as long run-out debris slumps could be imaged offshore Mt. Etna. Chiocci et al. (2011) observed a large bulge offsetting the margin that is deeply affected by widespread semicircular steps, which have been interpreted as being associated with large-scale gravitational instabilities.

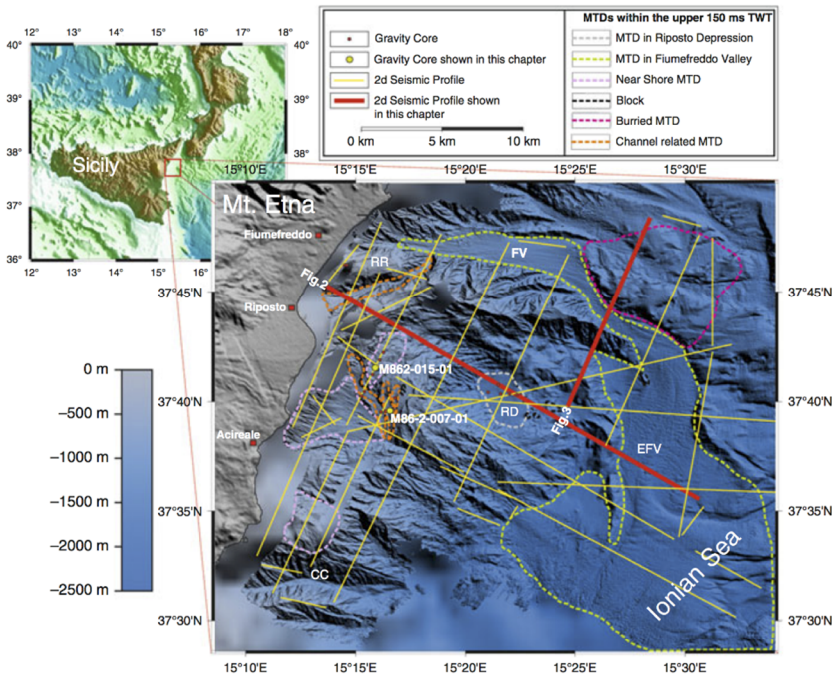

Fig. 27.1 Bathymetric map showing locations of seismic profiles collected during cruise M86/2 offshore Mt. Etna. *Dashed colored lines* display near-surface MTDs (Mass Transport Deposits). The *inset* map shows the general location of the working area. *RR* Riposto Ridge, *FV* Fiumefreddo Valley, *EFV* Extension of Fiumefreddo Valley, *RD* Riposto Depression, *CC* Catania Canyon

A variety of processes leading to a destabilization of the flank and possible catastrophic slope failures may act in addition to the ongoing deformation in the working area. These mechanisms include tectonic activity due to frequent earthquakes in the Calabrian Arc (e.g. Azzaro et al. 2000; Ferreli et al. 2002), high recurrence rate of volcanic eruptions and volcanic tremor (e.g. Simkin and Siebert 1994), and liquefaction of tephra layers, which was observed in comparable settings, e.g. by Harders et al. (2010). Furthermore, widespread incised gullies indicate ongoing highly variable hydrodynamic and gradational activity (Micallef and Mountjoy 2011), controlling the recent morphology in this area.

All these implications reveal that the area east of Mount Etna is a region, which is highly prone to submarine mass wasting. Several questions, however, remain open, including the spatial distribution of mass wasting and the role of abundant and widespread tephra layers. Based on new data collected during RV Meteor cruise M86/2 (December 2011/ January 2012), we focus on the relationship between widespread tephra layers and MTDs as well as on the identification of large- and small-scale features contributing to slope failures off Mt. Etna.

27.2 Data

All data presented in this manuscript are newly collected during RV Meteor cruise M86/2 (December 2011 to January 2012) and are presented here for the first time. High-resolution 2d reflection seismic data were acquired using a 1.7 l GI-Gun and a digital Geometrics GeoEel 104-channel streamer with a total length of 162.5 m and a hydrophone spacing of 1.56 m. Seismic data were processed with GEDCO Vista Seismic Processing V.11 including setting up the geometry, frequency filtering, normal move correction (NMO) with a constant velocity, stacking and time migration. Bin size was set to 2 m resulting in an average fold of 10. Bathymetric data were collected using the hull mounted Kongsberg EM120 and Kongsberg EM710 multi-beam echo-sounders. Parasound sediment echo-sounder data were acquired by an ATLAS DS-3/P70. In addition, a 10 m gravity corer was used for sediment sampling. All sediment cores were only examined visually as a detailed sedimentological analysis of the cores is not objective of this manuscript.

27.3 Results

27.3.1 Morphology of the Eastern Flank of Mt. Etna

Fiumefreddo Valley (FV) and its southern prolongation (EFV) (Fig. 27.1) mark the northern boundary of the eastern flank of Mt. Etna. This valley system hosts a wide spread hummocky topography, which is a strong implication for mass transport

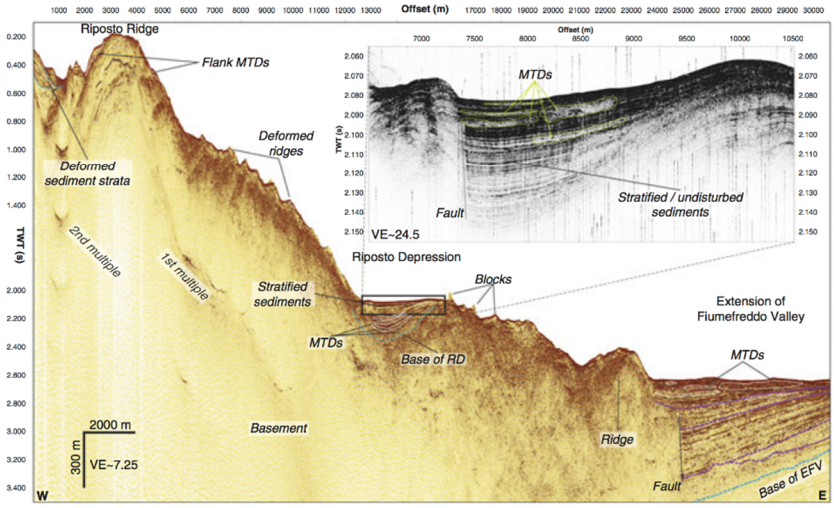

Fig. 27.2 2d reflection seismic profile M86-2-p407 and Parasound echo-sounding zoom-in of the Riposto Depression. The seismic section shows the distribution of proximal and distal sedimentary units and illustrates steep slope gradients. The Parasound echo sounding shows near-surface transparent units intercalated with well-stratified reflectors in the Riposto Depression. See Fig. 27.1 for location of profile

deposits (MTDs) at the seafloor. Riposto Ridge (RR) represents a major ridge in the North, which extends offshore in a curved shape towards the southern part of Fiumefreddo Valley; RR is strongly reworked by submarine canyon- and gully structures (Fig. 27.1).

Riposto Depression (RD, Figs. 27.1 and 27.2) is a flat depression, which covers an area of 7.25 km^2 and is surrounded by an amphitheater-like structure. This structure most likely represents the remnant of a major flank failure (Chiocci et al. 2011). Ridges surrounding the Riposto Depression show slope gradients of up to 20°. Large blocks and MTDs are visible especially on its eastern margin (Fig. 27.1), which can also be observed in seismic profiles (Fig. 27.2). The near-shore areas are characterized by funnel-shaped sedimentary systems, which host several incisions running down-slope to the East (Fig. 27.1). The southern boundary of the deforming part of Mt. Etna is marked by the Catania Canyon (Chiocci et al. 2011). In general, the entire flank offshore Mt. Etna is characterized by numerous small scale gully- and canyon like structures carving into the background morphology, which is commonly observable at steeply dipping continental margins (Micallef and Mountjoy 2011; Vachtman et al. 2013).

27.3.2 Seismic Evidence for MTDs

Most of the seismic units displaying high amplitude and discontinuous reflectors can be interpreted as MTDs. Profile M86-2-p407 (Fig. 27.2) represents a typical cross-section from the near shore areas to the southern extension of Fiumefreddo Valley. The profile shows four different settings:

- The Riposto Ridge is characterized by slope angles of up to 20° and prominent deformed ridges. The slope shows headwall-like structures, as indicated by widespread erosional truncations. Most of the depressions show an interlayering of chaotic seismic units interpreted as MTDs, and well-stratified sediments.
- The Riposto Depression is a small basin with a complex internal structure. The seismic record (Fig. 27.2) images well-stratified sediments in the uppermost 100 ms TWT underlain by three major high amplitude discontinuous units, which can be found below 2,150 ms TWT in the seismic record (Fig. 27.2). We interpret those units as MTDs. Parasound echo-sounder data allow a detailed view of the upper ~50 m of the sediments illustrating transparent units close to the sea floor as well as inter-bedded well stratified sediments (Fig. 27.2). The transparent/discontinuous units are interpreted as MTDs.
- The transition from Riposto Depression to the southern prolongation of Fiumefreddo Valley shows a rough topography. It reveals a field of blocks outcropping at the seafloor (Figs. 27.1 and 27.2). This hummocky topography may be formed as a result of one major or several smaller slope failures.
- The southern prolongation of Fiumefreddo Valley is imaged as a half-graben-like feature on the seismic profile (Fig. 27.2). The upper units are characterized by high amplitudes, discontinuous and more or less horizontal reflectors, while the lower units show a clear tilt. Further to the North, Fiumefreddo Valley is filled by high amplitude reflectors with varying continuity (Fig. 27.3).

A profile showing widespread MTDs around the Fiumefreddo Valley (Fig. 27.1) is shown in Fig. 27.3. Several chaotic units interpreted as MTDs are inter-bedded with well-stratified reflector packages representing the undisturbed background sediments. The area NE of Fiumefreddo Valley is of special interest. Billi et al. (2008) interpreted the morphology in this area as a large MTD originating from the head region of Fiumefreddo Valley based on an older data set. They considered a major sediment slide in this area as a potential trigger mechanism for the devastating tsunami, which followed the 1908 Messina earthquake. This hypothesis is strongly doubted by Argnani et al. (2009) based on modern bathymetric data. Argnani et al. (2009) show, that the morphology of the area is a product of long-lasting erosion without any trace of a 100 year-old large-scale landslide. The interpretation by Argnani et al. (2009) is well supported by the new seismic data. Thick stratified

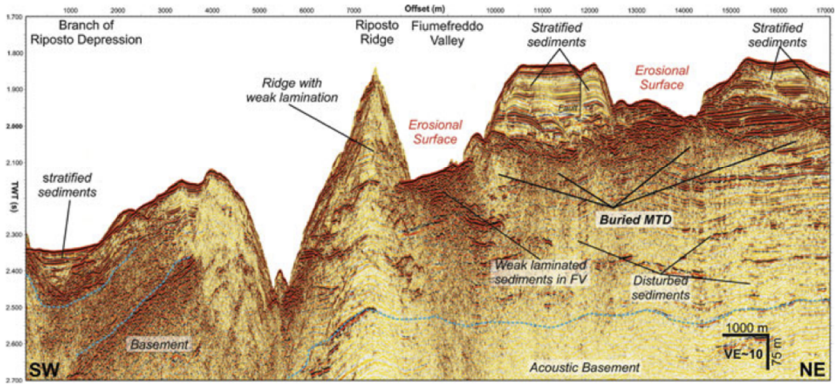

Fig. 27.3 2d reflection seismic profile M86-2-p404 traversing the northern edge of the survey area in a SW to NE direction. Especially the section from offset 8,000–14,500 reveals a stratified sedimentary unit, which is underlain by a large MTD. See Fig. 27.1 for location of profile

sedimentary units are found immediately below the sea floor (Fig. 27.3). These units are underlain by large MTDs, which were most likely deposited during the evolution of the Fiumefreddo Valley but not in present times. The buried MTDs indicate a long history of mass wasting at the eastern flank of Mt. Etna.

27.3.3 MTDs and Tephra Layers in the Sedimentary Record

Gravity cores were taken at several locations in order to sample near surface MTDs. Most of the cores show clear indications for MTDs, all of which host major tephra layers. To illustrate some typical features, sediment cores M86/2-007-01 and M86/2-015-01 were chosen. Gravity core M86/2-007-01 (Fig. 27.4a) with a total length of 433 cm was recovered southwest of the amphitheater structure at the eastern flank off Mt. Etna edifice (see Fig. 27.1 for location of core). It reveals a strong variation of deposits through the sediment column. Major tephra fallout deposits can be observed at 20–22, 58–61 and 325–331 cm (Fig. 27.4). In addition, two chaotic facies can be identified yielding intraclasts of up to 6 cm in diameter. Most remarkable feature in this gravity core is the section between 325 and 370 cm (Fig. 27.4b), as it bears a tephra layer with a thickness of ca. 6 cm, which is directly underlain by a ca. 40 cm thick chaotic unit.

Gravity core M86/2-015-01 (Fig. 27.4c) with a total length of 356 cm was recovered at the western edge of the amphitheater structure. Especially the lower section from 270 to 328 cm is of special interest, as it hosts a similar succession of MTD and tephra as described for the core M86/2-007-01 (Fig. 27.4d), as this MTD is directly overlain by a tephra layer. This chaotic layer features intraclasts of up to 9 cm in size with different compositions. Most prominent are tephra- as well

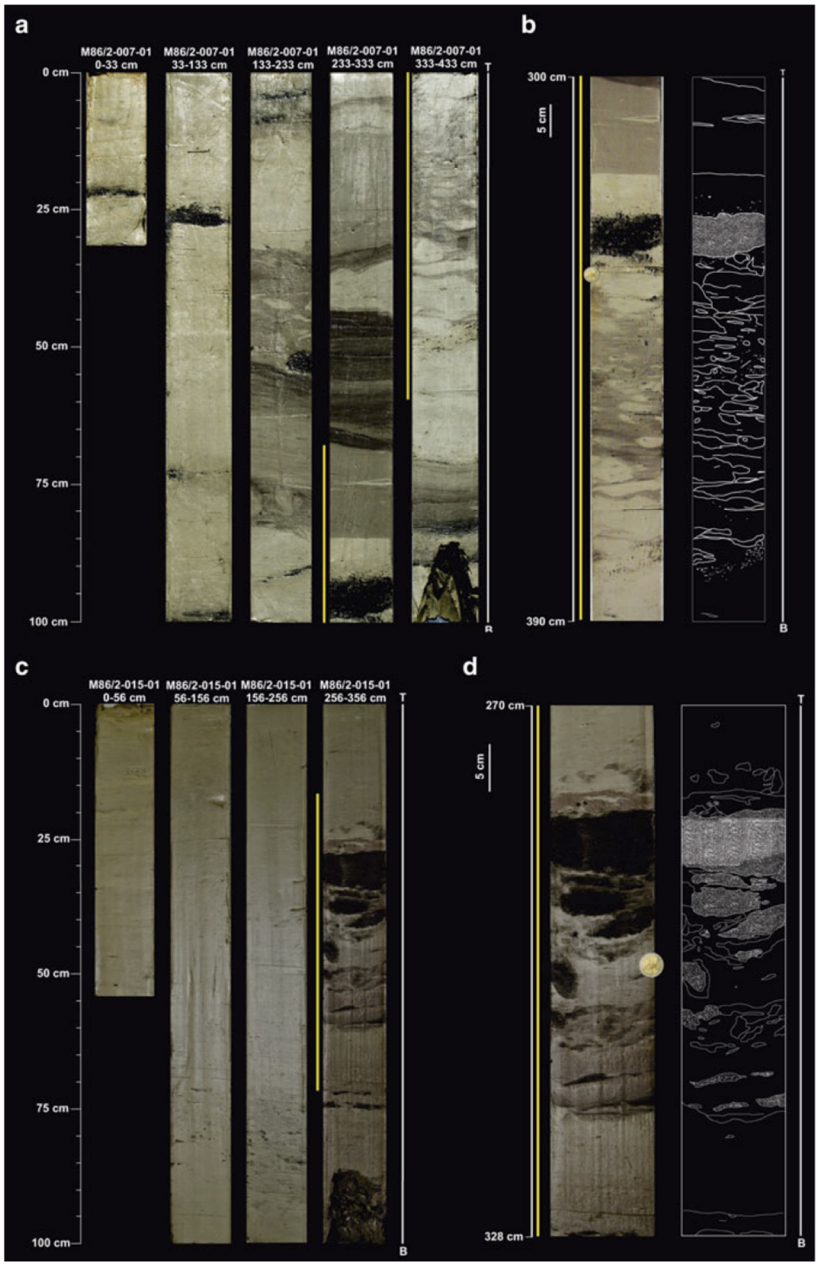

Fig. 27.4 (**a**) Gravity core M86/2-007-01 (**b**) Close up of Gravity Core M86/2-007-01 from 300 to 390 cm (**c**) Gravity core M86/2-015-01 (**d**) Close up of Gravity Core M86/2-015-01 from 270 to 328 cm

as clasts made out of fine to medium sands. As the composition of this chaotic unit hosts a mixture of sedimentary material available at the submarine slope of Mt. Etna, we consider this chaotic unit as a representative MTD for this region.

27.4 Discussion

27.4.1 MTD Distribution and History of Sliding

As previously described and discussed by Pareschi et al. (2006) and Chiocci et al. (2011), the entire survey area is strongly affected by submarine mass wasting. The new M86/2 high-resolution dataset reveals new insights into a long history of mass wasting and its strong connection to morphological features like the Riposto Depression. Especially seismic profile p404 (Fig. 27.3) provides indications for one or more ancient slope failure, as the prominent MTD is overlain by a well-stratified sedimentary unit with a thickness of ca. 200 ms TWT. Furthermore, Fiumefreddo Valley and its prolongation to the South (Figs. 27.1 and 27.2) seems to act as an important conduit. It collects debris and MTDs from the eastern flank of Mt. Etna and appears to restrict the sedimentary transport to the East and the Ionian Sea. The analysis of all available seismic data allows to document the regional and temporal distribution of large and small scale MTDs. Distal areas such as the southern prolongation of Fiumefreddo Valley show relatively small mass wasting deposits in the deeper sediment record, whereas high amplitude, discontinuous reflectors in the upper sediment column indicate larger scale MTDs in more recent times. For proximal areas, larger scale MTDs can be traced in sediment units deeper than 200 ms TWT. These MTDs can especially be traced within the Riposto Depression (Fig. 27.2), which shows a focus of large MTDs in the lower sedimentary units. The Riposto Depression represents a basin, which is strongly affected by mass wasting. It collects large amounts of transported sediments from the surrounding amphitheater structure with flank gradients of up to 20°.

Exposed and buried MTDs imply a long history of sliding and recent MTD generation in the working area strongly support the hypothesis of large-scale gravitational instabilities (Chiocci et al. 2011) and a long time activity of mass movements as run-out debris slumps (Pareschi et al. 2006).

27.4.2 Relationship between Tephra Layers and MTDs

The entire survey area is strongly affected by MTDs. Most general factors controlling slope failures include strong tectonic control and associated seismicity, over steepening of flanks due the deformation of the flank (Chiocci et al. 2011), volcanic eruptions, and possible liquefaction of tephra layers, which may act as a

slide plain and therefore entrain overlying sediments (Harders et al. 2010). Here we would like to focus on the role of tephra layers, as the identified succession of tephra layers directly on top of MTDs may be important for understanding possible slide triggering mechanisms in the working area. Harders et al. (2010) suggested for a comparable setting at the Middle America Trench that tephra layers act as detachment planes due to liquefaction during seismic activity. Nevertheless, no indication for such a process could be found in the working area offshore Mt. Etna. On the contrary the location of tephra layers immediately above the MTDs suggest a close link between emerging volcanic activity and slope failure. Volcanic tremor before an eruption may induce high seismicity and may trigger slope failures. Deformation of volcanic flanks during the rise of magma before an eruption and associated hydrothermal activity may further contribute to slope instability (van Wyk de Vries et al. 2000). Hence a slope failure would be followed by an eruption and the deposition of a tephra layer would occur immediately afterwards on top of the MTD. The consecutive succession of deposits was observed at several cores at different locations. No correlation between cores is possible but the different compositions of the tephra layers overlying MTDs suggest that different stratigraphic intervals were cored at different locations. We are aware that tephra does not behave like other particles in the water column (Carey 1997) as it may build vertical gravity currents, which lead to an inhomogeneous distribution of the widespread tephra layers. However, we are convinced that we sampled several slides with different ages, which show the typical succession of a MTD covered by a tephra. Hence, we consider the triggering of MTDs during emerging volcanic activity as being of general importance for the eastern submarine flank of Mt. Etna.

We also identified MTDs without a tephra layer on top indicating that other processes for slope stability are important as well. They may include oversteepening of the slope, toe erosion in areas with deep incisions, seismicity not related to volcanic activity, and high sediment accumulation rates. We also would like to point out that we have not cored any of the large MTDs identified in the seismic record as they cannot be reached without deep drilling. The clear indications even between small near-surface MTDs (identified in the cores) and volcanic activity let us assume that large failures are triggered by volcanic activity in a similar matter though a time lag between the MTD generation and the settling of tephra could lead to a similar observation in the sedimentary record.

27.5 Conclusion

Widespread MTDs could be mapped off the eastern flank of Mt. Etna edifice. MTDs at different stratigraphic levels indicate a long history of mass wasting. The distribution of MTDs is mainly controlled by pre-existing morphology. A typical succession of MTDs directly overlain by tephra layers indicate that volcano induced seismicity and flank deformation prior to an eruption act as important trigger mechanisms for slope failures on the eastern flank of Mt. Etna. This observation

was established at relatively small scale slides with thicknesses of up to 50 cm and in sediment depth less than 5 m. Seismic data show significantly larger buried MTDs, which were most likely triggered by similar volcanic processes in the past.

Acknowledgments Many thanks to the crew of RV Meteor for their help during the collection of data. The authors are thankful to Dina Vachtman and Klaus Reicherter for their reviews and constructive comments. This project was funded by the DFG and the Cluster of Excellence "The Future Ocean".

References

Argnani A, Chiocci FL, Tinti S, Bosman A, Lodi MV, Pagnoni G, Zaniboni F (2009) Comment on "On the cause of the 1908 Messina tsunami, southern Italy" by Andrea Billi et al. Geophys Res Lett 36:L13307

Argnani A, Mazzarini F, Bonazzi C, Bisson M, Isola I (2012) The deformation offshore of Mount Etna as imaged by multichannel seismic reflection profiles. J Volcanol Geotherm Res 251:50–64

Azzaro R, Bella D, Ferreli L, Michetti AM, Santagati F, Serva L, Vittori E (2000) First study of fault trench stratigraphy at Mt. Etna volcano, Southern Italy: understanding Holocene surface faulting along the Moscarello fault. J Geodyn 29:187–210

Billi A, Funiciello R, Minelli L, Faccenna C, Neri G, Orecchio B, Presti D (2008) On the cause of the 1908 Messina tsunami, Southern Italy. Geophys Res Lett 35:L06301

Borgia A, Ferrari L, Pasquare G (1992) Importance of gravitational spreading in the tectonic and volcanic evolution of Mount Etna. Nature 357:231–235

Branca S, Ferrara V (2013) The morphostructural setting of Mount Etna sedimentary basement (Italy): implications for the geometry and volume of the volcano and its flank instability. Tectonophysics 586:46–64

Carey S (1997) Influence of convective sedimentation on the formation of widespread tephra fall layers in the deep sea. Geology 25:839–842

Chiocci FL, Coltelli M, Bosman A, Cavallaro D (2011) Continental margin large-scale instability controlling the flank sliding of Etna volcano. Earth Planet Sci Lett 305(1–2):57–64

Doglioni C, Innocenti F, Mariotti G (2001) Why Mt Etna? Terra Nova 13:25–31

Ferreli L, Michetti AM, Serva L, Vittori E (2002) Stratigraphic evidence of coseismic faulting and aseismic fault creep from exploratory trenches at Mt. Etna volcano (Sicily, Italy). In: Ettensohn FR, Rast N, Brett CE (eds) Ancient seismites, Geological Society of America Special Paper 359, Geological Society of America, Boulder, pp 49–62

Gvirtzman Z, Nur A (1999) The formation of Mount Etna as the consequence of slab rollback. Nature 401:782–785

Harders R, Kutterolf S, Hensen C, Moerz T, Brückmann W (2010) Tephra layers: a controlling factor on submarine translational sliding? Geochem Geophys Geosyst 11(5):1–18

Micallef A, Mountjoy JJ (2011) A topographic signature of a hydrodynamic origin for submarine gullies. Geology 39:115–118

Pareschi MT, Boschi E, Mazzarini F, Favalli M (2006) Large submarine landslides offshore Mt. Etna. Geophys Res Lett 33:L13302

Simkin T, Siebert L (1994) Volcanoes of the world. Geoscience Press, Tucson, 349 pp

Vachtman D, Mitchell NC, Gawthorpe R (2013) Morphologic signatures in submarine canyons and gullies, central USA Atlantic continental margins. Mar Pet Geol 41:250–263

van Wyk de Vries B, Kerla N, Petley D (2000) Sector collapse forming at Casita volcano, Nicaragua. Geology 28:167–170

7 Conclusions and Outlook

7.1 Conclusions

A new 2D/3D hydro/seismo-acoustic acquired during RV Meteor cruise M86/2 allows a detailed investigation of the architecture of the bulged continental margin east of Mt. Etna in order to evaluate its proposed instability. The thesis combines the analysis of tectonic- and sedimentary processes, both playing an important role for large-scale continental margin instability. The main conclusions of this thesis are:

i) Architecture of the continental margin east of Mt Etna's edifice:

The morphology of the continental margin east of Mt Etna is dominated by a prominent bulge visible in morphological data. This bulge cannot be observed at the continental margin north and south of the volcano edifice. The entire margin is overprinted by multiple channels and gullies indicating a high grade of denudation. The central part of the continental margin east of Mt. Etna is dominated by an amphitheater-like structure; the semi-circular headwall is directly adjacent to a structural high. The structural high was mapped by means of 3D seismic data and shows a high grade of extensional and strike-slip tectonics.

It was possible do trace the limits of the continental margin instability with the new dataset. The Southern boundary is found as submarine continuation of the onshore Tremestieri-Trecastagni Fault System. The submarine continuation of the onshore fault system is imaged as a positive flower structure, indicating a transpressional tectonic regime north of the Catania Canyon. A prominent lineament at the top of an anticline is visible on bathymetric maps; this lineament is the morphological expression of the fault imaged by seismic data. The fault can be traced towards the toe of the continental margin. The northern boundary of the instability is described as the Pernicana-Provenzana Fault onshore but is not traceable as a distinct sharp boundary into the offshore realm. The prominent sedimentary Riposto Ridge is observed at the expected submarine continuation of the Pernicana-Provenzana Fault. The Riposto Ridge does not show any indications for brittle deformation in its uppermost strata, but is characterized by a diffuse grade of ductile deformation. In front of the toe of the continental margin, two concave anticlines were mapped and interpreted as the eastern limit of the moving flank. The sedimentary basins at the toe of Mt Etna's continental margin are addressed to a pre-Etnean genesis as they can be traced to the south of the volcano edifice though they might be overprinted by the continental margin spreading east of Mt Etna. A new model summarizing the architecture of the continental margin is shown in Fig. 19.

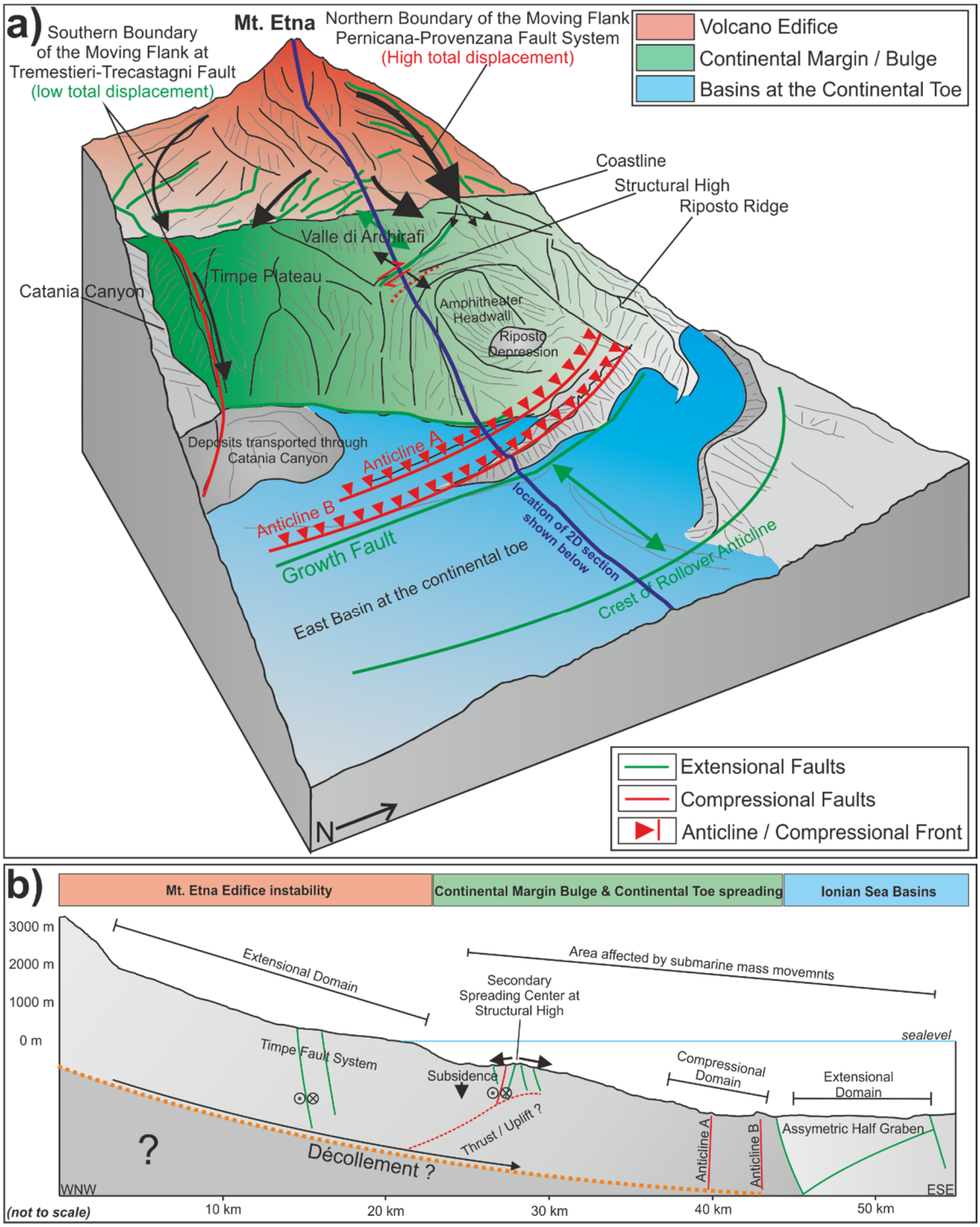

Figure 19: The model of continental margin and volcano flank instability generated in this thesis (See Chapter 4 MANUSCRIPT I for more information). The southern boundary of the volcano flank is located at the Tremestieri-Trecastagni Fault System and can be traced as a transpressional fault over the continental margin towards the continental toe. The northern boundary at the Pernicana-Provenzana Fault cannot be traced as a sharp feature into the offshore realm. Moreover, its movement is compensated by ductile and diffuse deformation in Riposto Ridge. The seaward extension of the moving flank is limited at two sub-vertical anticlines, in front of the continental margin. Whereas the eastern flank of the Mt Etna's edifice and the entire continental margin is affected by gravitational spreading and related instability, a secondary spreading center was mapped at the structural high directly west of the amphitheater headwall. The entire dataset implies a high grade of activity, as most of the observed faults and folds reveal a distinct surface expression at the seafloor. Furthermore, submarine mass transport deposits, traced at the continental margin and its toe, indicate a high recurrence rate of mass wasting events at the continental margin offshore Mt Etna.

ii) Characterization of continental margin instability:

The new data shows that the submarine continental margin east of Mt. Etna is overprinted by heterogeneous sets of faults. Furthermore, the area of the central continental margin east of Mt. Etna shows an area definitely not created by simple gravity gliding of the entire continental margin, as a secondary spreading center with indications for gravitational collapse and spreading is imaged by the new 3D seismic data. This implies a highly heterogeneous spreading mechanism, which is driven by gravity from the volcano edifice and gravity spreading at the structural high west of the prominent amphitheater. Nevertheless, a pre-Etnean décollement or glide plane could not be reliably mapped with our high-resolution seismic system due to a limited penetration. The distal extension of the continental margin spreading is marked by two concave anticlines at the continental toe east of Mt Etna; these anticlines are adjacent to a system of half grabens, which are related to rollover-anticlines. The continental margin spreading is highly active, as most of the observed faults are outcropping at the seafloor.

iii) Link between volcano flank instability and continental margin instability:

The most important onshore structures of the eastern volcanic edifice of Mt. Etna are the Pernicana-Provenzana Fault system as the northern boundary of the volcano flank instability, the Tremestieri-Trecastagni Fault System as the southern boundary, and the Timpe Fault System in the center of the eastern volcano edifice. Whereas the northern boundary seems to be dispersed into the offshore realm, it was possible to trace the submarine continuation of the Tremestieri-Trecastagni Fault System down to the toe of the continental margin. Furthermore, the new data implies a strong connection between the onshore Timpe Fault System and the newly mapped Valle di Archirafi Fault system, as they are creating the Giarra / Valle di Archirafi Wedge, which can be traced on- and offshore. This theory is strongly supported by analogue modelling of *Le Corvec et al. [2014]*, which suggests a connection of the Timpe Fault System to an offshore fault system. In addition, two concave anticlines are only observed at the continental toe east of Mt Etna but cannot be traced further north or south. All these findings imply a first order linkage of the volcano edifice and continental margin instability and gravitational spreading.

iv) Submarine mass transport deposits at the continental margin and the continental toe:

Widespread mass transport deposits were mapped off the eastern flank of Mt. Etna edifice. Mass transport deposits at different stratigraphic levels indicate a long history of mass wasting. The distribution of mass transport deposits is mainly controlled by pre-existing morphology. A typical succession of mass transport deposits directly overlain by tephra layers indicates that volcano induced seismicity and flank deformation prior to an eruption act as important trigger mechanisms for slope

failures on the eastern flank of Mt. Etna. This observation was established at relatively small scale slides with thicknesses of up to 50 cm and in sediment depth less than 5 m. Seismic data show significantly larger buried mass transport deposits, which were most likely triggered by similar volcanic processes in the past. The new dataset does not support the theory by *Billi et al. [2008]* that the 1908 tsunami was triggered by a submarine slide related to massive landslide deposits on the continental margin north of Mt Etna. The proposed slide deposits are overlain by ~ 150 m in-situ strata, which is strongly reworked by erosive processes of the adjacent canyons on the steep slopes of the continental margin east of Mt. Etna. The mass transport deposits proposed by *Billi et al. [2008]* seem to be the product of an ancient landslide event much older than 100 years.

Another striking feature in terms of submarine mass transports is the massive amphitheater-like structure, observed at the continental margin offshore Mt Etna because such semi-circular structures are commonly connected to massive submarine mass transport deposits formed during major slope failures. However, it was not possible to link a major mass transport deposit to the amphitheater-like structure; only small-scale mass transport deposits were mapped in an enclosed basin (Riposto Depression) and its surroundings downslope of the amphitheater-like structure. Nevertheless, it is still to evaluate, whether the amphitheater-like structure is an ancient scarp of a massive submarine landslide or the result of the complex teconic setting and the transtensional fault between Valle di Archirafi and the structural high.

The new findings imply a high geo-hazard potential of the entire area offshore Mt Etna, as the gravitational spreading of the continental margin can lead to slope over-steepening and the generation of weakened sedimentary units due to intense deformation. Within the sedimentary succession, the new dataset shows a variety of small- to medium scale mass transport deposits at the continental margin and the continental toe. Especially the geo-hazard potential at the steep amphitheater headwall has to be considered, as the domino-style fault system directly at its scarp implies a retrogressive growth of the fault system. Destabilization directly at the steep slopes of the amphitheater can result in future mass wasting events and may lead to a destabilization of the entire structural high next to Valle di Archirafi.

7. 2 Outlook

The submarine continental margin east of Mt. Etna displays a high grade of recent deformation, which illustrates the activity of a coupled gravitational instability. Onshore flank dynamics have been observed and monitored for more than 20 years and reveal a high geo-hazard potential due to sector collapses related to flank instability. However, only a few studies on Mt Etna's adjacent continental margin instability were carried out so far. One main outcome of this thesis is the setup of an enhanced model for the architecture and near surface tectonic processes of the onshore volcano flank and the offshore continental margin. The findings imply significant ongoing tectonic activity as most of the faults imaged in seismic data do show a surface expression at the seafloor. Nevertheless, the kinematic control, displacement rates, displacement velocities, and the link of offshore faults to the onshore faults and structures are still uncertain, as geodetic and InSAR measurements are limited to onshore regions. The development of marine geodesy networks is a new approach to measure relative fault displacements at the seafloor; marine geodesy is one of the most promising approaches for future fault and landslide monitoring in the submarine realm. The setup of a marine geodetic network at the continental margin east of Mt. Etna would allow quantifying several of the processes suggested in this thesis. Hence, a ship-time proposal for the deployment of the new GEOMAR geodetic stations was submitted based on the results of this thesis. The specific objectives of the proposed survey are:

i) Assignment of the movement of the continental margin and its link to the well-studied and monitored onshore flank
ii) Measuring of displacement rates along the southern boundary of Mount Etna's unstable flank and determination of its limits
iii) Validation of the hypothesis that the onshore Giarre Wedge and the offshore Valle di Archirafi Wedge are controlled by the faults of the Timpe Fault System and the Valle di Archirafi Fault System. This includes monitoring of the individual fault systems during and after volcanic activity.
iv) Determination of the stability of the amphitheaters headwall and its prominent fault displacement rates.

In addition to the deployment of a marine geodetic network, further studies need to be carried out at the continental margin offshore Mt Etna. Especially the mass wasting deposits identified in the Valle di Archirafi may document potential sector collapses of Mt Etna, such sector collapses are an important process during the volcanic evolution of Mt. Etna and represent a significant geo-hazard. Furthermore, the high grade of denudation at the continental margin leads to the formation of a variety of channels and gullies. A sediment budget study would shed some light on the erosional processes acting at Mt Etna's continental margin. These findings would help to understand the complex sediment transport pattern of volcanic and non-volcanic debris towards the toe of the continental margin.

8 Acknowledgements

Many Thanks to the Cluster of Excellence “The Future Ocean” for funding this project and the Integrated School of Ocean Sciences for interesting courses and interaction.

Many thanks to my first PhD Supervisor Sebastian Krastel for support, help, motivation, trust and especially for leaving headroom for creativity and the encouragement for new projects.

Many thanks to my second PhD Supervisor Jan-Hinrich Behrmann for his support, input and ideas during the last three years.

Many thanks to Cord Papenberg for his input, supervision and the 3D seismic data processing.

Many thanks to Jacob Geersen for his ideas, input and patient support during the preparation of the manuscripts.

Thanks to Morelia Urlaub for the nice collaboration and for setting up the MaGOMET ship-time proposal.

Many thanks to Francesco Latino Chiocci, Domenico Ridente and Federica Maisto for a wonderful research stay at Francesco’s working group at La Sapienza University, Rome.

Thanks to Deniz Cukur for our discussions, conferences and work at Sebastian Krastel’s group.

Many thanks to my Co-Authors, which supported me during the preparation of the manuscripts.

Thanks to the Master Students Irena Schulten and Julio Beier for the wonderful atmosphere during data processing and evaluation.

Many thanks to Mathias Meyer, Julia Schwab, Katja Lindhorst, Judith Elger, Peter Feldens and Heiko Jähmlich for the support and discussions during the last years!

Thanks to FB4 GDY and the working Group Marine Geophysics and Hydroacoustics for the nice support during data processing and evaluation.

Many thanks to the TLZ and especially Gero Wetzel and Torge Mathiessen for the steady support on- and offshore.

Many thanks to my girlfriend Sandra Sturmann, who was always supportive during my studies and my PhD phase.

Many thanks to my Family, Johannes Gross, Annette Gross, Nikolai Gross and Isabel Gross for their support and their introduction to the scientific world. Many thanks to Monika Korff for proof reading.

Many thanks to Kilian Etter for proof reading of the Thesis and discussions during the last months of my PhD phase.

Many thanks to my friends Emmanuel Porten, Arne Stichweh, Maik Brandt, Alf Brandt and Adrian Ernst for their steady support and their positive distraction during the last years!

9 Curriculum Vitae

Name:	Felix Michael Gross
Date of Birth:	01.02.1987
Place of Birth:	Freiburg im Breisgau, Germany
Permanent address:	Holtenauer Straße 207
	24106 Kiel

Education:

1997 – 2006	Goethe-Gymnasium Freiburg ím Breisgau Abitur 2006
2006 – 2009	Studies of Geosciences at Albert Ludwig Universität Freiburg Bachelor of Science
2009 – 2012	Studies of Marine Geosciences at Christian-Albrechts Universität zu Kiel Master of Science
Since Feb. 2012	Doctorate funded by the Cluster of Excellence “The Future Ocean” GEOMAR Helmholtz Centre for Ocean Research / Christian-Albrechts-Universität zu Kiel Supervisors: Prof. Dr. Sebastian Krastel-Gudegast Prof. Dr. Jan-Hinrich Behrmann